SELL, STORE OR MINE:

INTELLIGENT DECISION-MAKING FOR RENEWABLE GENERATION

Joana Barragan

August 30th, 2019

Supervised by: Professor William Knottenbelt

A thesis presented to Imperial College London in partial fulfilment of the requirements for the degree of *Master of Science in Sustainable Energy Futures* and for the *Diploma of Imperial College*

Energy Futures Lab

Imperial College London

SW7 2AZ

Acknowledgements

I would like to express my deepest and most sincere gratitude to my supervisor Professor William Knottenbelt, who has put great efforts in finding a project that would be both stirring and challenging. I am ever so grateful to have undertaken my dissertation under his counsel.

I'd like to extend my gratitude to Gavin Eves from the Sustainable Energy Futures department for supervising our year and his kind approach to solving any issue that would emerge. His disposition was outstanding and greatly appreciated.

I dedicate this dissertation to my fellow classmates and friends with whom I have had the chance to share great moments throughout the course of this Master. Their never-ending support comes greatly valued. I also dedicate my efforts to Ernesto José Petit Masci, for his kind and unwavering support throughout the course of my project; as well as to my family who never ceases to support me in all aspects of my life and to whom I would like to express my heart-felt gratitude.

And most importantly, praise to you God because through all these wonderful people you convey your love and care for me. You inspire me and guide me. May I always follow in your footsteps.

A thankful heart.

Table of Contents

Acronyms

AC	Alternating Current
ASIC	Application Specific Integrated Circuits
ATM	Automated teller machine
BBCT	Bumblebee Conversation Trust
BFL	Butterfly Labs
BRE	Building Research Establishment
BTC	Bitcoin (cryptocurrency)
CAPEX	Capital Expenditure
CNES	National Centre for Space Studies
COP	Conference of the Parties
CPU	Central Processing Unit
DC	Direct Current
DiffHor	Horizontal diffuse irradiation
DOE	US Department of Energy
DoS	Denial-of-service
E_Out	Energy injected into grid, mining or storage
EArray	Effective energy at array output
EES	Electrical Energy Storage
EIA	Energy Information Administration
EU	European Union
FiT	Feed-in tariff
FPGA	Field-Programmable Gate Array
GH/s	Giga-Hases per second (10^9 H/s)
GHG	Greenhouse Gas
GIS	Geographic Information System
GlobEff	Effective global irradiation, corrected for IAM and shadings
GlobHor	Horizontal global irradiation
GlobInc	Global incident irradiation on collector plane
GPU	Graphics Processing Unit
GW	Giga-Watt (power)
Hz	Hertz
IAM	Array incidence loss
IEA	International Energy Agency
IPCC	Intergovernmental Panel on Climate Change
IRR	Internal Rate of Return
ISO	Initial Stock Offering
kW	Kilo-Watt (power)
kWh	Kilo-Watt hours (energy)
LCOE	Levelized Cost of Energy
Li-ion	Lithium ion batteries
MPP	Maximum Power Point
MW	Mega-Watt (power)
MWh	Mega-Watt hours (energy)
NPV	Net Present Value
NREL	National Renewable Energy Laboratory
OECD	Organisation for Economic Co-operation and Development
OPEX	Operating Expenditure
PH/s	Peta-Hashes per second (10^15 H/s)
PJ	Peta-Joules (10^15 J)
PoW	Proof of Work
PPA	Purchase Power Agreement
PPP	Purchasing Power Parity
PR	Performance ratio
PV	Photovoltaic
R&D	Research and Development
RMS	Root Mean Square
ROI	Return on Investment
Rs	Indian Rupees
SHA	Secure Hash Algorithm
SIMD	Single instruction, multiple data
STC	Standard Testing Conditions
T_Amb	Ambient temperature
TH/s	Tera-Hashes per second (10^12 H/s)
TW	Tera-Watt (power)
TWh	Tera-Watt hours (energy)
UNFCCC	United Nations Framework Convention on Climate Change
YoY	Year-on-year

List of Figures

List of Graphs

List of Tables

1 Abstract

1.1 Background

Sustainable finance and proactive environmental measures emerging from international climate objectives and technological efficiency requirements are placing increasing pressure onto the deployment of renewables across the globe. Cost parity with fossil fuels has become the holy grail of the energy sector, and yet, their installation is not always straightforward, as many struggle to overcome the economic hurdles of the technology and rely still on subsidies and special solar tariffs. This thesis suggests that current financial models for renewable energy demand new revenues streams for the electricity generated, as well as flexibility to maximise profitability according to the specific market conditions and geographical location characteristics.

1.2 Scope and Objectives

The scope of this thesis is to analyse the impact of different revenue streams on profitability for the electricity generated from a solar PV site. The investigation considers the following profitability analysis for three different locations, namely Panjib in India, Huelva in Spain and Barstow in California, US.

Scenario 1 Selling the electricity generated to the grid with the GIS software PVSyst 6.8.3.

Scenario 2 Allocating the electricity generated to Bitcoin mining and selling electricity surplus to the grid within the different energy market conditions.

Scenario 3 Allocating the electricity generated to Bitcoin mining and storing electricity surplus in a 45 kWh Lithium-ion battery while continuing to generate profit through mining.

The objectives of the project include (1) the selection of three countries with high PV solar potential and different electricity market conditions, (2) the analysis of energy requirements of a defined crypto-mining site for an increased ROI, (3) performing a predictive analysis of the future value of bitcoin and the network mining difficulty with five different models ranging from optimistic to a more pessimistic setting, (4) filtering different variables to perform a sensitivity analysis to understand how the model is impacted, (5) analysing profitability resulting from the sale of electricity to the grid, using it to mine Bitcoins and selling surplus energy, as well as mining, storing and continue allocating stored energy to mine, (6) reaching conclusions on the main outcomes of the research.

1.3 Brief Description of the Methodology

The research offers a high-degree analysis performed in different computer programmes. The solar PV site of 12.75 kWp was modelled in the GIS software PVSyst 6.8.3 and the profitability performance of Scenario 1 was modelled within the same exercise, including a technical assessment of the PV system at each location, a loss assessment, the yearly profit and cumulative cashflows as well as a CO_2 balancing exercise.

The cryptomining model is divided into the historical and the predicted assessment of the future of the bitcoin price and the network hashrate (or mining difficulty) according to different scenarios which are based on the historical variability patterns of the network. The profitability of mining has been assessed on the one hand using pseudo-random models, namely an optimistic model, a medium-high profitability model, a medium-low profitability model, and a pessimistic model. On the other hand, a delimited random model has been used limiting the disparity observed in the historical variability factors of bitcoin price and network hashrate.

The financial analysis includes NPV, IRR and profitability performance for different parts of the analysis as well as sensitivity analysis with variables such as sun-hours, power unavailability (based on the days of sunlight), local electricity prices, battery replacement costs among others.

1.4 Summary of Main Findings

Assessing the different countries across all scenarios and predictive models, the research concludes that cryptomining, at the defined prediction and with the claimed assumptions, presents itself as a revenue stream that can maximize profit in the 25-year length of a solar PV site lifetime. Particularly, it was observed that whilst Huelva could not make its solar PV site profitable within the project length due to the fact that it competes against other conventional sources in the energy market, it is the location that benefits the most with regards to cryptomining potential as it has the largest rate of power availability in comparison to the other analysed countries. Cryptomining presents itself very profitable to all three countries; so much so that it provides 56%, 59% and 70% more profitability for Panjib, Huelva and Barstow, respectively, by storing electricity and mining further during off-sun-hour times (Scenario 3) than the resulting profitability from selling off surplus electricity (Scenario 2), even without energy storage costs. A summary table is provided in order to understand the profitability explicitly for each scenario and country (Table 1). Additionally, Graph 1 presents the performance of the most profitable scenario at the end of the project lifetime.

Historical & Predictive Results 2013-2037	**Panjib, India**	**Huelva, Spain**	**Barstow, US**
Scenario 1			
Net Investment	$ 47,057	$ 59,814	$ 47,848
Net Profit at End of Lifetime	$ 2,215	- $ 22,948	$ 34,825
Scenario 2			
Net Investment	$ 180,751	$ 193,508	$ 181,542
Average Net Profit at End of Lifetime*	$ 2,649,057	$ 2,762,119	$ 2,717,738
Scenario 3			
Net Investment	$ 246,049	$ 258,806	$ 246,840
Average Net Profit at End of Lifetime*	$ 4,146,426	$ 4,380,212	$ 4,608,889

* The net profit for scenarios 2 and 3 are presented as an average of the predictive models presented in Graph 1

Table 1. Net profitability at the end of lifetime results for all scenarios and locations, rounded to the nearest tens.

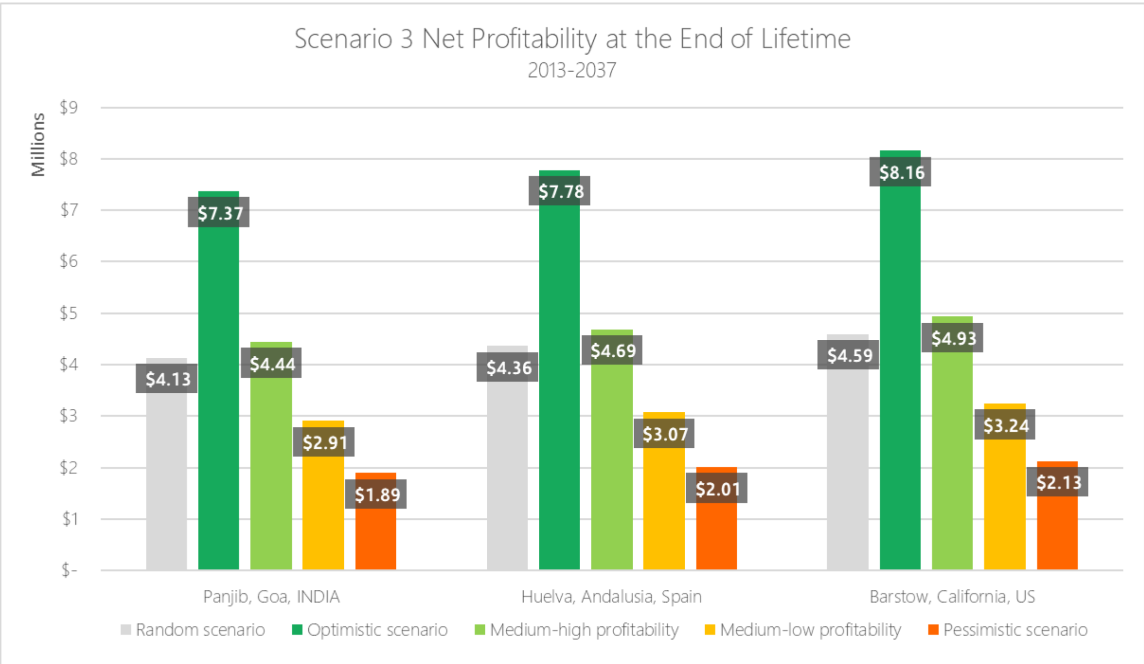

Graph 1. Net profitability at the end of lifetime (2013-2037) for all locations whereby energy storage is used to mine

2 Introduction

2.1 Context and Problem Definition

Renewable energy, in particular solar and wind deployment, have experienced an enormous uptake in the provision of energy to meet electricity demand, but it is no secret that there are several economic as well as technical barriers that the renewable industry still faces on order to compete against a fossil fuels economy, whereby 20-30% of companies and a fifth of world trade is related to fossil-fuels (Goldthau, 2018), and its infrastructure has been present throughout the course of a century. The shift to new distributed models – those that renewables incur in addition to centralized models – suggest a paradigm shift that comes under inarguably strenuous efforts across all levels of the energy supply chain, and even concerning consumer demand.

Profitability for the renewable sector is key and new ways of finding that profitability in order to make a project worth the while throughout the course of its duration need to be considered. Policy-making is key in making the first push towards the transition when uncertainties and risks are high, and renewables are certainly not risk-free. However, this is merely a short-term solution that cannot be withstood with a larger time horizon and a steadfast and cost-competitive establishment. Policies are already changing such as in China, India and the US whereby subsidies are reduced or eradicated such as in Spain and the goal is to make renewables a naturally attractive investment choice. Solar PV is one of the solutions which is ahead in the renewables race as it experienced the largest growth in generation in the renewable's realm with 570.8 TWh, larger than hydropower, wind and bioenergy (IEA, n.d.). According to the International Energy Agency (IEA), solar PV is on track to meet their Sustainable Development Scenario which requires an average growth of 16% from the year 2018 to 2030.

Selling to the grid may be more or less of a profitability choice depending on the country. For instance, in Spain solar electricity competes at the energy market prices of any other source whereas in other countries there is a specific tariff for solar-produced electricity. This thesis observes three different countries – namely India, Spain and California in the US – to understand the effect on the cashflow for the three different countries.

One of the profitability envisioned in this thesis is Bitcoin mining. Historically, Bitcoin has had a powerful impact on the profitability of miners, the generators of bitcoins. On the other hand, they have also become a new energy-intensive element of the electricity load as the energy required to sustain the Bitcoin network are very high due to its consensus mechanism, as will be explained in the succeeding chapters. This thesis examines mining as a profitability stream for electricity produced from solar PV systems which on one hand generates a certain degree of profitability and on the other reduces the carbon footprint of the activity given that the electricity supplied comes directly from a carbon-free source.

Another revenue stream will come from adding energy storage into the picture – along with its capital costs – and analyse how its presence affects the profitability of the system, but also the flexibility of what you can do with that electricity which can either mine for more hours or sell to the grid at peak times, if the tariff is variable.

2.2 Thesis Scope

The electricity produced from solar can be used in different ways, i.e. different profitability streams. The scope of this thesis considers the installation of a PV solar farm and the profitability of using the generated electricity by injecting to the grid or cryptomining. The model is based on historical sources for meteorological data and crypto values. In particular, this thesis looks at the more established cryptocurrency, Bitcoin.

Part of the thesis objectives was to select three countries or areas of implementation at different electricity market conditions, select a historical timeframe and generate the model based on studied assumptions. Since the PV simulation performed in PVSyst takes a project length of 25 years, a predictive modelling exercise has been performed within the crypto model as well based on several stated assumptions, within the 25-year timeframe starting in 2013 and leading towards a net profitability profile in 2037. The model has been performed on three different countries – namely India, Spain and the US – in order to understand how the meteorological and electricity market conditions impact on the profitability. Equally, since different system configurations will be assessed, the most profitable outlook will be recommended for each given location.

2.2.1 Aims

The **thesis aim** is to understand the profitability of different system configurations with regards to PV generation, cryptomining and energy storage, and how they impact in the profitability experienced in different locations in the globe. For this, three main scenarios are observed:

1. Sell the produced electricity to the grid at the established market electricity price
2. Dedicate the generated energy to mining Bitcoin and sell surplus electricity to the grid
3. Dedicate the generated energy to mining Bitcoin, store surplus electricity and continue generating profit from mining

It could (1) alleviate energy consumption from the grid during peaks, as the system would take the (estimated) high bitcoin mining loads from the grid, and (2) may provide additional incentives to cover or pay back the high renewable infrastructure costs, (3) or trigger further investments in new renewable infrastructure. (4) Additionally, it wouldn't be competing for resource use, as it would be based on a renewable energy generation.

2.2.2 Objectives

The specific objectives are further detailed below:

Identified Tasks	Description
1. Define scope of work	Timeframe, assumptions, solar PV farm size (etc.) definitions.
2. Selection of countries of study	Electricity costs vary greatly between countries and have a considerable impact on the profitability. Depending on their PV solar potential and electricity prices, three countries will be selected for contrasting purposes.
3. Analise Energy Requirements	A preliminary cryptomining estimation is to be carried out in order to set a power dimension to the PV solar farm to be designed.
4. Characterization of solar PV site	For each country, the technology, infrastructure size requirements, power output and cost elements have been defined.
5. Bitcoin price and network hashrate	Perform an analysis on the global historical and current status of bitcoin price and network hashrate.
6. Prediction in the crypto scope	A prediction exercise is to be developed in order to model the profitability coming from Bitcoin in the next 18 years (2013-2037), which depends on the value of Bitcoin and on the mining difficulty (network hashrate), as well as on mining technology progress.
7. Selection of variables for the sensitivity analysis	Identify the main variables for which the model will perform and the probability function for block generation and resource loss.
8. Profitability historical and predictive modelling	Model profitability performance in different scenarios: a) Profitability from selling the produced electricity to the grid at the established market electricity price b) Profitability from using the generated electricity to mining Bitcoin and sell surplus electricity to the grid c) Profitability from using the generated electricity to mining Bitcoin, store surplus electricity and continue generating profit from mining.
9. Results, analysis and discussion	Compare financial results and assess the results.
10. Overall conclusions	Provide an overall conclusion to the analysis carried out.

2.3 Renewable Energy Perspective

The renewable energy industry has peaked over the past decade and many countries have experienced a massive deployment in renewable technologies (Andoni, et al., 2018). According to Skea, there are two main energy drivers for the renewable explosion: climate and energy security (Skea, 2018).

2.3.1 *Climate*

The UN Framework Convention on Climate Change (UNFCCC) came into force in 1995 and was accepted by 195 nations, aiming to stabilize greenhouse gas (GHG) concentrations released in the atmosphere. The 2015 Paris Climate Agreement sought to reinforce the global response to climate change and the threat it poses (Skea, 2018).

Major national and international institutions have defined roadmaps to achieve ambitious targets. For instance, the European Commission has given the EU member states a binding target whereby 20% of their final energy consumption must originate from renewable resources by 2020 (European Commission, n.d.). Added pressure has come from the Intergovernmental Panel on Climate Change (IPCC)'s report of October 2018 with regards to the environmental impact of a temperature increase of 1.5°C above pre-industrial levels. According to the report, limiting the temperature increase to the studied level is highly challenging and requires rapid actions which, in turn, alleviate other world objectives (IPCC, 2018).

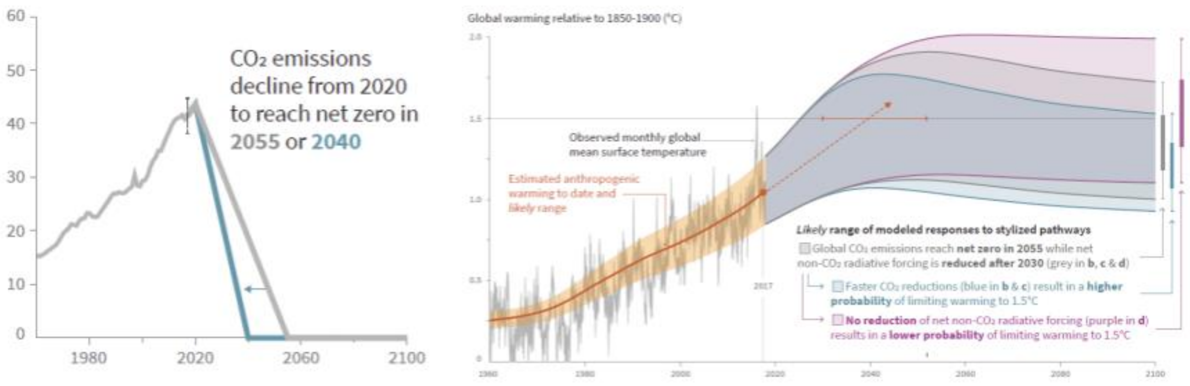

Graph 2. Required decline of CO2 emissions, expected global warming relative to pre-industrial levels *(IPCC, 2018)*

2.3.2 *Energy Security*

The Energy Information Administration (EIA) has projected a 28% growth in energy consumption between 2015 and 2040, primarily from non-OECD countries (including China and India and for which energy consumption is highly correlated to socioeconomic development) (Doman, 2017).

This increase in energy demand puts stress to the current energy, environmental and economic issues the world is seeing today.

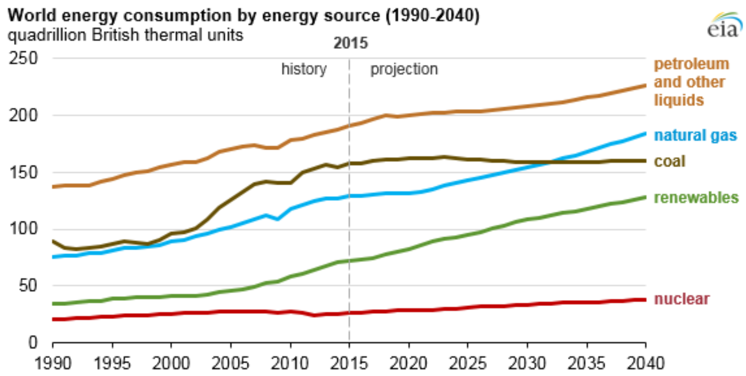

Graph 3. World energy consumption by energy source (1990-2040) *(Doman, 2017)*

As seen in Graph 3, fossil fuels will continue to lead the world energy supply as studies on oil reserves indicate to real physical constraint to their provision in the short to medium term (Skea, 2018). In a 2040 Energy Outlook report by ExxonMobil, 70% of the growth in transportation fuels is still allocated to diesel, not H_2-fuel cell vehicles (Skea, 2018).

In parallel, the use of natural gas will expand. In a 2040 Energy Outlook, ExxonMobil expects a 150% growth in nuclear and natural gas power generation for non-OECD countries (Skea, 2018). Renewable energy (wind and solar) will also increase but, according to Skea, it will not dominate the energy market and the EIA seems to agree. In addition, the current trend in electrification will increase demand for electricity specifically (Skea, 2018). These forecasts for energy consumption highly intensify the problems coming already from the energy transition in itself, as the world requires a rapid and efficient one. In addition, given the natural physical allocation of resources around the globe, the energy sector has developed to become highly interconnected and energy dependent, putting stress into political relationships with other nations to protect energy supply within borders (see Figure 1).

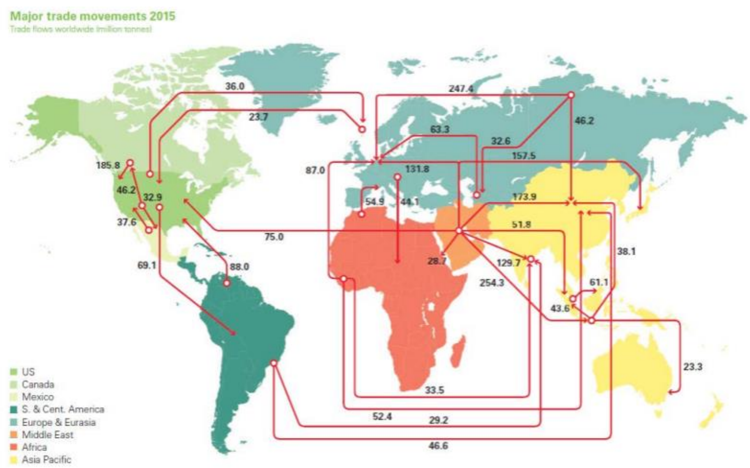

Figure 1. Major trade movements of 2015 *(Skea, 2018)*

In broad terms, this leads to the need for a transition from the centralized paradigm to more distributed models, and to minimize energy peaks and ensure peak demand is met. Despite their intermittent configuration according to the available source, local renewable energy is being encouraged with greater intensity despite the high initial costs.

2.3.3 Energy Costs of Renewable Deployment

The world is currently experiencing an energy transition. Pearson identifies the following parameters which are inevitably involved in any transition: (1) the use of resources and their impact on the environment, (2) fuels and energy conversion technologies, (3) infrastructure and transport networks, (4) institutions and market participants, (5) policy instruments and their regimes, (6) economic, social and cultural variables, (7) and people's behaviour, lifestyles and health (Pearson, 2018).

Transiting from a status-quo scenario towards a less-established and more unpredictable set-up comes with its uncertainties, risks and, ultimately, higher costs. However, as the technologies gains more and more recognition and market share, technology costs are driven down. The Levelized Cost of Energy (LCOE) is a measure used to compare how much it costs to produce one unit of energy, expressed in real currency value to remove the effect of inflation. As shown in Graph 4, the LCOE is presented in a range. For solar photovoltaic (PV), the LCOE would depend on solar irradiance and the technology's efficiency.

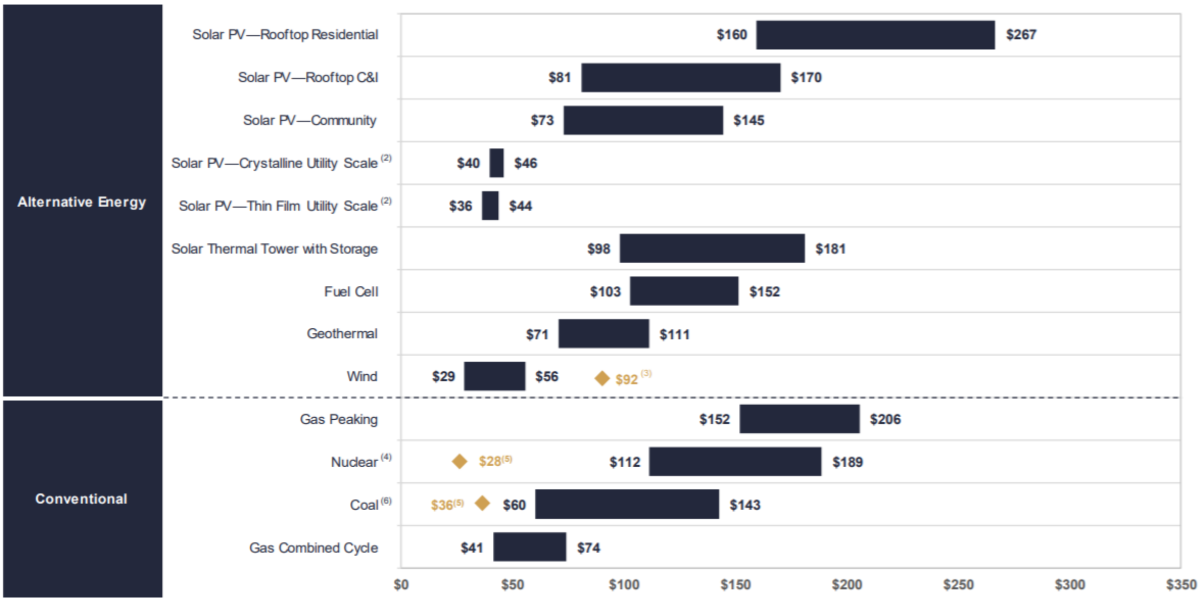

Graph 4. LCOE per MWh of different energy conversion technologies *(Lazard, 2018)*

According to Fraunhofer Institute for Solar Energy Systems' report, PV systems are experiencing a decreasing trend in LCOE for all its technology types including (Kost, et al., 2018). This decline in renewable LCOE, particularly in wind and solar, leads to a reduction in renewable energy prices represented in Graph 5. For instance, the last auction for wind in the UK cleared at £74.50 and £57.50/MWh which are record low-prices for the wind industry and talks are already being broadcasted about a subsidy-free deployment of offshore wind in the 2020s.

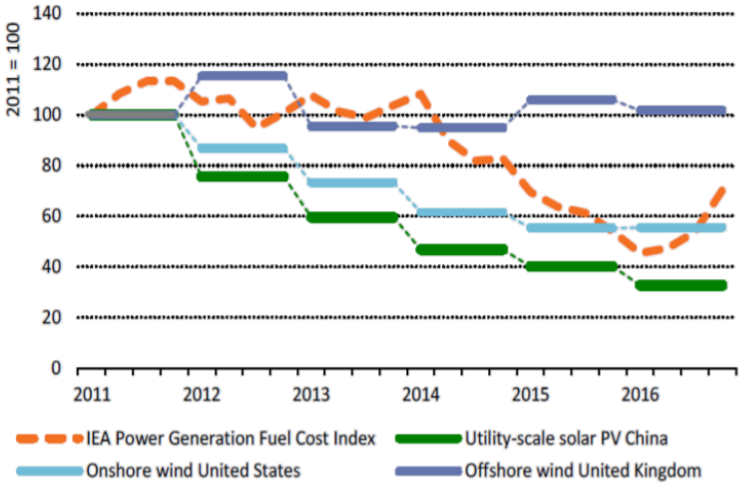

Graph 5. Renewable energy prices are falling *(Skea, 2018)*

Specific to solar PV, Graph 6 shows how the cost of manufacturing a photovoltaic module has been decreasing over time. Swanson's Law portrays the learning curve profile for PV cells in terms of cost performance and installed capacity or shipments (Partain, et al., 2016). It is named after the founder of SunPower Corporation, Richard Swanson, who observed that PV price falls by about 20% as capacity doubles (Motyka & Sanborn, 2015). Nelson believes that the drop in PV price is driven by (1) R&D to reduce the cost of PV capacity, (2) as well as regulation, policy and consequent investment to drive the learning curve by actual deployment (Nelson, 2018).

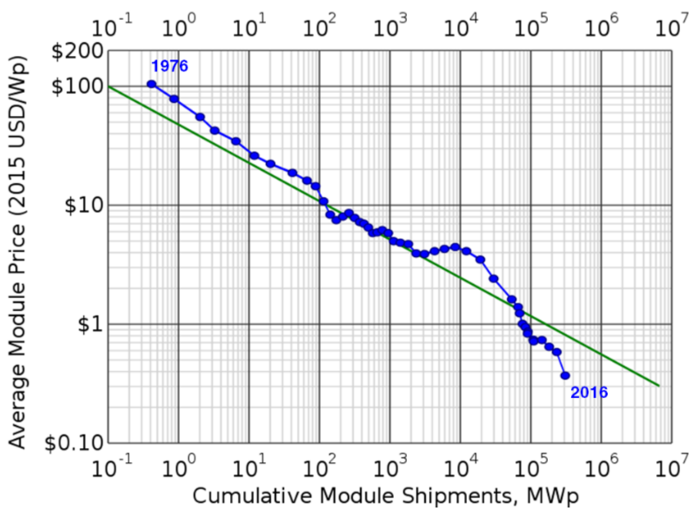

Graph 6. Swanson's Law PV module cost learning curve *(Nelson, 2018)*

Nevertheless, PV solar modules remain expensive and usually require subsidies. The cost of the PV module is about 33-50% of the total capital cost of the system (IRENA, 2012). Table 2 provides average PV costs for the UK. Financial pay back depends on solar irradiance, the technology efficiency and regional electricity prices, amongst other factors.

Table 2. Average PV costs in the UK *(Evergreen Energy, 2017)*

Size of Solar Installation	**Approximate cost**	**Approximate annual output (kWh)**	**Annual system benefit** (savings and FiTs)
2 kW	£3,400	1,700	£167.03
2.5 kW	£4,250	2,125	£199.33
3 kW	£5,100	2,550	£239.20
3.5 kW	£5,950	2,975	£292.30
4 kW	£6,800	3,400	£334.05

2.3.4 Stand-Alone Solar Photovoltaic Farms

The radiant power on Earth from the Sun is about 100,000 TW. To put this in perspective, the global electricity consumption is of about 2 TW, out of which about 80% are covered from fossil fuels and nuclear power. Less than 2% of electricity production comes from solar photovoltaics (Nelson, 2018). This is changing. Solar photovoltaics are gaining a lot of transaction as technology benefits are more and more recognized. Large-scale solar farms are seeing a tremendous growth globally given the high pressures to reduce the environmental impact for energy generation, as well as the readily-available solar resource in many parts of the world. Over the years, the solar PV market has increased, predominantly in Europe and China (Graph 7). India and China alone have 100 GW plans of solar deployment for the next 3 years (Farrokhfal, et al., 2015). In 2018, the European Commission lifted tariffs no Chinese-imported solar panels and this is expected to drive the costs of solar panels down by 30% in Europe (PV Europe, 2019).

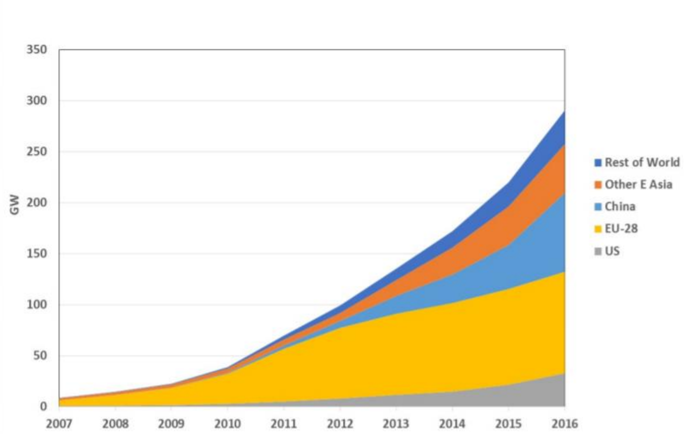

Graph 7. Global solar PV *(Skea, 2018)*

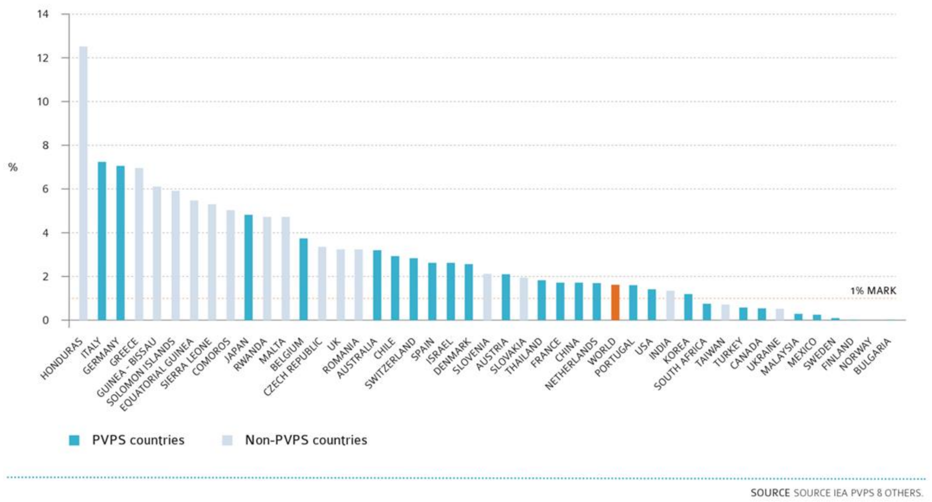

Graph 8. PV contribution to the electricity demand in 2016 *(Nelson, 2018)*

Solar PV's efficiency and investment validation is not the same for every country in the world. Electricity production is very much dependent on the geographical solar irradiance and the number of sun-hours as shown in Graph 9.

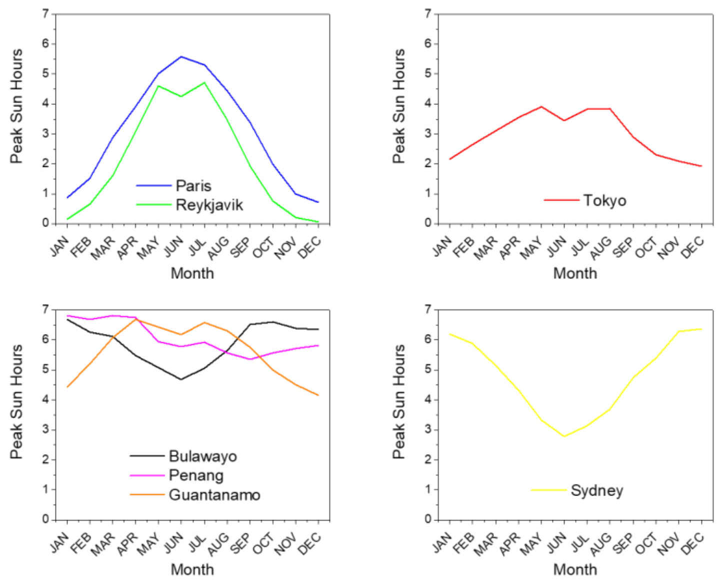

Graph 9. Example of peak sun-hours in different countries *(Nelson, 2018)*

Technical Definition

Solar farms are large-scale application of solar panels made up of photovoltaic modules that capture photon energy from the Sun and convert it into low-carbon electrical energy. This is done by exciting electrons into high energy states with incoming photons through semiconducting materials. Specifically, it relies on the solar photon flux density (Nelson, 2018).

According to Nelson, solar energy conversion to electricity requires (1) photon absorption across an energy band gap through a semiconducting material, (2) physical separation of photogenerated charges, (3) and asymmetric cell contacts through a p-n or n-p junction connected to an external circuit. The power conversion efficiency for the best single-junction solar cells stand at 26.7% (Nelson, 2018) and for perovskite cell it stands at 20.9% efficiency, the latter developed by Dr Jizhong Yao from Imperial College London and CEO of Microquanta Semiconductor (Peleg, 2018).

Solar photovoltaics don't have moving parts and consist of (1) the panel with PV modules, (2) a mounting frame, (3) electric cabling, (4) and inverters to convert Direct Current (DC) to Alternating Current (AC) to be used in the grid or on onsite applications. Additional features the optimize solar capture are the sun trackers, isolators and metering kits (Burke, 2015). To maximize energy output at different conditions, Badejani et al. propose a voltage-based maximum power point unit (Badejani, et al., 2007).

At current technology stage, the average lifespan of photovoltaic cells stands at 30 to 40 years before replacement, but conversion efficiency reduces by-0.5% per year after 25 years. Inverters converting DC to AC power generally need replacement after 15 years (Park Insurance, 2019).

Land Space

Solar farms can be designed according to power output targets, and consequently the area used for solar PV arrays can vary greatly from 1 to 100 acres, typically in rural areas (Burke, 2015). According to Park Insurance estimates, for the UK and its insulation profile it would take about 25 acres (0.1 km^2) to generate 5 MW of power output (Park Insurance, 2019). Solar PV farms can be categorized in different ways; one of them is whether they are on-grid (grid-connected systems) or off-grid (stand-alone systems) from the national or regional grid (Burke, 2015).

To define the system, it is important to identify (1) latitude, (2) annual mean of daily sun angle, (3) average power produced per PV area, (4) wind speed mean and (5) the average variation in wind direction (Badejani, et al., 2007). From there, the technical requirements can be specified to meet the load required.

Planning

Rigorous planning and approval frameworks are usually in place for large-scale solar PV implementation given the use of space and the opportunity cost of the project (Burke, 2015). Approval from the local planning authority and environmental agencies is key before developing a solar farm in rural areas. The Building Research Establishment (BRE) provides a good practice guide for solar farm developers with regards to solar development (BRE, 2014), community engagement (Waters, et al., 2015), biodiversity (Parker & Greene, 2014) and agriculture (Scurlock, 2014).

Once approved, to finance a PV farm can (1) either gather the necessary funds to finance the whole project, (2) or bring together a cooperative team of stakeholders who will benefit from the benefits of the implementation (Park Insurance, 2019). As renewable energy grows, incentives for developers in the field have increasingly been reducing. In the UK, Renewable Obligation (RO) subsidies were removed for 5 MW farms or above (Burke, 2015) and in April 2019, the feed-in-tariffs (FiTs) scheme was revoked as well (Shrestha, 2019).

To implement a solar farm, it is key to examine the (1) solar resource (radiation) available in the selected location and its variability (daily, seasonal, etc.), (2) the topography of the region and orientation of the solar panels, (3) as well as the proximity to grid infrastructure if the site online (Park Insurance, 2019).

Environmental Impact

Apart from generating energy from a renewable source, in a 2015 UK House of Commons briefing paper Burke states that the physical mounting of PV arrays was reported by Bumblebee Conversation Trust (BBCT) to have positive effects on the land by creating microhabitats and small ecosystems. This in turn boosts the value of the land for future agricultural purposes (Burke, 2015). However, overall environmental and wildlife impacts mainly depend the location and the president of National Centre for Space Studies (CNES) presaged that the large-scale implementation of solar PV could be damaging to the biosphere (Palz, 2011).

2.3.5 Solar PV Surplus Generation

Renewable technologies generate electricity whenever the resource is available. As more and more renewable technologies are installed the risk of over-supply increases. Conventional means of energy supply must cover energy demand peaks, independent on the varying weather conditions (wind blowing, solar availability) and varying peak conditions (traffic, 6pm tea time, TV peak). When grid reliability needs to be ensured, the constant conventional and predictable energy supply is not the one that gets stopped when there is over-supply. Energy from renewable sources is. This is referred to as *curtailment*. Curtailment occurs due to: (1) predicted or unpredicted decrease in demand, (2) decrease in price of other less environmentally-friendly technologies or their fuels, (3) over-supply of resource, (4) unavailability of energy storage systems. To understand the curtailment phenomenon, it is interesting to look at the state of California.

California has expanded 1,02 GW from 2016 to 2017 (Nyberg, 2018).. In April 2017, 64% of electricity load was supplied from solar and wind sources (CAISO, 2016). "*The growth in these preferred resources is nothing short of phenomenal"*, California's ISO declared in 2017. But they also predicted 6-8 GW of solar PV curtailment in 2017. In 2016, 8.5% of the day's output was curtailed from large-scale solar farms, mainly to reduce congestion and system-level reliability issues (Paulos, 2017).

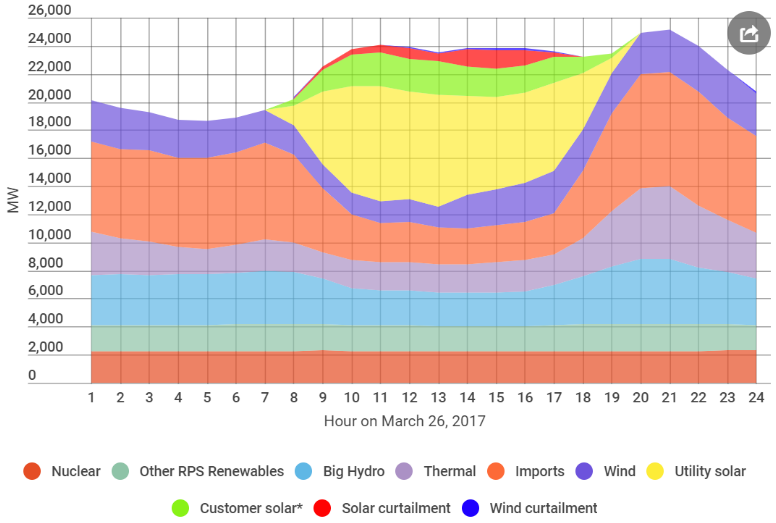

Graph 10. Solar and wind curtailment in California *(Paulos, 2017)*

California's ISO identifies three types of curtailment: (1) economic dispatch, (2) self-scheduled cut, (3) and exceptional dispatch; where economic dispatch is the most predominant. As observed in Graph 11, it is not seasonally constant. The winter months of 2016 have a lower curtailment rate than winter months of 2017, for instance. Therefore, it is something very difficult to predict. Based on data for California, solar PV suffers more economic curtailment than wind (Graph 12).

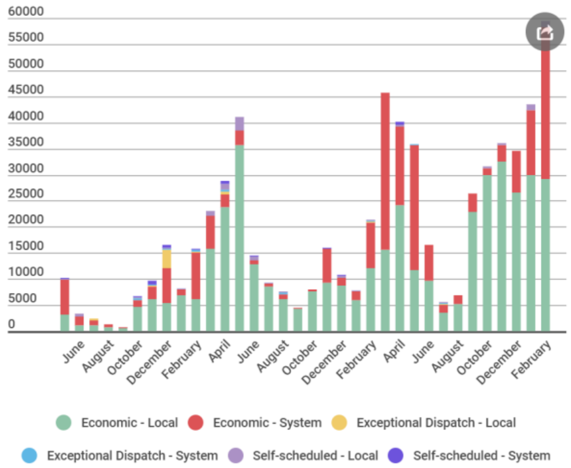

Graph 11. Types of curtailment for California's state *(Paulos, 2017)*

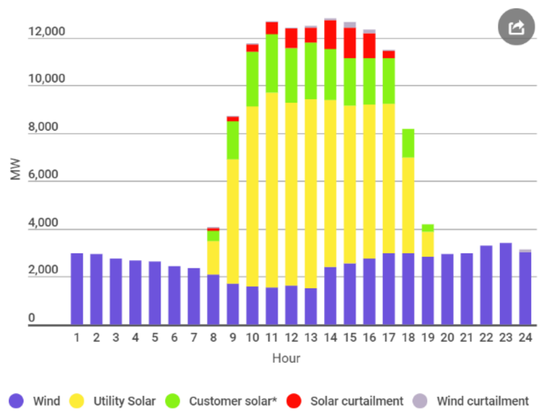

Graph 12. On March 26th, 2017, solar PV experienced more curtailment than wind in the state of California *(Paulos, 2017)*

Similarly to Graph 10, Graph 13 portrays what is commonly known as the *duck curve*. It represents the electricity demand peaks and off-peaks throughout the day. The duck's tail starts at a 04:00-06:00 am, followed by a downward movement until 03:00 pm and then by a very steep increase which reaches a peak at around 06:00 pm, reaching the duck's head. Given the solar hours during the day, solar energy is precisely harnessed when the electricity demand is not as demanded. Consequently, this idea leads on to a high risk of over-supply of solar energy during the middle of the day (CAISO, 2016). However, this profile might not be the same for summer as the peak air conditioning demand rises during the through of the curve.

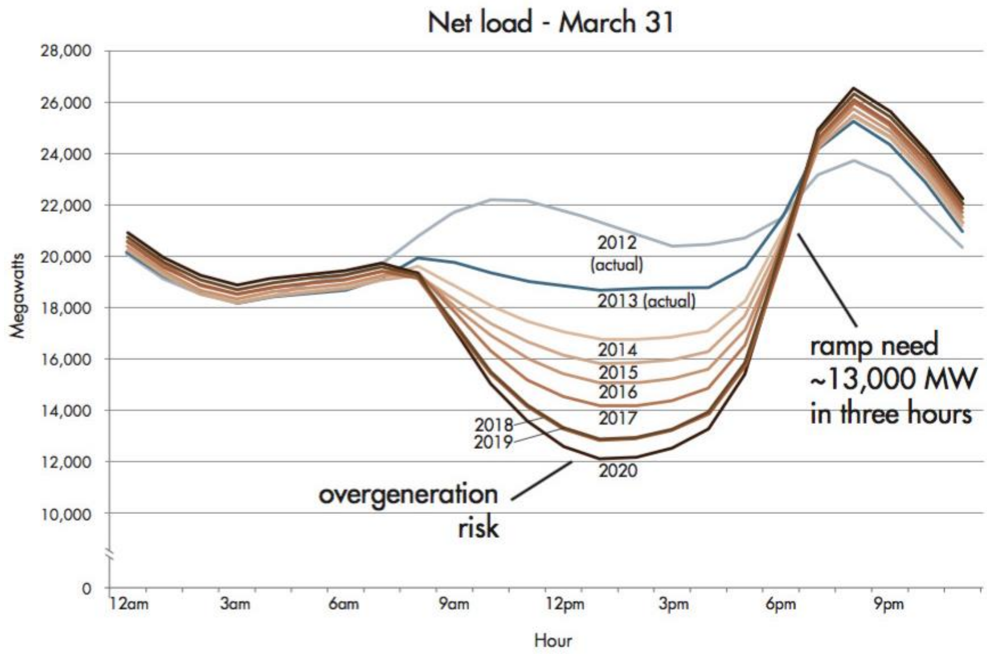

Graph 13. The duck curve shows steep ramp requirements and overgeneration risk *(CAISO, 2016)*

The National Renewable Energy Laboratory (NREL) with assistance of the US Department of Energy (DOE) provide an analysis of the US' curtailment tendencies in different states with regards to both wind and solar generation (Bird, et al., 2014). According to Schermeyer et al., Germany curtailed 4.7 TWh of distributed generation from renewable energy in 2015 – equivalent to 478 million euros of compensation. They suggest the amount of curtailment will increase and, with it, compensation for renewable energy generation readiness (Schermeyer, et al., 2018).

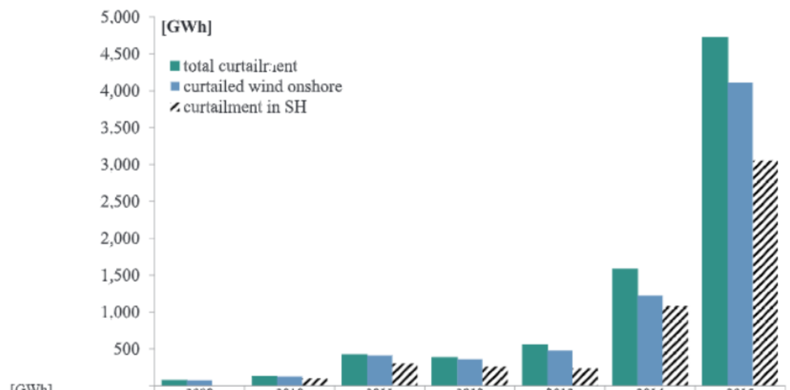

[GWh]	2009	2010	2011	2012	2013	2014	2015
total curtailment	74	127	421	385	555	1,581	4,722
curtailed wind onshore	73	125	410	358	480	1,221	4,110
curtailment in SH		100	308	262	239	1,092	3,055

Graph 14. Curtailment in Germany from renewable energy resources *(Schermeyer, et al., 2018)*

2.4 Energy Storage

2.4.1 Intermittency of Renewables Technologies

92.8% of Uruguay's electricity consumption is provided form renewable energy (UTE, 2018), whilst for Costa Rica, the figure rises up to 95% (Climate Council, 2019). In 2016, Portugal produced its electricity demand from renewable sources alone for four days (Lewis, 2016). Whilst we are seeing great improvements in the renewable energy sector for countries who have an abundance of renewable resources, not every country is like that. Additionally, over 40% of the renewable energy electricity supply for these countries is provided from stable and predictable hydropower capacity.

In particular for renewable technologies that are meant for distributed systems – such as solar and wind – their most contested drawback is their intermittency and unpredictability (daily, monthly, seasonal or yearly). This stands as one of the main stoppers to full national dependency on renewable energy, as the sun doesn't always shine, and the wind doesn't always blow. It also affects stability at grid-scale and large-scale power systems (Kim & Chang, 2014). Graph 15 portrays an example of the hours of sunlight at which photons can be captured, and the hours at which wind blew in a specific location. It is plotted against the energy use of the day.

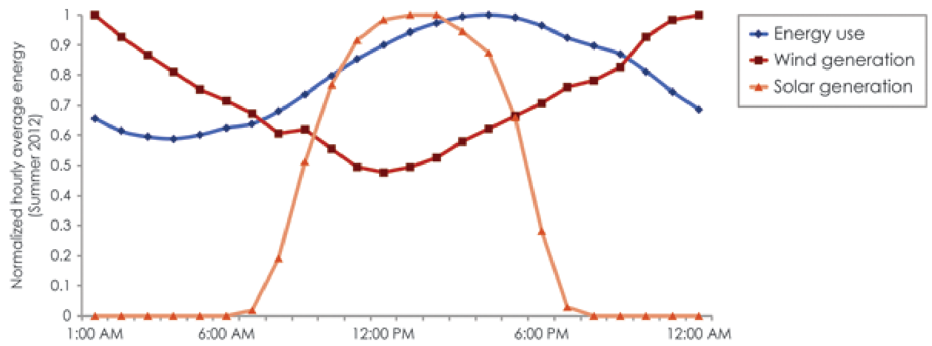

Graph 15. Example of resource variability over the day against energy use *(Clayton, et al., 2018)*

Given the lack of renewable resource control, the need for established energy storage technologies arise. These propose a model whereby energy can be stored through different technologies (mechanical, electrical, chemical, electromagnetic, etc.) which act as buffers to collect energy from the resource when there it exists and consume it at the time it is demanded. Currently, the global capacity of power storage is 176 GW (2017), less than 2% of global power production capacity (Center for Climate and Energy Solutions, n.d.). Graph 16 portrays the gap difference in the US of large-scale battery storage against the planned power capacity in the US.

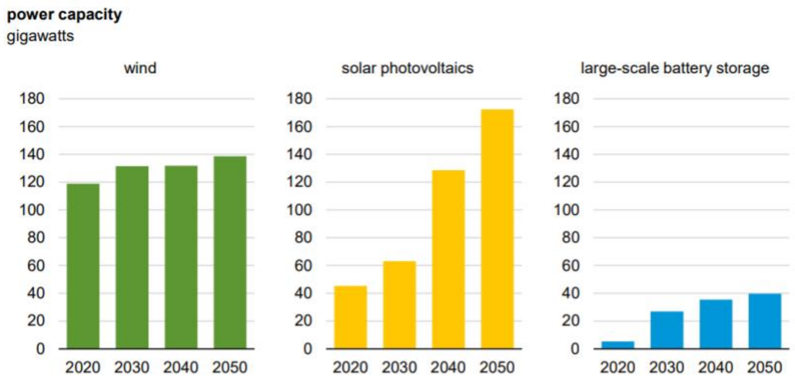

Graph 16. US large-scale wind, solar, and battery storage capacity projections *(EIA, 2018)*

2.4.2 Electrical Energy Storage Technologies

Electrical Energy Storage (EES) technologies, such as batteries and supercapacitors, can store the electrical energy which has already gone through a process of conversion from the resource to the electrons. Batteries for instance, store electricity in DC which is at which the electricity is generated, and which will later need to be converted to AC for grid purposes and household uses (SolarChoice, 2019).

EES can alleviate the mismatch between supply and demand without the need to increase electricity generation (Kim & Chang, 2014), whilst providing stability for the grid. Nonetheless, it can also be a strategic asset towards maximizing profits for renewable energy generators. With regards to solar energy, electricity harnessed during sun hours, excess energy be stored and sold at electricity demand peak-times where the electricity is more expensive and where the payment for electricity supply would be higher. The architecture of an EES is provided in Figure 2.

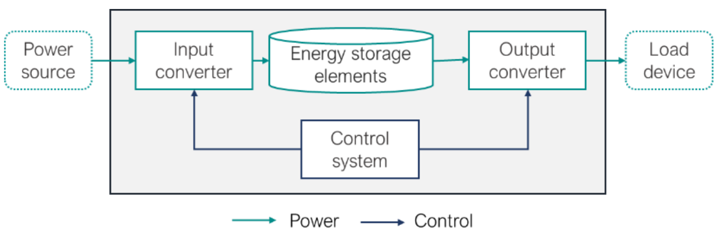

Figure 2. EES system architecture *(Kim & Chang, 2014)*

Electrical Energy Storage Technology Comparison

Kim & Chang identify the following favourable characteristics for EES assets:

Table 3. Desirable characteristics for EES *(Kim & Chang, 2014)*

Characteristic	Desirability	Description
Cycle efficiency	High	Ratio of energy output at discharge over energy input at charging cycle
Cycle life	Long	Maximum number of charging or discharging cycles before the capacity drops below a set percentage, and the battery needs to be replaced
Self-discharge rate	Low	Speed at which energy is lost even if under no load
Energy density	High	Maximum energy storage per volume (m^3) or weight (kg)
Power density	High	Maximum power rating per volume (m^3) or weight (kg)
Capital cost	Low	Cost per unit energy (kWh) or unit power (kW)

For each, Kim & Chang have also been able to gather their key characteristics for some representative EES technologies. As provided in Table 4, it can be observed the supercapacitors have a very good power density (W/kg) and cycle efficiency, but its self-discharge rate is very high and energy density very low. Lithium ion (Li-ion) batteries have high power and energy density and a good self-discharge rate, whilst maintaining a high cycle efficiency. Meanwhile, metal-air batteries have irrefutable high energy density but suffer in cycle efficiency.

Table 4. EES technologies comparison *(Kim & Chang, 2014)*

EES Technology	Power density W/kg	Energy density Wh/kg	Capital cost $/kWh	Cycle efficiency %	Cycle life	Self-discharge per day
Lead-acid battery	180	30 – 40	74 – 222	70 – 90	500 – 800	0.1 – 0.3
Li-ion battery	1,800	150 – 250	1,040 – 1,484	80 – 90	1,200	0.1 – 0.3
NiMH battery	250 – 1,000	30 – 80	450 – 1,000	66	500 – 1,000	2
NiCd battery	150	40 – 60	296 – 890	70 – 90	1,500	0.2 – 0.6
Metal-air battery	-	450 – 650	74 – 296	< 50	100+	Very small
Super capacitor	1,000 – 2,000	2.5 – 15	2,000	> 93	100,000+	20 – 40

Lithium-Ion Energy Storage

The most common EES technology is the Lithium-ion battery which began getting technology traction in the 1990s and are now considered to be one of the most advanced options in the energy storage market (Deng, 2015). Its upsurge is intensified for its use in electric-powered vehicles (Graph 17).

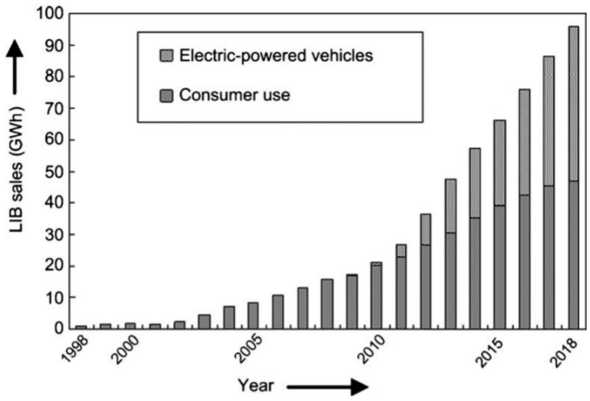

Graph 17. Demand for Li-ion batteries until 2015 *(Deng, 2015)*

As indicated in Table 4, it is characterized for high power, low discharging rate and high charging rate, long life and high capacity (Deng, 2015). This is due to its position in the periodic table, being a light and highly electropositive atom (Schlogl, 2013).

In this type of battery, Li-ion cells can be arranged (1) in parallel to enhance the current, (2) in series to increase the voltage, (3) or in a hybrid configuration. The cells are configurated in modules and packs. For instance, Tesla cars model S and X have 7,104 Panasonic 18650 battery cells in 16,444 modules with a storage capacity of 85 kWh (Pressman, 2017).

A Li-ion cell consists of a cathode, a Li-ion electrolyte and an anode. A microporous polymer membrane is typically used to separate the electrodes, allowing ions to move between the electrodes but inhibiting the electrons from moving across the separator (Deng, 2015). The cell is represented in Figure 3 according to its charging and discharging states.

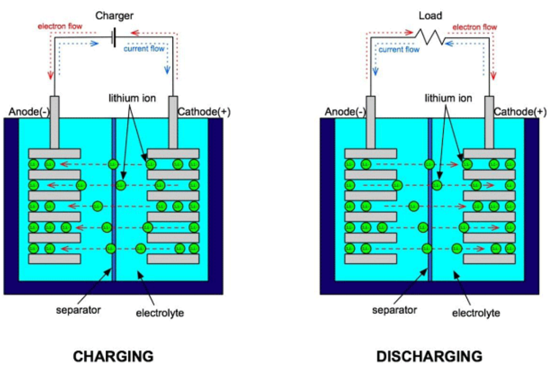

Figure 3. Charging and discharging of a Li-ion battery *(The Electric Energy, n.d.)*

2.4.3 Energy Storage Costs

The cost of Li-ion batteries per stored energy ($/kWh) remains high, but it has decreased since the 1990s. Battery costs depend on technology characteristics such as power and energy capacity (EIA, 2018). Back in 2014, the mean retail price stood at 0.1 $/kWh according to the EIA and battery packs for electric vehicles cost $600/kWh. Deng estimated that this could be reduced to $200/kWh by 2020 (Deng, 2015). Currently, Tesla Model 3 and General Motors 2017 Chevrolet Bolt's battery packs are valued at 190 and 205 $/kWh, respectively (UCS, 2018). That is a 67% decrease in battery packs for vehicles in just 4 years. However, batteries need to be replaced every 4-10 years according to technology charging/discharging cycles, efficiency and use and this increases the investment required for battery storage use. Bloomberg New Energy Finance offers the battery pack price reduction as shown in Graph 18. They forecast a continuous fall in the battery pack to fall to $94/kWh by 2024 and $62/kWh by 2030 (Goldie-Scot, 2019). However, the availability of resources also has an impact on technology. Goldie-Scot presents the argument of increased battery costs if Lithium price increases but believes the effect will not be as impactful on the technology (Goldie-Scot, 2019).

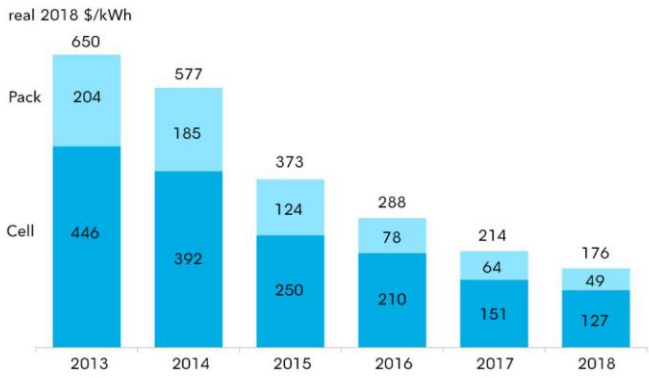

Graph 18. Li-ion battery pack price per unit energy stored with pack-cell cost split *(Goldie-Scot, 2019)*

The EIA has released a report on the US battery market trends for large-scale energy storage, where battery costs are analysed based on the nameplate duration (EIA, 2018), as described below. The nameplate duration is defined as the energy capacity over power capacity (Marcy & Fields, 2018).

Table 5. Nameplate duration as described in EIA report for battery cost assessment *(EIA, 2018)*

Nameplate Duration	Value
Short-term duration	Systems with < 0.5 hours in nameplate duration
Medium-term duration	Systems with 0.5 – 2 hours in nameplate duration
Long-term duration	Systems with > 2 hours in nameplate duration

According to the EIA's report for large-scale storage, battery costs for short-duration are less expensive than medium and long-duration per unit power capacity ($/kW). Conversely for unit energy capacity ($/kWh) the long-duration batteries will be cheaper than short-duration as energy costs are spread out, as shown in Graph 19.

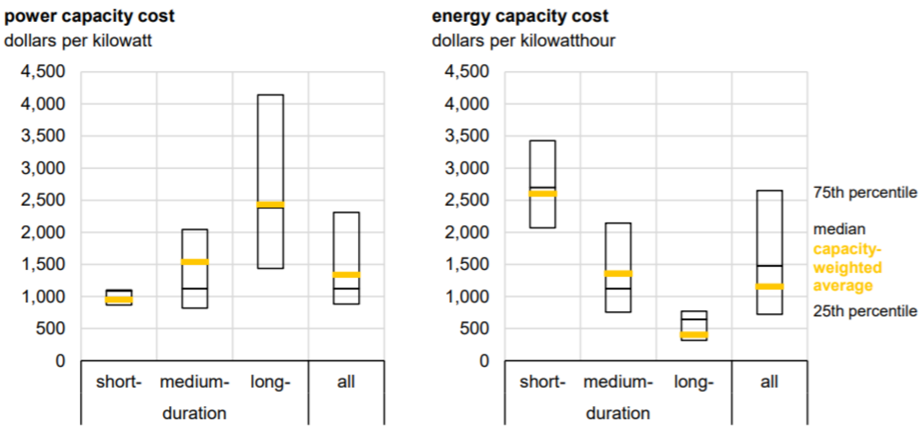

Graph 19. Total installed cost of large-scale battery storage by duration *(EIA, 2018)*

2.4.4 Energy Storage Replacement Costs

Additionally, batteries need to be replaced according to its technical characteristics, efficiency and usage profile (charging and discharging). According to Zakeri and Syri, replacement costs for batteries range from $185 to $550 per MWh. They point out that the replacement time needs to be taken into account for projects with long duration. For Lithium-ion batteries with 365–500 cycles per year, batteries should be replaced every 5 years (Zakeri & Syri, 2015).

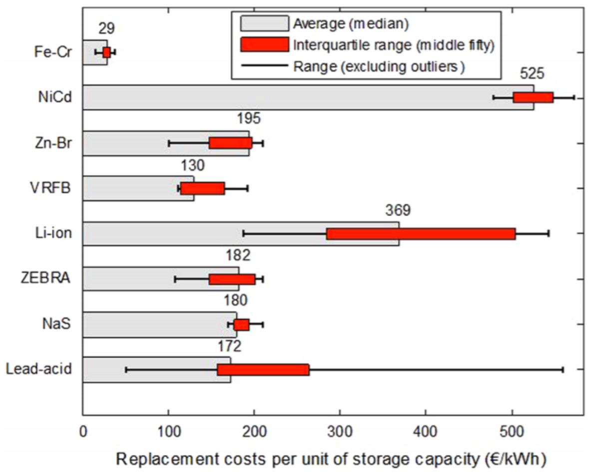

Graph 20. Replacement costs per unit of stored energy (Zakeri & Syri, 2015)

2.5 Crypto-Mining Energy Consumption

2.5.1 Blockchain & Bitcoin

The blockchain is regarded the digital revolution of the 21st century in the chronology of computing development and it is often referred to as the second era of the internet (Tapscott, 2016). Whilst, the Internet in itself became a platform of information or data exchange from which value can be extracted, the main hypothesis for blockchain is that it is a medium through which real value and assets are directly exchanged without the need of an intermediary governing and controlling the exchange parameters or making profit from the exchange. In this unrestrained and objective setting, the blockchain cryptographically registers and validates transactions permanently and immutably, allowing users to be in control of their transactions in a traceable manner. Blockchain 1.0 refers to the issuance and trade of cryptocurrencies, whereas Blockchain 2.0 denotes the use of blockchain for smart contracts and Blockchain 3.0 alludes to smart contracts and transaction dynamics which attain a much higher level of autonomy within the network (Brilliantova & Thurner, 2018).

This paper will provide a brief overview of Bitcoin, the first conceptualization of the blockchain in the fintech realm. It is worth noting however, that there are contrarian arguments with regards to the “storage of value” definition for Bitcoin given that its instability causes it to become more of a speculative investment instead (Seibert, 2019).

Bitcoin was launched in 2008 by Satoshi Nakamoto, the pseudonymous creator of the blockchain, to eliminate the unnecessary mediation costs and time from banks and other financial institutions currently managing day-to-day transactions (Nakamoto, 2008). The Bitcoin network is a “*randomly connected overlay network of a few thousand nodes, controlled by a variety of owners*” (Wattenhofer, 2016). It is a homogeneous network, without a pivotal jurisdiction; and it is a global network which only requires access to Wi-Fi. It works under the concept of *state replication* whereby all partaking actors in a distributed system play under the same network rules and command sequences (Wattenhofer, 2016).

The popularity of Bitcoin has grown ever since Nakamoto’s whitepaper was released, although not always reflected in the Bitcoin price fluctuations (Graph 21). Early January 2017, Bitcoin reached a total value of $16 billion with 16 million bitcoins in circulation (Vranken, 2017) and by the end of the same year a bitcoin was priced at $20,000, an increase of 1,700% (Andoni, et al., 2018). Intentionally or unintentionally, Bitcoin’s vogue has opened the door to many other blockchain implementations in a plethora of applications, albeit not always suitable for blockchain technology. Blockchain has remarkable potential in solving security issues as the world becomes more and more connected through the Internet of Things, for instance (Khan & Salah, 2018).

Aggregating all bitcoins, the current global value and volume stand at $157.7 billion and $8.9 billion/day, respectively (Li, et al., 2018). The number of nodes in the Bitcoin network has been estimated from the number of open ports (Bitnodes, 2019) which are key to validate the Bitcoin network and to play by the rules. Based on this estimation, as of the 1st of April 2019, the United States owns 24.84% of public nodes, followed by Germany (18.41%) and France (6.28%) (Figure 4). However, it is very difficult to know the exact number of full nodes available in the network.

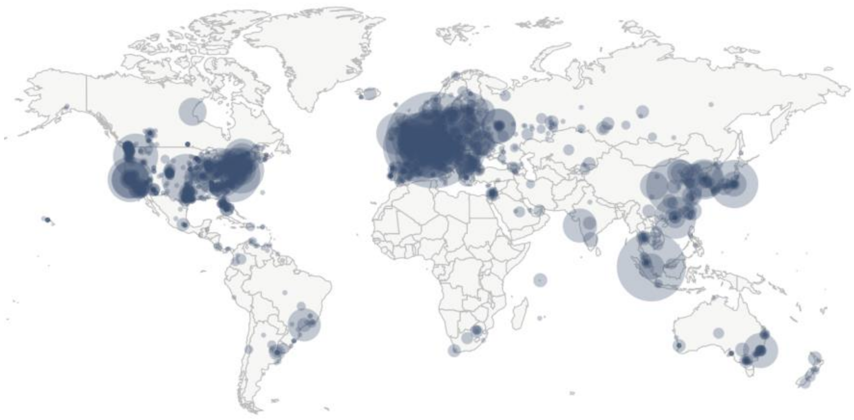

Figure 4. Global distribution of nodes in the Bitcoin network as of April 1, 2019 *(Bitnodes, 2019)*

This network trades transactions between nodes through a digital token, namely the bitcoin. A bitcoin is a cryptocurrency that is transferred through this peer-to-peer network without the need of a regulatory or intermediary political power, such as a bank or another financial arbiter (Shi, 2016). Each transaction performed in the network is gathered into blocks which must be verified through a consensus mechanism (Chapter 2.5.3) by all the nodes in the network. This has been designed intentionally so that the network can be sustained and protected from attackers and manipulation. Once validated, the block is added to every component in the network (Narayanan et al. 2016), thus creating a *distributed ledger* system. Every node has a local replica of the network at that point in time. Since its launch, Bitcoin has had its ups and downs, reaching a peak in 2017 (Graph 21).

Graph 21. Bitcoin price extracted on the 23rd of July 2019 *(CoinMarketCap, n.d.)*

2.5.2 Reward Transaction

The number of transactions in each block depends on the time taken to put a transaction in the block and the time taken to reach a consensus (Blockgeeks, 2018). The number of transactions for Bitcoin stands at roughly 7 transactions per second so, theoretically, about 4,200 transactions are validated in one block.

In the set of transactions contained in a block, the first one is referred to as the *reward transaction*, directed towards the block miner as the recipient, who is rewarded, not according to time or energy consumed, but based on block release. The number of bitcoins in the reward transaction depends on a fixed value – so that the increase in demand does not increase the supply which is set at 21 million bitcoins (Hayes, 2018) – and on transaction fees from the transactions included in the block.

The fixed value reward was initially set at 50 BTC but follows a halving reward scheme which is part of the protocol (Chapter 0). The reward transaction value should be close to the amount of energy and capital costs (hardware) invested in mining the block (Wattenhofer, 2016). As more transactions are carried out, more power is required and there are greater transaction fees.

2.5.3 Consensus Mechanism using Proof-of-Work

In the absence of an authoritative unit (permissionless setup), a consensus mechanism is used in distributed systems to attain the necessary agreement within that system or network to validate its current state and transaction order. It is the underlying framework through which the structure of the blockchain is created from the genesis block (first block in the blockchain) to the lead (block with the latest transactions) (Andoni, et al., 2018).

There are several types of distributed consensus algorithms for blockchain networks, out of which the present study will give an emphasis on Bitcoin's Proof-of-Work (PoW) mechanism. The consensus model is key in ensuring that coins are only spent once, thus avoiding double-spending, and they are established by game-theoretic rewards to miners. A consensus must satisfy the following properties: (1) agreement for the same transaction value from all partaking nodes, (2) all nodes must have a finite time, (3) and the decided value will be the node's input value for validity (Wattenhofer, 2016).

In order to limit the denial-of-service (DoS) attacks, Bitcoin uses the "Hashcash" Proof-of-Work mechanism (Andoni, et al., 2018). The PoW consensus mechanism requires the mining node to prove that it has put in work to add a block to the blockchain (Baliga, 2017) and is rewarded a bounty – agreed throughout the network – and a transaction fee (Andoni, et al., 2018). The longest chain the blockchain will be the valid blockchain where new blocks are added, as they represent the largest portion of consensus, and therefore, the most validated and secure chain

(Vujičić, et al., 2018). However, the PoW model is vulnerable to the possibility that a mining pool – i.e. joined computing power working towards mining a single block – might control 51% of the mining power (Baliga, 2017).

Dominance, however, is a phenomenon that could theoretically occur in a PoW network by being in control of 51% of its mining power (Baliga, 2017). Therefore, consensus algorithms must be able to deal with malicious nodes and acts within the network. Bohme et al. claim that more than 173 MW of electricity are continuously consumed by PoW calculations and equates this to 20% of a nuclear plant power output (Bohme, et al., 2015). More on energy consumption is discussed in Chapter 2.5.8.

Nevertheless, PoW remains one of the most efficient and secure consensus mechanisms, albeit the most energy consuming. A trade-off presents itself with PoW between energy resources (and waste) and system security. PoW algorithms are known for to be very energy intensive in the validation of transactions and block consolidation; however, they are a critical element in guaranteeing system security in trustless blockchain applications, such as Bitcoin (Andoni, et al., 2018).

2.5.4 Main Technical Concerns about Bitcoin

CAP Theorem

In the late 1990s, Eric Brewer (computer scientist) introduced a trade-off between three important characteristics of a distributed data system, including blockchain networks: consistency, availability and partition tolerance (Figure 5). A distributed system can satisfy only two of these three characteristics. For the left-out property, the *best effort* approach is taken (Gilbert & Lynch, 2012).

- **Consistency:** all network nodes must return the same output with relation to a given input and be in agreement with regards to the current state of the network or system (Gilbert & Lynch, 2012).
- **Availability:** the network or system is fully operational and can process incoming requests (Gilbert & Lynch, 2012)
- **Partition tolerance:** when facing network partition (i.e. physical disconnection, software errors, incompatible protocol errors) the distribution system should be able to continue operating with partitions amongst nodes (Wattenhofer, 2016)

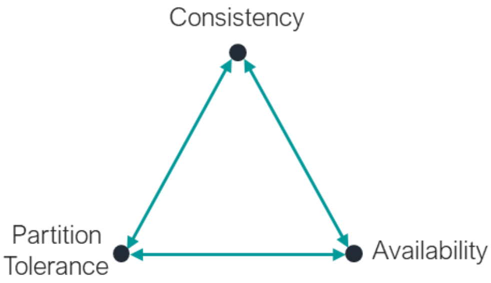

Figure 5. CAP Theorem trilemma for distributed systems *(Wattenhofer, 2016)*

For the blockchain space and for most distributed systems, partition tolerance is a go-to metric to ensure. Therefore, if *availability* is picked over *consistency*, there will always be a response from the network, but data may not be up-to-date (Arvind, et al., 2018). In the scope of Bitcoin, a financial and monetary blockchain, updated data is of high importance. However, blockchain is an example of *Availability-Partition Tolerance* with best-effort or eventual *Consistency*, given that all the nodes provide a good performance with regards to consistency as they all see the same register (Bahga & Madisetti, 2016).

Bitcoin Scaling

The increased popularity discussed above (and represented in Figure 6) has raised the concern of scalability as a primary issue.

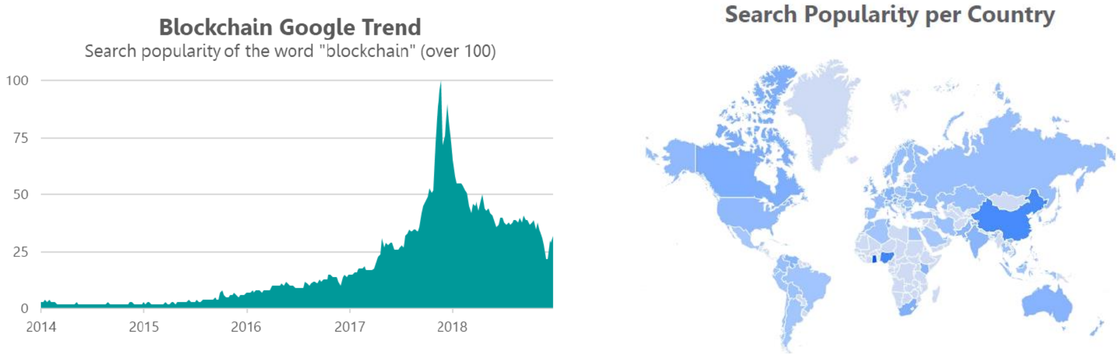

Figure 6. Blockchain awareness and popularity on Google search and per country *(Google, n.d.)*

More transactions to be validated put pressure on the block limit of 1MB and the established block frequency of 10 minutes (Croman, et al., 2016). The number of transactions depends on (1) the time to add a transaction on a block, (2) and the time to reach consensus, a process that occurs linearly (Blockgeeks, 2018).

Scaling is a real issue for Bitcoin. Whilst Bitcoin's network bandwidth does not go over 7 transaction/second (t/s), Ethereum process 20 t/s, Litecoin 56 t/s, PayPal 193 t/s, Ripple 1,500 t/s and VISA 24,000 t/s. A new platform, namely Credits, has been able to process 488,403 t/s at peak load (Credits Blockchain, 2018). The slow transaction time began grabbing people's attention when users reported in May 2017 that they had to wait for 4 days for transaction confirmation. To make it faster one could pay higher transaction fees, but this made no sense in some cases. As Coin Telegraph reports, a $3 coffee could have transaction fees of the equivalent to $15 (Coin Telegraph, n.d.).

As the network expands, there are some solutions that are studied or have been implemented. Segregated Witness or Segwit2x (exclusive to Bitcoin) is a parallel chain, or *off-chain data storage*, that stores signature data in Merkle tree arrangements, as 65% of data in a transaction is signature data. This (1) reduces the size of each individual transaction, (2) thus increasing the number of transactions that can be included in a block, (3) decreases the transaction fees, (4) makes block confirmation time shorter, (5) and resolves the quadratic hashing problem which would come with block size increase as signature hashing scales quadratically (Blockgeeks, 2018).

Because there is no central regulator who can change the rules and instead the debate is spread across the community, if the community is divided, then so will the outcome. This is what happened with Bitcoin Cash in 2017, Bitcoin's *hard fork.* Developers, such Amaury Séchet, an ex-Facebook developer, who did not agree with off-chain data storage (storing signatures elsewhere) and who believed SegWit was a temporary contrivance, promoted the creation of Bitcoin Cash, a new version of Bitcoin. Glance states "*The argument has not just been about technology. There are ideological and commercial interests driving the various players*" (Glance, 2017). Bitcon Cash has been able to raise the network bandwidth to 61 t/s by increasing the block size eight times (8 MB) and they also made some technical arrangements on the signature handling (Coin Telegraph, n.d.).

Developers and researches are still in the lookout for new frameworks that solve scalability issues in decentralized peer-to-peer networks. Huang et al. describe Aura, a peer-to-peer blockchain technology with "unlimited and sustainability scalability", whereby it claims that with an increase in the number of nodes, the computation capacity increases exponentially (Huang, et al., 2018). The crypto-world remains expectant of future scalability problems in Bitcoin and other altcoins, as well as what new creative solutions the crypto-community will come up with.

2.5.5 Bitcoin Crypto-Mining

There are two main types of nodes in the Bitcoin network: a user node and a miner node. As aforementioned, every node in the network receives a newly validated block approximately every 10 minutes, consolidated into a block by the so-called mining nodes, or miners. Miners are computers in the network that have enough computational resources to validate and generate blocks which are related to complex – and therefore energy intensive – mathematical problems that need to be solved for the transactions to be verified and compiled (Shi, 2016). Since Bitcoin does not require an in-between political power, the block validation and bitcoin issuing must rely on two things: (1) the consensus mechanism discussed above and (2) reward incentive engineering for miners (Shi, 2016), namely the Bitcoin halving reward system which will be discussed in the following chapters (Chapter 0).

Mining is the process performed by miners solving for these algorithms to validate blocks and add them to blockchains in return of transaction fees and the block mining reward, a bounty programmed by the network. In literature, this is referred to as *coinbase transaction*, as portrayed in Figure 7 (Vujičić, et al., 2018). Mining is attractive precisely because of its financial enticements, although this will be further discussed in Chapter 2.5.7. Miners compete for the coinbase transaction by investing computational resource. The probability of winning the mining race for individual miners is usually described as the *contest function* (Dimitri, 2017).

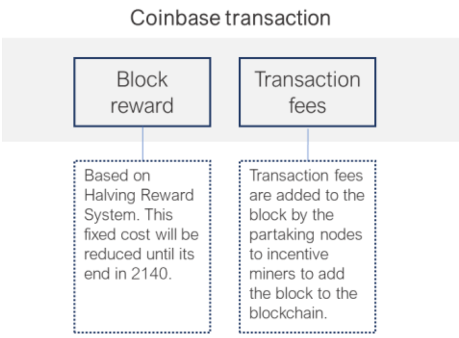

Figure 7. Explanatory diagram of coinbase transaction

However, the more nodes, the slower the network becomes and more computational power it requires. The difficulty in crypto-mining is determined by the increasing time and hash power (computational power) demands given the large node network and the blockchain growth. This intensification shows no sign of abatement as blockchains are created to be more and more complex as they expand. The block generation process through mining is controlled and readjusted via Bitcoin's algorithmic protocol every 2 weeks so that the block validation time remains relatively constant at around 10 minutes (Vujičić, et al., 2018), although block confirmation time varies depending on the network activity and the transaction fees (Andoni, et al., 2019). This is necessary to keep up with the improvements made from mining hardware and its computing power (Vranken, 2017). Some key elements relevant to mining are discussed below.

Bitcoin Halving Reward System

When Bitcoin was launched in 2008, the reward for validating a block was 50 bitcoins (BTC) and designed to be halved every 210,000 blocks (Vujičić, et al., 2018), approximately every 4 years. As of today (28th of March 2019), the coin reward is 12.5 BTC (Bitcoin Block Half, 2019) and will be reduced to 6.25 BTC in approximately one year. Given the bitcoin limited supply of 21 million bitcoins, the halving process will halt when it reaches 1 Satoshi, or 10^{-8} BTC (Vujičić, et al., 2018) which will happen in the year 2140. Miners will still verify blocks but will now rely on transaction fees alone to cover hardware and operational costs (Vranken, 2017).

Hash Rate & Mining Efficiency

The hash rate is the whole network's computing power rate in a second-by-second basis (Li, et al., 2018). For Bitcoin the estimated hash rate is shown in Graph 22.

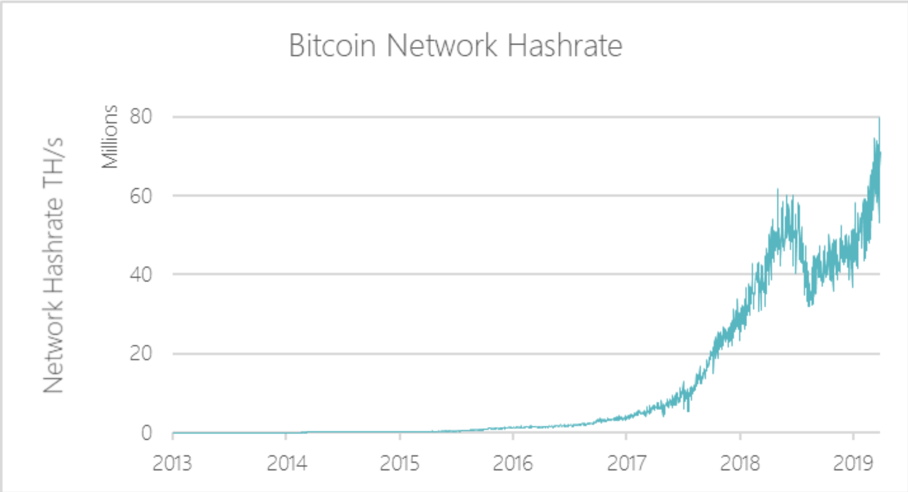

Graph 22. Bitcoin estimated hash rate over time, shown in tera hashes per second

The mining efficiency is obtained by calculating the ratio between the number of hashes per second over the power consumed in the same timescale. The mining performance is assessed by comparing different mining efficiencies for different miners, mainly dependent on their algorithms. Li et al. performed an experiment with nine cryptocurrencies (altcoins) and placed a power meter to analyse the computer power usage, which was the primary source of electricity. For PoW, Li et al. show that mining power and mining hash rate follow a linear relationship (Li, et al., 2018).

2.5.6 Mining Hardware

The Mining Arms Race

In order to solve block algorithms, miners have to invest in computing hardware with sufficient computing power and quality. Mining nodes have been changing throughout according to the power needs of the intensifying algorithms:

Table 6. Hash rate and energy efficiency of first to fourth generation miners *(Vranken, 2017) (Shi, 2016)*

Hardware	Introduction	Hash rate (h/s)	Energy efficiency (h/J)
Central Processing Unit (CPU) in standard computers	2009	10^5 - 10^8	10^4 - 10^5
Graphics Processing Unit (GPU) on display cards	Late 2010	10^6 - 10^9	10^5 - 10^6
Field-Programmable Gate Array (FPGA)	Mid 2011	10^8 - 10^{10}	10^7
Application Specific Integrated Circuits (ASIC)	Early 2013	10^{10} - 10^{13}	10^8 - 10^{10}

Dimitri argues that the decision to mine really depends on the competitors' efficiency for block generation (Dimitri, 2017). Today, ASICs is the most widely used technology as they hold the highest efficiency for hashing computations. They were first launched to the bitcoin mining market by Butterfly Labs, ASICMiner and Avalon (Vranken, 2017). With the high reward bitcoin incentives and the high Bitcoin price of 2017, the mining community raced for the latest and best mining devices in the market. High mining rewards encouraged miners to keep upgrading their systems (Wattenhofer, 2016). Those who did not adapt to the growing computing speed requirements were out of the game, without earning any profits and whilst paying off energy and hardware costs. The overall mining efficiency of miners has increased, and miners are able to even finance their own hardware and software upgrades (Vranken, 2017).

As shown in Table 6, Bitcoin initially allowed mining for normal personal computers. Now this is not enough. On the one hand, we have ASIC chip manufacturers performing large hashing computations in data centres located onsite in cool areas where they can minimize energy costs (Vranken, 2017). Many large miners select locations close to cheap electricity generation units where the ambient temperatures remain low. In Iceland for instance, 98% of the electricity production comes from renewables, including hydroelectric and geothermal power plants, and was a major miner hub back in the hype of 2017. It was estimated that by the end of 2018, more than 100 MW would have been consumed by mining activities in Iceland (Sigurdardottir & Rigillo, 2018) which – if taken as at a year-basis – is about 17,000 Icelanders' energy consumption, about 5% of the population.

On the other hand, the mining community has moved to mining pools. A *mining pool* is a large community of individual miners that share their computing resources to solve transaction and block algorithms. Initially, crypto-mining in Bitcoin was meant to decentralize the issuance of bitcoin, but now there are some rising concerns with colluded power in major mining pools. For instance, Greenberg & Budgen claim that 58% of bitcoins are mined in China in focused groups near coal power stations (Greenberg & Budgen, 2018). For instance, even Bitcoin has launched a pool where the hash rate currently stands at 712.68 Ph/s whereas for Bitcoin Cash it is 238.55 Ph/s (Bitcoin, n.d.).

Mining Pools

As previously mentioned, mining pools pay individual miners when a block is generated by a pool member after it found a successful input (Equation 1), according to their individual power contribution. Mining pools are managed by a *pool manager*, who only send block headers to the miners and they return a nonce field, thus facilitating the communication within the pool (Bachrach, et al., 2015).

The *Shapley value* is a game theory concept based on dividing the gains and costs among parties according to the value of contributions (Serrano, 2007). Some mining pools follow the same reward distribution arrangement, except for hardware and energy costs coverage. Energy costs are covered indirectly by the PoW contributions from each node and the corresponding reward from the mining pool, albeit not directly reflective; and infrastructure costs are compensated with time and block generation.

After examining pool mining dynamics through cooperative game theory analysis, Bachrach et al. deem a better node coordination from mining pools and in general that they experience higher bitcoin rewards. They conclude that to maximize profit, the mining strategy would benefit from algorithms that would switch pools automatically, according to the varying conditions of each pool and team instability caused from high transaction loads (Bachrach, et al., 2015).

Figure 8 identifies Antpool and F2Pool as the two largest mining pools with almost a third of Bitcoin mining activities (Shi, 2016). This figure is also backed by Bohme et al. In June 2014, the no longer operative mining pool GHash briefly controlled 50% of the mining power which threatened the network and Bitcoin community with the 51% attack or manipulation. This would give the pool manager the ability to alter the system logs and perform malicious activity on the chain if they so wished for (Bohme, et al., 2015).

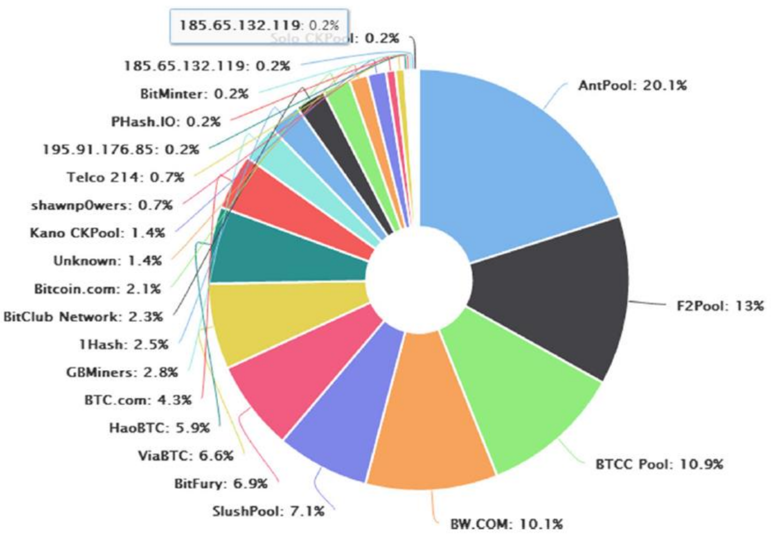

Figure 8. Bitcoin computing power distribution *(Shi, 2016)*

According to Bachrach et al, theoretically it would take 1.9 years for a miner with state-of-the-art mining hardware to mine a single block. Many miners who look for steady incomes choose to join mining pools, to receive a portion of the mining gains (Bachrach, et al., 2015).

Mining Appliances

Underpinning Bitcoin's success and popularity is a sequence of big technology developments at both software and hardware levels. Since Bitcoin's first transaction in 2009 from a CPU, the technological ecosystem has invested a vast amount in competing for computational rates. The technological innovation began at a horizontal scale and at enthusiast-level.

Taylor has mapped the mining difficulty upward trend against the mining technologies due to rising exchange rates and technology improvement as shown in Graph 23. The dots indicate the introduction of the new mining technology. Mining pools began emerging at the end of 2010 and miners began receiving small steady transactions, instead of one-off large transactions (Taylor, 2017).

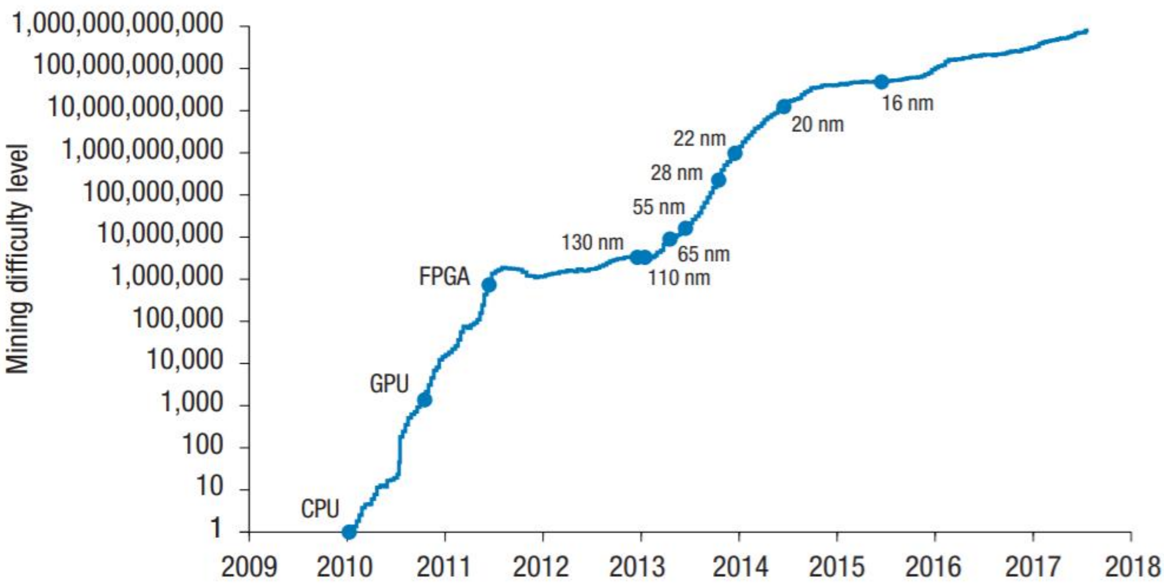

Graph 23. Mining difficulty level plotted with mining hardware upgrades *(Taylor, 2017)*

Table 7. Hash rate improvement for different technologies *(Taylor, 2017)*

Technology	Mega Hash rate per second
Overclocked 6-core CPUs (example: Inter Core i7-990x) with SIMD extensions	33 MH/s
Nvidia GPUs (example: GTX 570)	155 MH/s
AMD GPUs (example: 7970) operating at 200W	0.675 GH/s

Xilinx Spartan-6s operating at 60W	<0.675 GH/s
Bitmain Antminer S9 using 16-nm ASICs	13.5 TH/s

Graph 24 portrays the daily revenue per mining performance since 2010 and where the horizontal lines represent the energy costs per day for each mining technology (Taylor, 2017). Mining revenue for a given mining hardware must always be greater than the energy costs otherwise their profitability becomes negative and either the miner must (1) upgrade their technology, (2) forfeit the mining arms race.

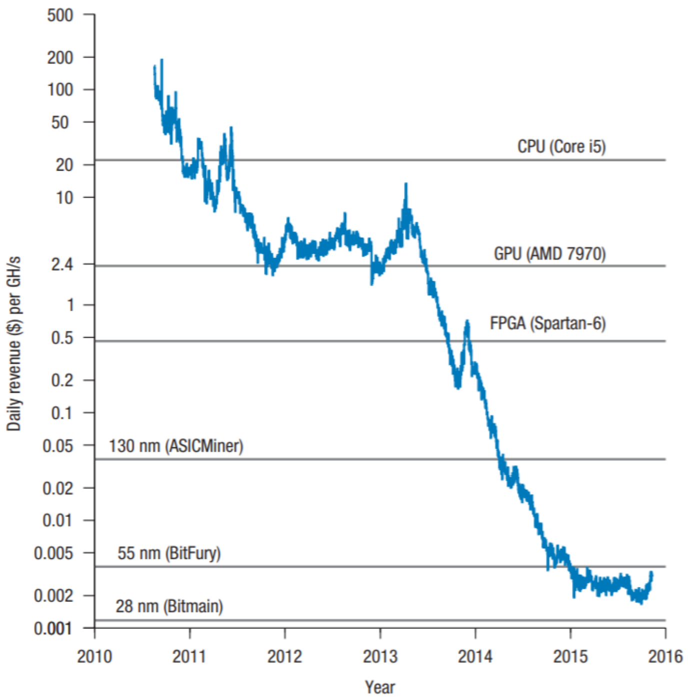

Graph 24. Daily revenue for mining performance *(Taylor, 2017)*

CPUs are the first-generation miners with the following basic computation for the source code (Taylor, 2017).

```
While (1)

      HDR [kNoncePos]++;

      IF (SHA256(SHA256(HDR)) < (65535 << 208)/DIFFICULTY

return;
```

Algorithms have been optimized such as the one discussed by Taylor with regards to *mid-state buffer*, whereby an intermediate hash value is created from the block header and some initial megadata from the block. An SHA256 process takes 64 rounds of encryption computation (Taylor, 2017).

In late 2010, GPUs were rapidly adopted. Taylor claims that the growth equated to 3.2 billion GPUs were attained for mining activities. GPUs were much more accessible for hobbyists than the following FPGA technology. GPUs scaling led to increased power and cooling demand, each GPU consuming about 300 W thus exceeding the power density supported by data centers and residential electricity grids (Taylor, 2017).

A year later, FPGAs came into the mining market, but it was difficult for this technology to compete against the high-volume GPUs which were already being sold in large retail sites such as Newegg. However, FPGAs could break-even after two years on the total cost of ownership (TCO) given that they were five times more efficient than the preceding technology (Taylor, 2017).

After their FPGA miners, Butterfly Labs (BFL) launched in 2012 the ASIC mining technology with three hardware rigs with a pre-order value over $250,000 on the first day of launch (Taylor, 2017):

Table 8 Butterfly Labs ASIC technology for mining hardware *(Taylor, 2017)*

BFL Technology	Cost	Hash rate
Jalapenos	$149	4.5 GH/s
Singles	$1,299	60 GH/s
Mini Rigs	$30,000	1,500 GH/s

These machines could make 20-50 times more revenue in BTC per invested US dollar, even at these high capital costs (Taylor, 2017).

In order to impede BFL from overtaking the global mining activity, ASICMiner was founded to sustain an ASIC data centre, similar to a mining pool. However, the mining community did not quite understand their business model and eventually, ASICMiner began to sell hardware (Taylor, 2017). Avalon, a renowned FPGA manufacturer, did not want to be left behind. Their first mining hardware was priced at $1,299 and offered hashing at 66 GH/s with 600 W (Taylor, 2017). However, the paradigm has shifted to vertical corporate-owned large ASIC (20 nm and 16 nm) data centres to perform mining computations and the ASIC war began in order to make rigs the more efficient, better designed and with a greater hash rate.

2.5.7 Bitcoin Mining Economics

Mining Economics & Profitability

Mining takes up resources. A miner would want to pay-off their mining expenses as well as make a certain degree profitability (unpredictable). A miner has to make the decision whether to invest their resources at a cost of C per second or not. At cost C and Bitcoin value V , a miner is able to make trial-and-error guesses at a hash rate of r trials per second ($r = f(C)$) then the number of hashes computed at that cost will be H. To make the investment worth it if the amount earned $\frac{rV}{H}$ should be greater than the cost, therefore the following needs to be met (Kroll, et al., 2013):

$$H < \frac{rV}{C}$$

However, the miner is not alone in the mining arms race. It competes against many other nodes with different computational profiles and the block mining rate is kept constant at roughly 10 minutes. By assuming N miners and B new blocks per second,

$$B = \sum_{i=1}^{N} \frac{r_i}{H}$$

If we take the global sum or total (represented with a dash on top of the variable), then:

$$\frac{\bar{r}}{B} < \frac{\bar{r}V}{\bar{C}} \qquad \bar{C} < BV$$

Global equilibrium for reward in currency per second should be equal to the total cost of mining:

$$\bar{C} = BV$$

A miner would have to assume the costs of the physical location where the mining equipment would be installed in addition to the costs associated to the energy consumption to fed into the algorithm computing process, as shown in Table 9. Therefore, miners are amortizing their hardware and other capital expenditure (CAPEX) costs, in addition to the operating costs (OPEX). This leads to the marginal component in addition to the fixed component of costs C in bitcoin mining (Kroll, et al., 2013). The expect profit of a miner would increase if its marginal cost decreases whilst its competitors' marginal cost increases (Dimitri, 2017).

Table 9. Identification of cost elements and revenues for a large miner *(Vranken, 2017)*

Costs	**CAPEX**	**OPEX**
Physical location	Space Purchase, Physical assets	Space Rent, Maintenance
Energy	Room conditioning, Physical cabling, miners, cooling equipment, etc.	Electrical power to run mining software, Cooling, Maintenance
Revenues	**Value**	**Price**
Block reward	12.5 BTC/block	Variable with the market
Transaction fee	Variable	Variable with the market

According to Taylor, the cost of capital goods should not be greater than the sum of the exponential payment decline shown in Graph 24 minus energy costs plus the resale value of the currently owned hardware (Taylor, 2017).

Transaction fees are the other component of the mining reward scheme in the Bitcoin network. With every block transacted, a Bitcoin nonzero value is left as gratuity for the miner to motivate them to add their block to the chain (Taylor, 2017). No matter the size of the transaction, Kroll et al. argues that a miner would be better off by accepting the transaction, no matter how small it is; otherwise, another miner would take it. Pushing transaction costs up would require a consensus agreement between all miners to avoid mining blocks with a transaction fee lower than a set target (Kroll, et al., 2013). But given the uncontrolled nature of Bitcoin, this calls out to the prisoner's dilemma in game theory where the actions of the opponent are not known (Table 10). The overall network would benefit from miners' collaboration, but the cooperating miners will not guarantee their individual profitability.

Taking that a block is generated every 10 minutes, in a day 288 blocks are generated daily. The total mining reward without any fees is therefore 3,600 BTC (according to the 12.5 BTC as the halving mining reward), out of which the average daily reward transaction – i.e. transaction fees – is about 50 BTC (Kroll, et al., 2013). That is 0.17 BTC in transaction fees per block generated on average.

Table 10. Miner's prisoner's dilemma when facing a low block transaction fee or reward transaction

	Miner B mines the block	**Miner B does not mine the block**
Miner A mines the block	A∪B would get the small transaction fee	Miner A gets the small transaction fee, Miner B is left with nothing
Miner A does not mine the block	Miner B gets the small transaction fee, Miner A is left with nothing	Transaction would increase and A∪B would get a higher fee

Kroll et al. believe that transaction fees will not be crucial in the development of mining economics long-term under current rules. However, Bitcoin is the "first mainstream open-source currency" (Kroll, et al., 2013). Current rules are already changing through Bitcoin open-source governance in:

(1) reducing blocks with low transaction values, otherwise called *Bitcoin dust*. The minimum transactional value is proposed to change from 1 satoshi, or 10^{-8} BTC, to 5,430 satoshi.

(2) After the 2013 Bitcoin's fork, the mining community decided to take Bitcoin's chain in version 0.7 as the reference chain, even if it was smaller than version 0.8, thus going against one of blockchain's main principles with regards to the longest consented blockchain (Kroll, et al., 2013)

Similar to Graph 24, Graph 25 shows the block reward value plus the transaction fees awarded to miners. At the end of 2012 and in mid-2016, the mining reward went through the having reward process, and that is why the miner revenue decreases. Whenever the revenue falls below the green horizontal lines representing the estimated daily energy cost, miners are impelled to upgrade their hardware to not lose profit; but whilst miners are still making profit or haven't reached the break-even point, they stick to the technology they have (Vranken, 2017). For mining pools, the revenue coming from a generated block is split according to computational contribution amongst the participating miner nodes.

Graph 25. Daily revenue per Gh/s for miners 2011-2016 *(Vranken, 2017)*

Mining Death Spiral

A major parameter affecting Bitcoin mining is based on confidence on the value of Bitcoin. As seen in the equations above, the value of the reward V depends on the cryptocurrency's market value – which is equivalent to other currency values – which in turn, fluctuates frequently and with it, the incentive to mine or to invest in mining equipment. Kroll et al. identify this pattern as a spiral death: confidence loss in Bitcoin would decrease the price, thus disincentivizing mining which would reduce again confidence in the fiat currency (Kroll, et al., 2013).

As the struggle for winning the race for solving the block algorithms tightens, capital expenditure increases for miners. Many miners are not able to keep up investing and partaking in the arm race, as incentives depreciate with time and infrastructure costs continue increases. This pattern seems to put off newcomers from joining the mining network too. Consequently, the trending danger is that bitcoin issuing might be centralizing with time into only those mining entities that have enough computing resources, in a smaller and less competitive community, eventually creating an oligopoly. In 2016, Bitcoinchain.com reported that 85% of the blocks were mined by five large Chinese mining nodes (Vranken, 2017).

For future miner improvements, the only foreseeable modifications are to do with ASICs migration to new design efficiencies, given little micro-architectural alterations can be made with regards to the SHA-256 algorithm. As a result, Vranken expects a slow-down in mining efficiency and performance (Vranken, 2017).

2.5.8 Bitcoin Mining Energy Consumption

"*Bitcoin has bene designed with no consideration of its environmental impact*" (Truby, 2018). Bitcoin, through its PoW consensus fabric, portrays a rather detrimental prospect with regards to the consequences on energy usage whilst the world faces the current environmental concerns. Bitcoin does not deny that it wasn't designed to be eco-friendly. The following lines are provided by Bitcoin in an infographic: "*Bitcoin Mining is intentionally designed to be resource-intensive and difficult so that the number of blocks found each day by miners remains steady over time, producing a controlled finite monetary supply. Individual blocks must contain a proof-of-work to be considered valid*." (Bitcoin, n.d.).

Miners are incentivized to add blocks to the longer chain, thus agreeing on the system state (Wattenhofer, 2016). The issue with bitcoin mining is that only the first miner that solves the algorithm gets the reward. That means that the energy consumption allocated to solve one block mathematical problem is not solely constituted by the energy consumed by the winning miner, but by all of the mining nodes that were aiming at solving the problem and being rewarded.

Therefore, behind the upward movement of the crypto-market is the growth in energy consumption related to cryptocurrency mining of Bitcoin and other altcoins. Literature shows that there is vagueness in our understanding of energy consumption of crypto-mining and therefore it is quite difficult to put a bold or even approximate number to the mysterious value. The estimated energy usage allocated to Bitcoin mining was 63.99 TWh in 2018 (Li, et al., 2018) based on the Bitcoin revenues assigned to paying off electricity costs. According to Li et al., the only certain figure is the minimum annual electricity of Bitcoin mining of 23.38 TWh, computed from the average network hash rate of 27,235.27 PH/s (Li, et al., 2018). Studies have been made to estimate the power consumption of Bitcoin by taking the hash rate in h/s and dividing it over the energy efficiency in h/J (O'Dwyer & Malone, 2014). Literature shows an energy consumption in the range of a 10 MW small power plant to 3-6 GW, the equivalent a country such as Denmark or Ireland (Deetman, 2016).

Truby reports that Bitcoin mining is responsible for 0.14% of global electricity generation, albeit it bases this statement on dubious sources (Truby, 2018). It is also claimed that Bitcoin and Ethereum consume the equivalent value to $1 million in hardware costs and electricity in one day (Andoni, et al., 2018). Pilkington forecasts that in the future Bitcoin could be using 60% of world electricity production, namely 13,000 TWh (Pilkington, 2015). In 2018, the estimated energy consumed per transaction was 200 kWh for Bitcoin, compared to 37 kWh and 0.01 kWh for Ethereum and Visa, respectively (Truby, 2018). Another source forecasted a few years back that it would require 5,500 kWh of energy to mine only one bitcoin in 2020, equivalent to a semester of an average American household electricity consumption (Deetman, 2016).

In Bitcoin, each block is characterized by a hash of 256 bits as it is based upon the SHA-256 cryptographic method (Vujičić, et al., 2018). To find a uniformly arbitrary number x between 0 and 2^{256}-1, the hash for block B is computed by multiplying the hash function twice, as follows (Vranken, 2017). Generating one block equates to 2^{71} double-hashes, where each double-hash takes 512-bit blocks and performed a few thousand of computational operations (Taylor, 2017).

$$h(B(x)) = SHA256 \cdot SHA256(B(x))$$

The randomly obtained values are what was previously expressed as the nonce. Miners aim to find a hash number that must below a given network target which is redefined every 2016 blocks to maintain the block generation rate at every 10 minutes (Nakamoto, 2008). This is because, as the network mining capacity increases, it becomes easier to mine blocks and therefore the difficulty needs to be adjusted so that it always takes 10 minutes (Taylor, 2017). The successful input x is defined as (Bachrach, et al., 2015):

$$h(B(x)) < T$$

Equation 1

The target T can be defined in terms of the algorithmic difficulty D and where T_{max} is the maximum target number (about 2^{244}):

$$D = \frac{T_{max}}{T}$$

Thus, trying random inputs, the success probability that a nonce matched a valid hash value can be expressed as follows (Vranken, 2017):

$$p = \frac{T}{2^{256}} = \frac{T_{max}}{2^{256}D} \approx \frac{1}{2^{32}D}$$

Vranken observes that at rate r, the time t to reach a valid hash number is set for every 10 minutes (or 600 seconds) to validate a block:

$$t = \frac{1}{p \cdot r} = \frac{2^{32}D}{r} = 600 \text{ s}$$

The hash rate is therefore obtained as:

$$r \approx \frac{2^{32}D}{600}$$

Adding the mining energy efficiency μ to the equation gives an estimated power P:

$$P = \frac{r}{\mu} \approx \frac{2^{32} D}{600\, \mu}$$

The power usage is presented in Graph 26 shows that the actual mining power consumption can vary from 45 MW to 450 TW for January 2017. The figure of 450 TW is impossible as the annual consumption at that time peaked at 2.3 TW, and therefore Vranken proposes a more realistic approach based on revenue from bitcoin mining ($1.9 million). The upper bound was then calculated to be from 400 MW (assuming an electricity price of $200/MWh) to 2.3 GW (assuming an electricity price of $35/MWh). Vranken concludes that mining is only profitable with ASICs and that in practice the energy consumption lies between 100-500 MW or 3-6 PJ per year. He compares the figure against:

- gold mining and recycling, both estimated at 500 PJ
- printing banknotes and minting coins at 40 PJ
- ATMs and bank branches transactions at 2,340 PJ

Compared to these numbers he states that the energy consumption is very small (Vranken, 2017).

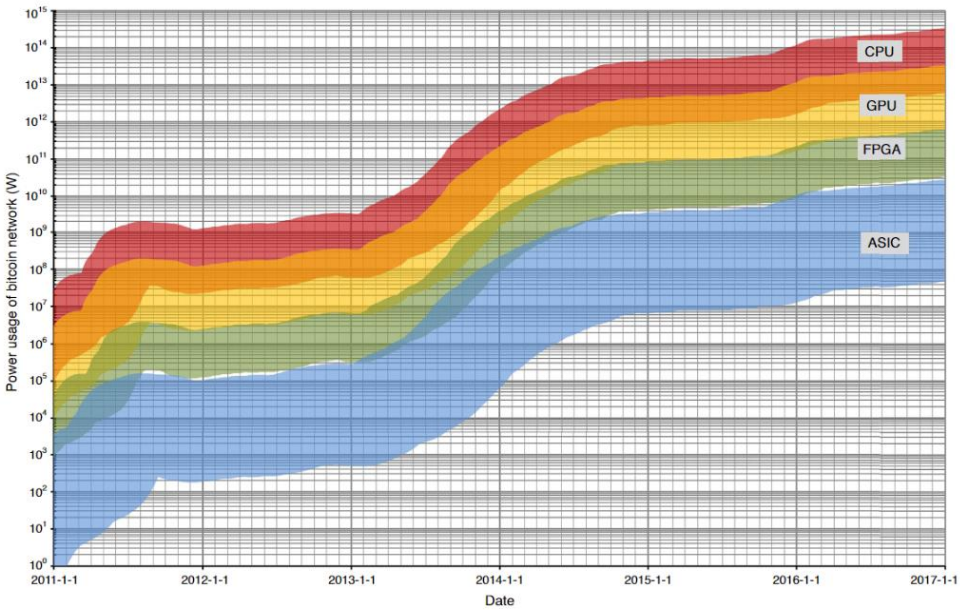

Graph 26. Power consumption for different Bitcoin mining devices *(Vranken, 2017)*

Due to the very mysterious and secretive nature of cryptocurrencies and the every-changing number of cryptocurrencies in the market, it is very difficult to perform an accurate study on mining energy consumption status. All in all, it seems that there is a lack of homogeneous understanding of the energy consumption required for validating transactions and consolidating blocks, although it is implicit to be of a considerable amount.

The need for regulation has been proposed in literature (Truby, 2018), but the challenge of the decentralized untamed nature of Bitcoin – as well as other permissionless blockchains – sets a difficult barrier to overcome in the attempt of enacting energy consumption limits in the decentralized and distributed arena.

2.5.9 Mining other Cryptocurrencies

Most miners diversify their mining portfolio by dedicating their energy consumption to mine different cryptocurrencies – or altcoins – according to the market value of each and to seek profitability from the cryto-market. Other (currently) profitable altcoins include Ravencoin, Grin, ZENCash, AEON, Electroneum (ETN), Bitcoin Gold (BTG), Feathercoin (FTC) and Monero, to name a few. Whattomine.com provide a list of cryptocurrencies that can be mined, their hashrate and the power required. It also provides a profitability comparison against Ethereum (Whattomine.com, n.d.).

Most mining concepts provided above apply to altcoins in addition to bitcoin, including the mining arms race and mining hardware, mining pools, and most part of the mining economics and energy consumption.

3 Methodology

3.1 Case Specification

The very first step of the research is to select three countries, in order to understand how profitability is relative to different scenarios and under different energy market conditions.

To select the countries the following two parameters will be used towards the selection:

- **Electricity cost**: electricity prices that a cryptomining centre would have to pay when not taking electricity from a free renewable source.
- **Photovoltaic Power Potential**: availability of solar resource to produce electricity to power the crypto-miners or electricity to the grid.

A country selection was performed in order to identify countries with high solar radiation per unit area, plotted against the electricity prices parameters for the same countries. The analysis compared overall 54 countries, as shown in Graph 27, after a process of elimination as outlined below. The electricity prices data was obtained from the IEA report of 2019 (IEA, 2019).

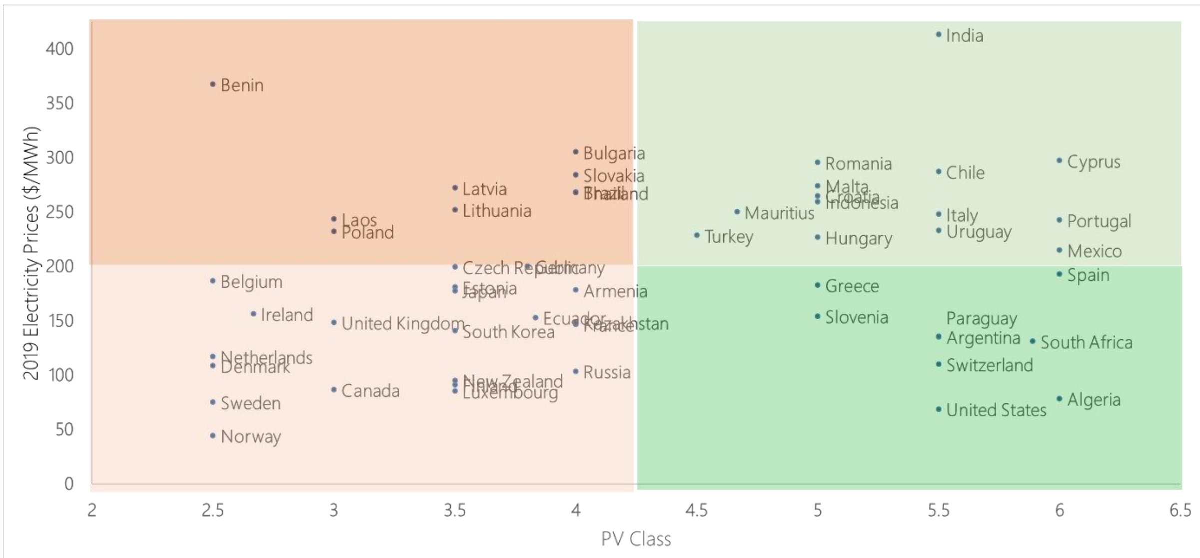

Graph 27. Country distribution according to PV class and electricity prices

After analyzing the options, India, Spain and the United States have been selected. All three countries have a high national PV class in the range of 5.5-6 and present a variation of low to high electricity prices. Together they also represent countries at different developing stages, socially and in wealth which makes it more interesting for comparison.

Additionally, due to their high PV potential they have all since an increase in solar PV capacity growth. For comparison purposes, Graph 28 portrays the net solar PV capacity added to the electricity network across the years 2016 and 2018. The consequent step is to decide a particular region within the country and for this, specific characteristics to each country are provided in the succeeding chapters.

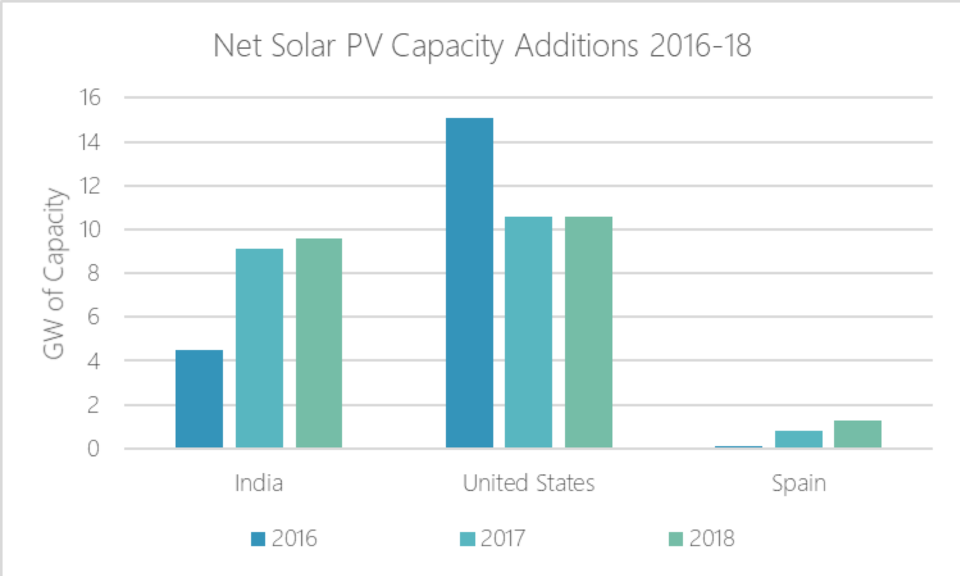

Graph 28. Net solar PV capacity additions 2016-2018 (Bellini, 2019) (Bahar, 2019)

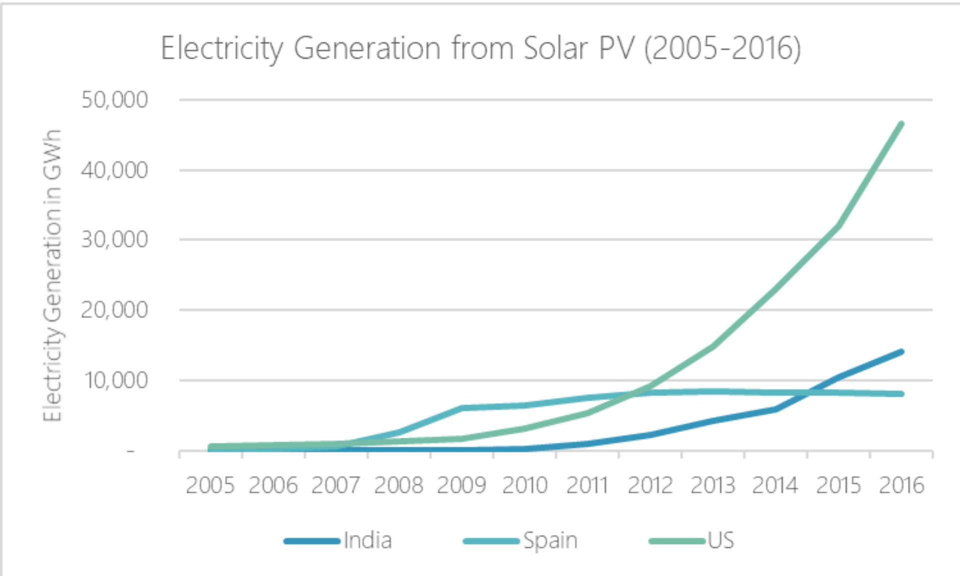

Graph 29. Electricity generated from solar PV from 2005 to 2016 (IEA, 2016)

Data Collection

At country selection stage, the following criteria is regarded to provide valuable insights:

- **Data availability**: data that can be accessed freely, or access permits are granted.
- **Data quality**: data is obtained from trusted party, consistent and up-to-date. In the meteorological data obtained from PVSyst, as shown in the plots of Appendix A.1 (p.115) whereby irradiation values in the scatter-plot surpass the clear sky upper limit, it can be observed that data is not always consistent and discrepancies exist, but that it is still indicative and therefore it can still be used.
- **Data variety**: relative analysis benefit for comparative purposes in terms of electricity affordability and resource availability.

The International Energy Agency (IEA) granted access to the latest *World Energy Prices 2019* issue for the purposes of the research. Several steps were followed:

1. Available data for years prior to 2013 is not considered, as the present thesis consists of an historical analysis from the existence of cryptocurrencies and the available data.
2. Countries that have more than one gap or inconsistencies in industry electricity prices across the period that spams from 2010 until 2018, are equally disregarded for the selection.
3. Countries where the portion greater than 6% of a day's wages goes into electricity usage will not be considered (Portugal, Slovak Republic, Poland, Hungary, Czech Republic, Mexico, Estonia, Greece).

The electricity prices data is provided in US dollars per MWh, and US dollars per MWh using Purchasing Power Parity (PPP), an economic theory that helps for purposes of comparison match electricity prices of different countries.

The solar radiation is collected from the US Government's Open Data (Data.Gov, n.d.) website and checked against the Geographic Information System (GIS) software PVSyst 6.8.3.

3.1.1 Case Specification for India

Solar Radiation Profile

Kar et al. suggest that renewable energy plays a key role in India's energy mix. 58% of the country´s total surface receives an annual average radiation is 4 to 7 kWh/m^2/day with 300 days of sunshine a year, data which coincides with the average daily radiation obtained from Data.Gov, and the solar PV potential is of 6,000 GW. This means that, in theory, India has the capacity to generate 500,000 TWh every year, assuming 10% conversion efficiency (Kar, et al., 2016), which is more than 300 times India's energy demand from 2018.

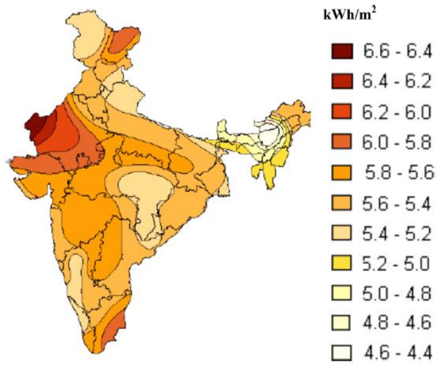

Figure 9. Solar Irradiation distribution in India (Kar, et al., 2016)

Different regions have been examined in India and consulted against the meteorological data files included in the PVSyst database for particular technologies. In the end the city Panjib located in Goa, in the Western region of India, was selected. Graph 30 shows the meteorological monthly conditions for the location according to the PVSyst database.

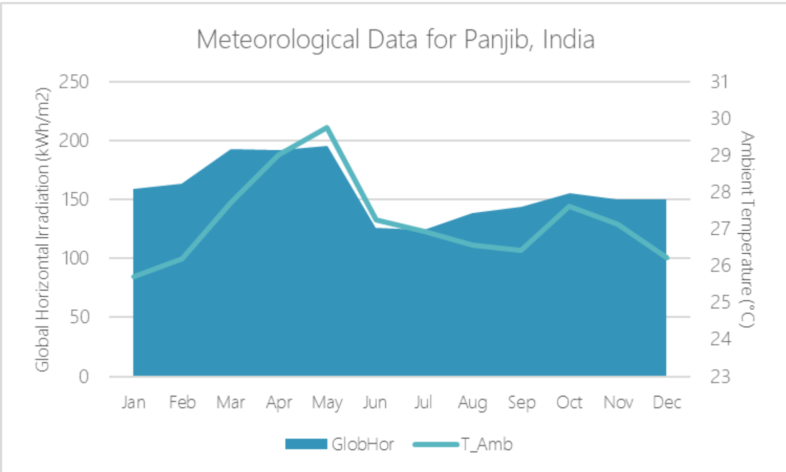

Graph 30. Meteorological data for Panjib, Goa, India (PVSyst, 2019)

PV Current Capacity and Future Targets

In 2016, India had 38.82 GW of total renewable capacity – i.e. 13.12% of the countries power production – (Kar, et al., 2016) and generated 14,130 GWh of electricity from solar energy, whereas in 2010 it merely produced 113 GWh (IEA, 2016), as shown in Graph 29.

India has determined plans for the future of its energy mix. Initially after the COP 21, it had plans to increase its solar capacity to 100 GW as part of its ambitious plant to achieve 175 GW of renewables capacity by 2022. However, in June 2018 it increased the global renewables target to 225 GW (IBEF, 2018).

Electricity Market and Prices

Solar energy generated can be sold to the grid with a corresponding feed-in tariff for solar which is set through bidding process, and changes according to the technology development. The tariff was lowered in 2016 from 8.56 Rs/kWh to 7.08 Rs/kW and energy producers must sign a purchase power agreement (PPA) with their energy company. Table 11 represents the tariffs offered for new commers to the solar market, whereas the previous stay with their agreed-on tariff.

Table 11. Tariff for solar electricity in India (India Times, 2016)

	Without subsidy Rs/kWh	With subsidy Rs/kWh
1 kW to 10 kW	7.08	6.03
10 kW to 50 kW	6.61	5.63
50 kW to 100 kW	6.14	5.23

Solar energy in Goa receives a 50% subsidy up to 100 kW capacity installed, out which 20% from the state and 30% by the Ministry of New and Renewable Energy. The 50% are marked based on the capital costs of the project. Furthermore, planning permissions are no longer required for building a solar farm in the state of Goa (IEA, 2019).

3.1.2 Case Specification for Spain

Solar Radiation Profile

Spain receives 300 days of sunshine a year on average (Endesa, 2018), a very favourable figure for the solar profile in the country. The radiation profile was analysed for the regions in Spain with the greatest global irradiation profile and contrasted with the available data on PVSyst. Huelva (1829 kWh/m^2) was the city with the greatest amount of solar irradiation followed by Malaga (1829 kWh/m^2) and Almeria (1827 kWh/m^2), all located in the Southern area of Andalusia (Figure 10). The annual meteorological data for Huelva is provided in Graph 31. Meteorological data for Huelva, Andalusia, SpainGraph 31.

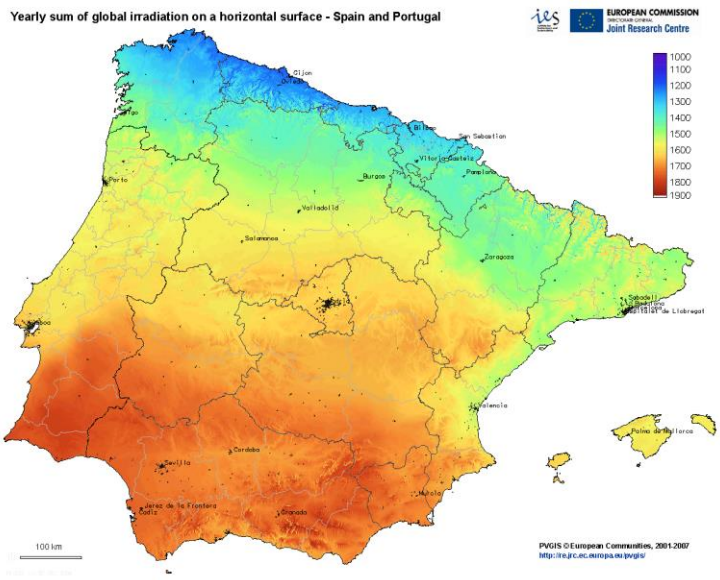

Figure 10. Yearly sum of global irradiation, Spain and Portugal (Alves, 2016)

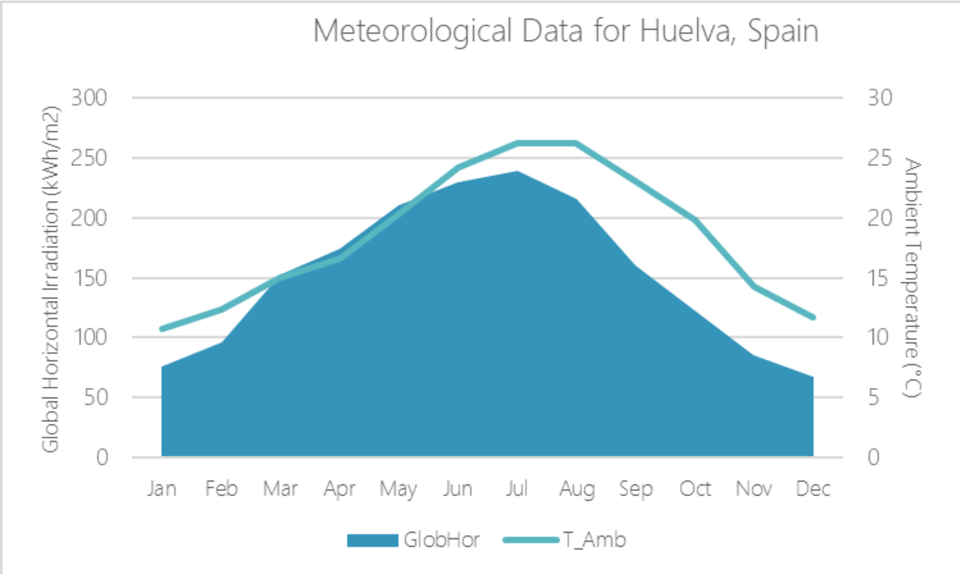

Graph 31. Meteorological data for Huelva, Andalusia, Spain (PVSyst, 2019)

PV Current Capacity and Future Targets

In 2016, Spain generated 8,070 GWh of electricity from solar energy, whereas in 2005 it merely produced 41 GWh (IEA, 2016), as shown in Graph 29. In 2018, Spain produced 45.8% of its electricity from renewable energy – wind leading – given good weather conditions. In 2017, solar PV provided 4.5% of the country's gross generation (REE, 2017) with the regions of Castilla La Mancha (925 MW) and Andalusia (878 MW) installing the highest number of solar PV capacity (Tsagas, 2018). In 2018, Andalusia contributed to 18.9% of Spain's PV solar generation (REE, 2019).

Electricity Market and Prices

In Spain there is no special tariffs for solar as they were abolished in 2014 for renewable energy. Solar electricity is sold to the grid mix at normal market value. For the purposes of this model, the value data for Operador Del Mercado Ibérico De Energía Polo Español (OMIE) was used as a stable value for tariffs in Spain as 0.07 $/kWh, taken from the average tariff of 2018 (OMIE, 2018). Graph 32 portrays the change in annual average tariff which goes down below 0.045 euros per kWh produced hindering solar electricity from making an actual profit. In addition, the approximate cost of injecting solar energy into the grid is of 1,000 euros plus taxes (distribution company, installation, metering, administrative) and Monera believes that it is not worth injecting Spanish solar electricity to the grid (Monera, 2018).

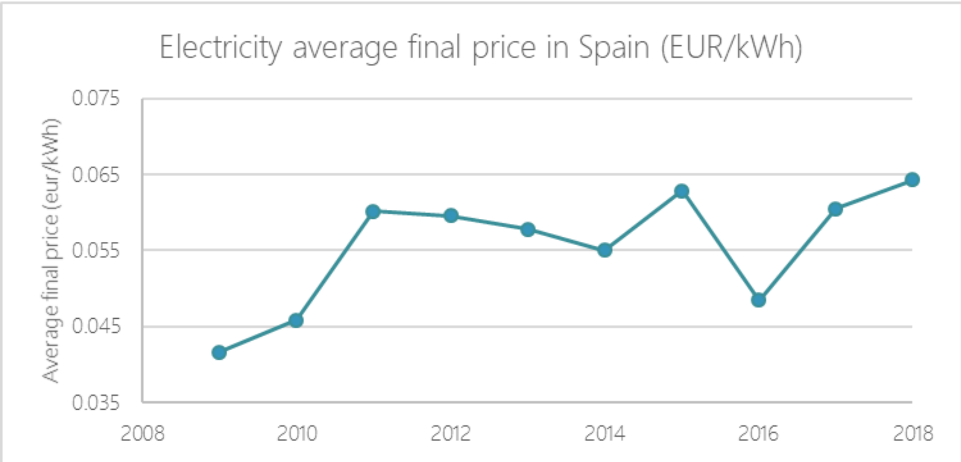

Graph 32. Electricity average final price in Spain (OMIE, 2018)

3.1.3 Case Specification for California in the US

Solar Radiation Profile

The US experiences on average a solar irradiation rate of 5 to 7 kWh/m^2 per day, where the most highly-irradiated states are California, Arizona and New Mexico in that order (NREL, n.d.). California experiences 284 days of sunlight (Bestplaces, n.d.). Several locations with different irradiation profiles (Figure 11) have been observed in California and contrasted against the available data on PVSyst. The area of Barstow combined both high-irradiation profiles and geographical suitability due to its non-urban profile and desertic characteristics. The monthly meteorological one-year data is provided in Graph 33. Meteorological data for Barstow, California, US Graph 33.

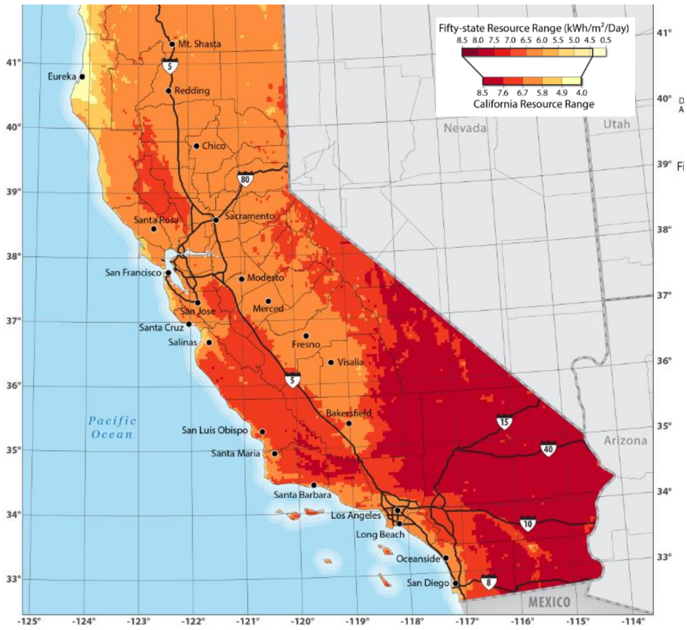

Figure 11. Solar irradiation profile in California, US

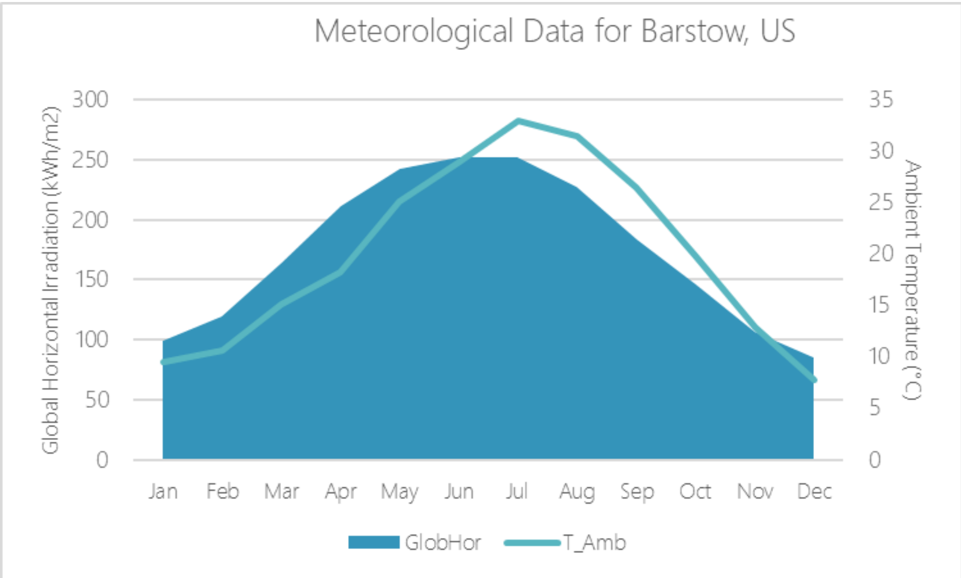

Graph 33. Meteorological data for Barstow, California, US (PVSyst, 2019)

PV Current Capacity and Future Targets

Renewable energy sources provide 17% on average across the US states. Specifically, in California renewables meet 31.36% of the electricity demand (IEA, 2019). In 2016, the US generated 46,633 GWh of electricity from solar energy, whereas in 2005 it produced 524 GWh (IEA, 2016), as shown in Graph 29. The solar industry experienced a boom in 2016. However, according to Mackenzie Power & Renewables, the annual US solar installations decreased in the year 2017 and 2018 (Graph 34). By the end of 2019, an increase of 13GW in power terms is expected due to the fall in PV costs (SEIA, 2019).

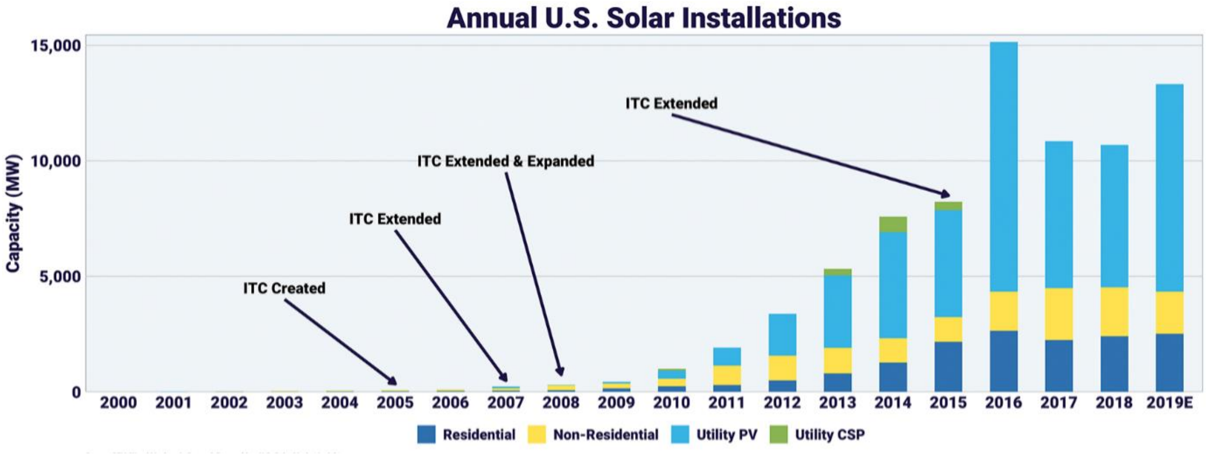

Graph 34. Annual US solar installations (SEIA, 2019)

The whole state of California has 25 GW of installed PV capacity. It is by far the leading state with regards to this renewable technology, with the runner-up state, North Carolina, has 5.4 GW of installed capacity (SEIA, 2019). The US Solar Energy Industries Association indicate that the growth will continue to resume after 2019 in their 5-year forecast (Graph 35), surpassing by 2021 a net PV installed capacity of 100 GW.

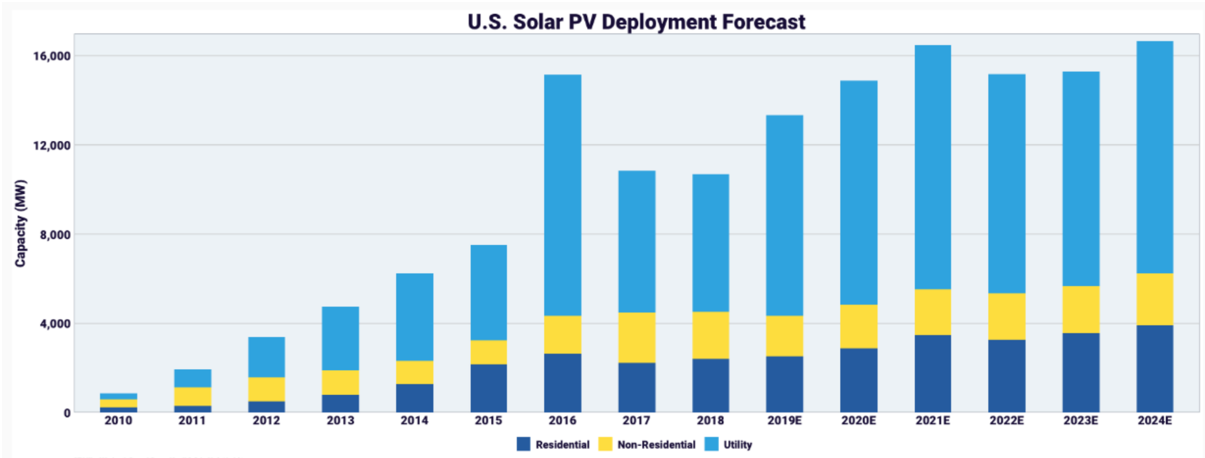

Graph 35. US solar PV growth forecast (SEIA, 2019)

Electricity Market and Prices

California relies on the California Independent System Operator (CAISO) to manage the bulk electricity generation and bring together electricity demand and supply for the state. Electricity prices change according to a region’s demand and supply as observed in their price map (CAISO, 2019). However, the state has a specific solar tariff managed by California’s Public

Utilities Commission, named the Renewable Market Adjusting Tariff for renewable generators below 3MW of installed capacity and which offers a fixed price for the electricity produced (CPUC, 2018). The fixed price for the purposes of this modelling was considered to be 0.139$/kWh.

3.2 Crypto Model Methodology

3.2.1 Mining Profitability Methodology

The purpose of this section is to characterize the potential profitability coming from directing electricity from solar PV towards the computing power a mining technology requires to mine cryptocurrencies. For the purposes of this thesis, Bitcoin (BTC) is the cryptocurrency studied.

The model was produced in an Excel spreadsheet along with the Energy Storage Modelling. Table 12 shows the tabs and a description of the computation or database included in it.

Table 12. Crypto-model Excel sections summary

Crypto Model Tab Name	Tab Description
BTC Price	Database of the historical Bitcoin (BTC) price value from the 28th of April 2013 until the 23rd of July 2019. It includes daily open, highest, lowest, close, volume and market cap values in US dollars. For modelling purposes, the close value of the BTC is taken.
BTC Halving Reward	The calculation of halving rewards for block generation in the mining scope is presented here and estimated to be 4 years in the future.
Miner Technology Characterization	
Mining Technology Options	The different mining technologies evolved through gradual technology adoption are presented here with their operating and cooling power requirements, market price and operating hashrates. The number of miners has been optimized to increase the ROI of the system, according to the revenue from cryptomining. The capital costs for the system are calculated based on the number of miners.
System Definition for Multiple Technologies	The actual model is developed here. According to the date from 28-04-2013 until 23-07-2019, the technologies change. The required mining hours is calculated based on the network hashrate at each given date. For simplicity, it is assumed that the bitcoin reward is returned daily as a % contribution of the computing power provided, as it would for a pool mining and that every time the block would be generated. It is an initial approach towards calculating the maximum potential gain, the upper limit. The electricity demand and cost are also calculated.
Results	The results change based on the country selected (sun-hours, electricity costs, sun availability factor) and the aggregate revenue from BTC is calculated, as well as the net electricity savings from not purchasing electricity from the grid, ROI and payback time.
ROI Sensitivity Analysis	A sensitivity analysis has been performed to see how the calculated ROI is affected by changing sun-hours, electricity costs and sun availability factors for

	all three locations.
NPV and IRR Analysis	The Net Present Value (NPV) and Internal Rate of Return (IRR) have been calculated for the historical period for all three locations.
Energy Calculation	The yearly energy demand calculation has been performed in order to characterize the PV solar system presented. Each miner power and energy requirements are calculated per year. Used also for additional profit calculations.
BTC Variability	An analysis of the variation between Close to Open prices, High to Low prices and the daily variation from the Close value is performed here. The adoption point is set as the point in time when the BTC price exceeded 1,000 USD value.
YoY Variation	From the adoption point, the year-on-year variation of the BTC price is analysed but no real pattern is extracted as the BTC market is very speculative and is driven by market movements that cannot be foreseen.
BTC Prediction	Two scenarios are presented: a pseudo-random optimistic scenario whereby the value of BTC increases by 10% YoY and a pseudo-random pessimistic scenario whereby it decreases by -10% YoY.

The model takes into account the varying hashrate of the network to calculate the mining potential of selected mining technology. It incorporates the technological evolution of the industry, based on the model provided by Vranken (*Graph 25*).

Based on the graph, the technologies listed in Table 13 have been selected in the model. The model allows for change in the number of technologies to see how this would impact on the ROI for each country scenario. However, for purposes of this model, 8 ASIC batch 1 (110nm), 8 ASIC Antminer S1 (55nm), 1 ASIC Antminer S4 (28 nm), 1 ASIC Antminer S7 (28 nm) and 1 ASIC Antminer S9 (16nm) have been selected as the most profitable structure to an increased ROI whilst being guaranteed energy from the PV system. The overall miner power usage was characterized by the number of years in operation, and for each country with its respective sun-hours, both the total power (kW) and energy consumption (kWh) required was identified.

The energy consumption required can also be calculated and this is then used to calculate the electricity savings from mining without consuming from the grid, as well as the energy configuration required from the solar PV in terms of power and energy. A ROI sensitivity analysis was calculated based on changes of these variables.

Table 13. Mining technology options in technology adoption for the crypto-model

Mining Technology	**Adoption Date**	**Hashrate** GH/s	**Power Consumption (incl.cooling)** W	**Unit Purchase Cost in USD**
ASIC batch 1, 110nm	01-01-2013	66.3	1,193.5	$1,299
ASIC Antminer S1, 55nm	01-10-2013	180	693.0	$299
ASIC Antminer S4, 28 nm	01-09-2014	2,000	2,695.0	$1,400
ASIC Antminer S7, 28 nm	01-09-2015	4,860	2,329.3	$1,823

ASIC Antminer S9, 16nm	01-06-2016	13,500	3,080.0	$6,125

Technology evolution is assumed to be the same for each geographical location and with the same capital costs. However, the operating conditions depend on the country's (1) peak-sun hours – i.e. how much energy will be generated and for how long the mining will be able to operate without storage throughout the day –, (2) power unavailability or how many days the country experiences a shaded sky, and (3) electricity cost per kWh for each country as a baseline for comparison. As indicated in Table 12, a sensitivity analysis is performed and will be discussed to understand the impact of any change in these three variables for the system's ROI. The baseline scenario is presented in Table 14.

Table 14. Baseline characteristics for each country

Country	Electricity Cost $/kWh	Peak Sun-Hours	Unavailable Days	Power Unavailability
Panjib, Goa, India	$ 0.07	5.5	65	17.8 %
Huelva, Andalusia, Spain	$ 0.23	5.4	45	12.3 %
Barstow, California, US	$ 0.17	5.9	81	22.2 %

The profitability is measured through the varying Bitcoin halving reward, whereby from 2009 until 2012 it was 50 BTC, from November 2012 until July 2016 it was 25 BTC and from July 2016 until approximately July 2020 every block generated is rewarded with 12.5 BTC. Any prediction forward, it is assumed that the block reward halves every 4 years based on the fact that the difficulty of the network is re-adjusted so that a block is generated every 10 minutes.

Through the network hashrate and the varying technology hashrates the potential BTC per second, hour, day or year can be calculated. Aggregated from the 24th of April 2013 (date in which Bitcoin quality data is available) until the 27th of July 2019 (date when a line was drawn in the modelling), the overall profitability for the time period can be assessed assuming that the potential profitability is proportional to the computing power implemented, as it would be in a pool mining structure. Furthermore, a Net Present Value and Internal Rate of Return were analysed for all three cases, looking exclusively at the mining system, assuming the electricity was fed from a PV solar source.

3.2.2 Predictive Mining Modelling

Because the PV model lasts 25 years from 2013 until 2037, ideally the profitability should be compared against a 25 mining-period. Since the model only has mining profitability calculations from 2013 until 2019, a predictive modelling has been developed in order to forecast the future bitcoin and network hashrate value. This modelling exercise was performed in Excel spreadsheet, with the following subsections.

Table 15. Excel distribution for the predictive mining modelling

Crypto Model Tab Name	Tab Description
BTC Variability	An analysis of the variation between Close to Open prices, High to Low prices and the daily variation from the Close value is performed here. The adoption point is set as the point in time when the BTC price exceeded 1,000 USD value.
YoY Variation	From the adoption point, the year-on-year variation of the BTC price is analysed but no real pattern is extracted as the BTC market is very speculative and is driven by market movements that cannot be foreseen.
BTC Prediction	Two scenarios are presented: a pseudo-random optimistic scenario whereby the value of BTC increases by the rates presented in Table 16.
Hashrate YoY Variation	The daily variation of the network hashrate since adoption point (day when BTC surpasses $1,000 worth), to understand its historical upper and lower limits as well as the average value.
Hashrate Prediction	Outline of the different scenarios portrayed in Table 16 for Bitcoin network hashrate.
Prediction Analysis	This section brings together the different levels of both bitcoin price and hashrate prediction, and also gathers the assumptions towards technology progress in the period spreading across 2019-2037 (mining capability and price, considering a steady period before technology change of 2 years). It calculates the profitability based on a selected country (sun-hours, power unavailability)
Prediction Results	In this tab, the results every country are bought together including net revenue making and the ROI.

The bitcoin price and network hashrate were modelled according to historical data and different forecasting scenarios, portrayed in Table 16.

Table 16. Bitcoin value and Bitcoin network hashrate predictive mode scenarios

Model	Description
Bitcoin Value Predictive Model	
B.0	Delimited random model based on a scenario whereby the bitcoin value (in USD) is forced to vary daily between 20.16% and -23.06%, the overall scope of historical bitcoin price from day-to-day variability.
B.1	Pseudo-random model based on a scenario whereby the bitcoin value (in USD) is forced to vary daily between 25% and 10%, making Bitcoin mining more valuable.
B.2	Pseudo-random model based on a scenario whereby the bitcoin value (in USD) is forced to vary daily between 10% and -5%, making Bitcoin mining less valuable.
B.3	Pseudo-random model based on a scenario whereby the bitcoin value (in

	USD) is forced to vary daily between -5% and -20%, making Bitcoin mining even less valuable over time.
B.4	Pseudo-random model based on a scenario whereby the bitcoin value (in USD) is forced to vary daily between -20% and -35%, making Bitcoin mining have less value than the other scenarios.
Network Hashrate Predictive Model	
H.0	Delimited random model based on a scenario whereby mining difficulty (network hashrate) is forced to vary daily between 81.2%% and -42.2%, the overall scope of historical network hashrate from day-to-day variability.
H.1	Pseudo-random model based on a scenario whereby mining difficulty (network hashrate) is forced to vary daily between -40% and -10%, making Bitcoin mining easier.
H.2	Pseudo-random model based on a scenario whereby mining difficulty (network hashrate) is forced to vary daily between -10% and 20%, making Bitcoin mining less easy.
H.3	Pseudo-random model based on a scenario whereby mining difficulty (network hashrate) is forced to vary daily between 20% and 50%, making Bitcoin mining more difficult.
H.4	Pseudo-random model based on a scenario whereby mining difficulty (network hashrate) is forced to vary daily between 50% and 80%, making Bitcoin mining very difficult.

The restricted random scenarios (B.0 and H.0) make use of a random variability factor that is demarcated by fixed upper and bottom limits, namely the maximum and minimum daily variability numbers experienced historically, and outlined in Table 16, using the Excel formula shown in Equation 2.

=RAND()*(Upper_Limit – Bottom_Limit) + Bottom_Limit

Equation 2

The value is calculated by multiplying the obtained delimited random value by the bitcoin price or network hashrate value of the same day of the previous year.

For the pseudo-random scenarios (B.1-2-3-4 and H.1-2-3-4), the same formula is used for the calculation of the variable but in this case, a particular outcome is forced on the model. Whilst the values will always lie between the upper and bottom limits obtained from historical values, the purpose of this exercise aims to force a particular behaviour in the predicted bitcoin price and network hashrate.

Table 17. Model and their predictive behaviours

Model Behaviour	Bitcoin Value and Network Hashrate Models
Optimistic (higher profitability)	Models B.1 and H.1
Medium-High profitability	Models B.2 and H.2
Medium-Low profitability	Models B.3 and H.3

Pessimistic (lower profitability)	Models B.4 and H.4

According to Table 17, the optimistic forecast on the behaviour of the system (higher profitability) will occur when the bitcoin value has a positive growth behaviour and a low increase in mining difficulty (network hashrate), as predicted by the models B.1 and H.1, respectively. As the bitcoin value experiences more and more negative variability and/or higher positive variability with regards to the network hashrate, the behaviour will turn more and more pessimistic and render less profitability.

In order to achieve non-changing results, the formula in Equation 2 was frozen under a certain random variability average illustrated below (

The bitcoin price and network hashrate were modelled according to historical data and different forecasting scenarios, portrayed in Table 16.

Table 16) for the different models:

For the bitcoin value model at the delimited random model (B.0), the results shown in Graph 36 are portrayed. The daily average variability is of 17.49% and can range from -23.06% and 20.16% from the previous day.

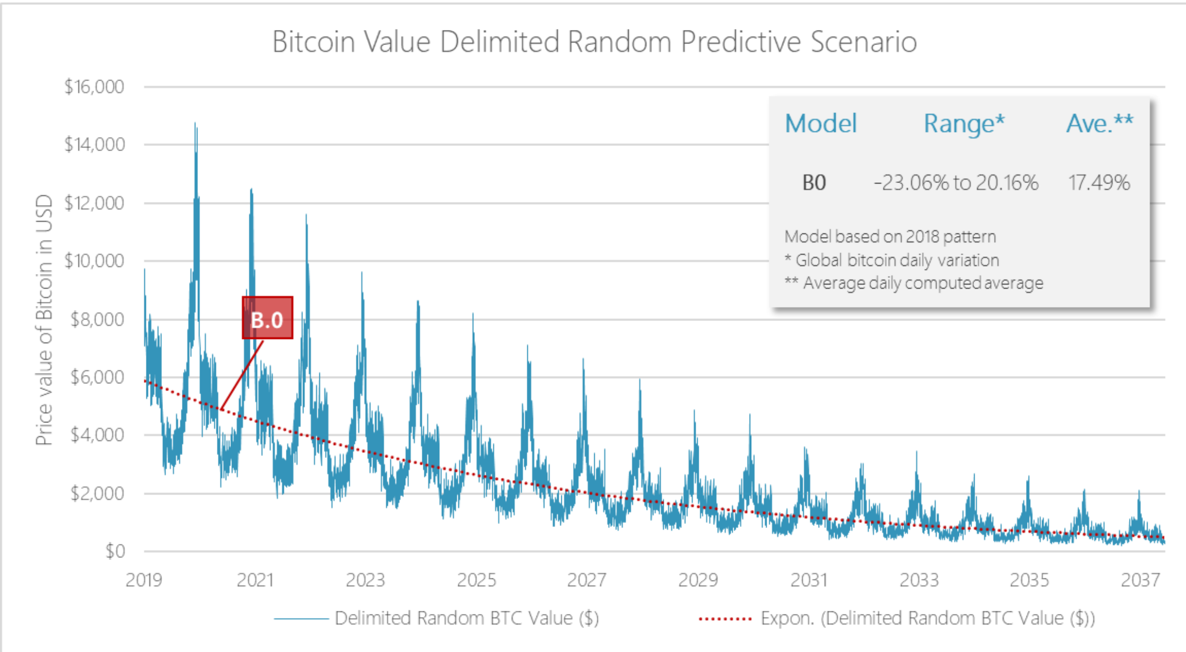

Graph 36. Bitcoin value delimited random predictive scenario (model B.0)

For the pseudo-random scenarios described, the variations shown in Graph 37 portray the positivity or negativity of each model, B1 being the more optimistic and B4 the more pessimistic. In the long-run it is observed that the value falls for all models, given the pattern of the baseline

2008. It is also observed that the average variability correctly falls in between the specified range for each scenario (Graph 37).

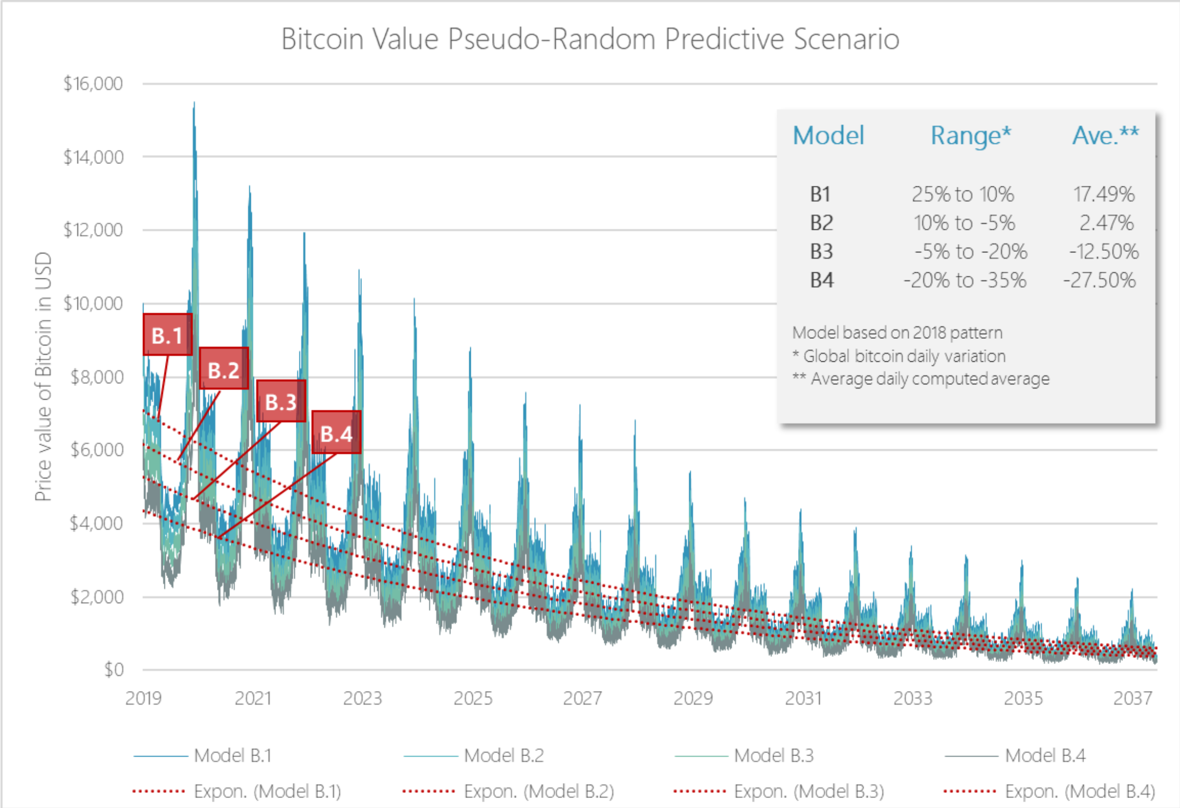

Graph 37. Bitcoin value pseudo-random predictive scenario (models B.1, B.2, B.3 and B.4)

The same exercise has been performed for the network hashrate predictive model. The following are encountered (Graph 38 and Graph 39). The random model (H.0) has an average variability factor of 18.60% between the range -41.22% and 81.18%, and it is observed that the mining difficulty increases over time, considerably from 208 onwards.

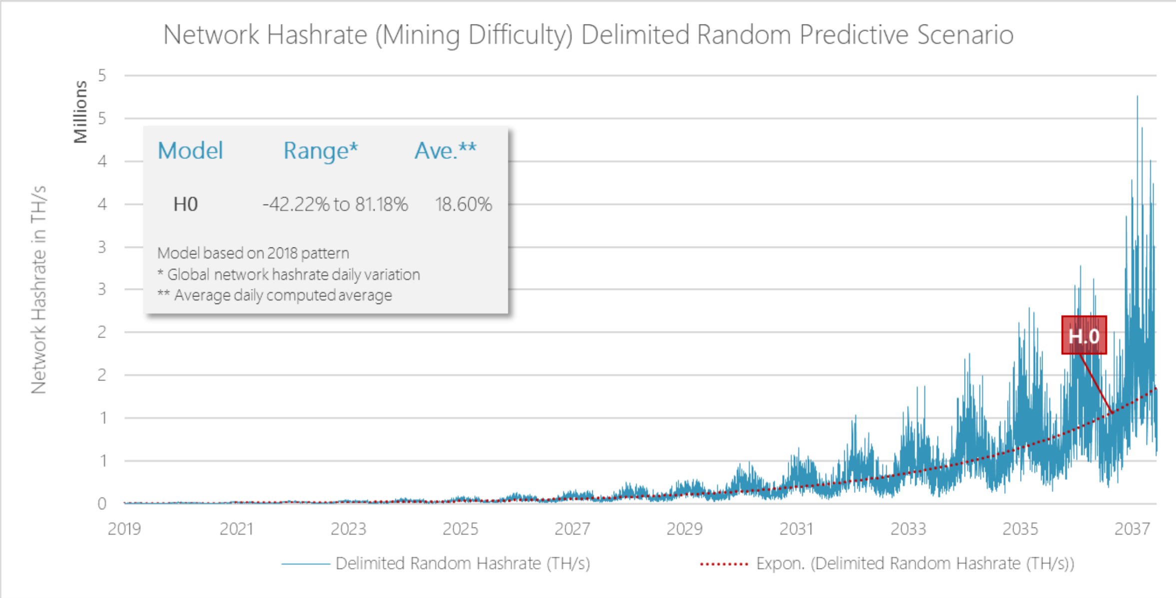

Graph 38. Network hashrate delimited random predictive scenario (model H.0)

For the pseudo-random models (H.1, H.2, H.3 and H.4) is observed that all averages fall in between the specified range as expected. Furthermore, the positivity and negativity of the models can be observed, being the model H.1 the most optimistic as the mining difficulty does not change as much as H.4, for instance.

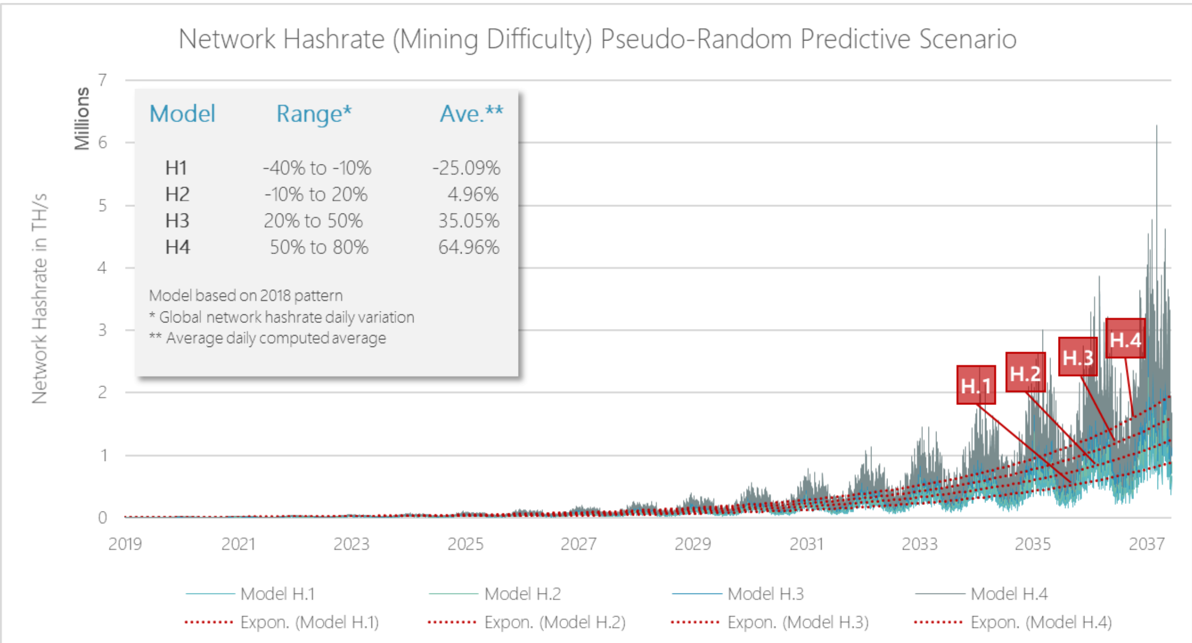

Graph 39. Network hashrate pseudo-random predictive scenarios (models H.1, H.2, H.3 and H.4)

3.3 Solar PV Model Methodology

The photovoltaic system design software PVSyst 6.8.3 was employed for the PV system characterization for the different locations selected, namely Panjib in India, Huelva in Spain and Barstow in the United States.

Through the calculation of the required mining power and energy requirements – including cooling demand – the necessary power and energy production was calculated. Initially, the model was defined for 12.75 kW of nominal power capacity for 10 mining devices of the first-generation ASIC batch 1, 110nm in 2013, i.e. the most demanding mining characterization that concluded in the highest ROI. Additional energy-intensive mining devices could have been added but the ROI would have been negatively affected due to high technological capital costs. However, once the model produced results, the daily generated energy computed from the annual energy output was less than the energy requirements to mine. Therefore, the mining devices from the first batch were reduced to eight for all countries.

The power capacity remains constant for all countries as a point of comparison. Depending on each country, the sun-hours and the energy generation change and that will incur an impact on the overall ROI, NPV and IRR.

3.3.1 Preliminary PV Assessment

A preliminary comparison of irradiation values for different regions of India, Spain and California in the US was performed, combined with an assessment of the available geographical locations and meteorological data included in the PVSyst 6.8.3 database. The meteorological data will determine the sun path throughout the year. Several locations are contrasted, but the following were selected:

- **Panjib** in the Western state of Goa is selected for India. The MeteoNorm 7.2 (1998-2013) station is used as the data source. Appendix A.1.1 provides the meteorological data extracted.
- **Huelva** in the Southern region of Andalusia is selected for Spain. The MeteoNorm 7.2 (1996-2010) station is used as the data source. Appendix A.1.2 provides the meteorological data extracted.
- **Barstow** in the Eastern region of California is selected. The MeteoNorm 7.2 station is used as the data source. Appendix A.1.3 provides the meteorological data extracted.

The detailed meteorological characteristics of every location is also provided in Appendix A.1, including horizontal global and diffuse irradiation, monthly ambient temperatures, the global incident in the collector plane, the effective global energy per area and effective energy at the output of the array, the disposable energy and the performance ratio. The output data for the provided geographical location is performed through a PVSyst hourly-steps simulation throughout a year and extrapolated to all years.

Based on the calculations obtained from the Crypto Model for the mining power requirements, the array nominal net power is set as 12,75 kWp. PVSyst provides a preliminary assessment which allows us to compare the impact on cost of different types of solar cells. Initially, the modules are selected as ground-based, standard, free-standing modules with mono-crystalline cells, but the required area, investment and net energy cost for different types of cells was calculated for comparison purposes (Table 18).

Table 18. Comparison of polycrystalline and thin-film cell technology against monocrystalline cells (PVSyst, 2019)

Compared against Monocrystalline Cells	% Increase in Area Requirements	% Increase in Investment Requirements	% Increase in Energy Costs
Polycrystalline cells	+6.4%	+1.4%	+6.7%
Thin-film cells	+60.3%	+12.2%	+13.3%

3.3.2 Module Angle Optimization

It is assumed that no near shadings exist. The albedo factor is set as 0.26 for fresh grass in Panjib and Huelva, and 0.38 for desertic landscapes in Barstow.

For all cases, the modules are assumed to be fixed tilted planes for which the tilt and azimuth are decided upon the yearly irradiation yield and does not vary according to seasonality. Initially, the simulation is executed with an optimal angle identified through an imprecise trial-and-error approach. The azimuth is defined as the angle between the South point of the horizon and the direction in which the panels face. Once the simulation has produced results, an additional optimization exercise (Table 19) changing the tilt and azimuth from 0° to 50° and -90° to 90°, respectively in 20 steps, concluded the following optimal plane tilt and orientation:

Table 19. Tilt and azimuth optimization for Panjib, Huelva and Barstow

	Optimal Plane Tilt	Optimal Plane Orientation (azimuth)	Global Irradiation kWh/m^2	Energy Generated MWh / year
Panjib, Goa, India	21.2°	-4.7°	1,892.6	19.56
Huelva, Andalusia, Spain	34.2°	4.7°	1,830.4	21.58
Barstow, California, US	34.2°	-4.7°	2,088.9	23.55

A more detailed table is provided in Appendix A.2 (p.120) with the consequent graphs for each location. The simulation was then executed again with the new optimal angles and the results were produced from the new setting.

3.3.3 Photovoltaic System Configuration

To define the PV array system, the planned power of 12.75 kWp – as obtained in the Crypto model – is introduced and a generic brand of PV modules with 60 Si-monocrystalline cells with a nominal power of 250 Wp are selected, with an efficiency profile based on irradiation as shown in Graph 40.

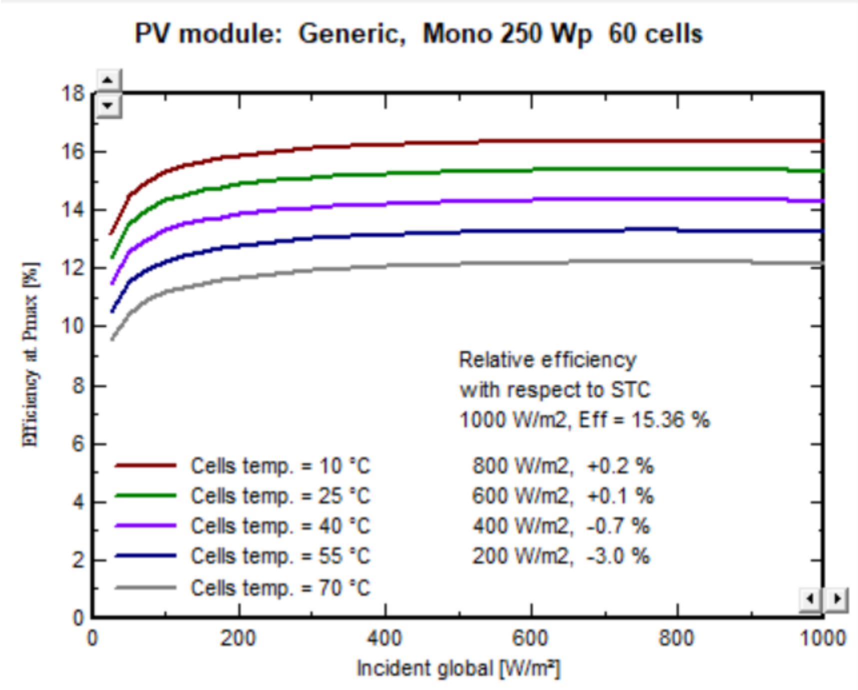

Graph 40. PV module efficiency at maximum power as a function of the incident global irradiation for the selected PV technology (PVSyst, 2019)

Figure 12 shows the schematic of the PV system designed. The PV array is connected to the inverter which converts the DC output into AC for grid purposes. For the cases analysed in this thesis, both selling to the grid and mining locally are envisioned. In practice, a converter (DC-DC, constant voltage) would be used to use the energy locally for mining is assumed to incur the same conversion losses and investment requirements. When analysing the mining versus selling model, the same energy output is taken for simplification purposes, as the energy out of the array versus the energy out of the inverter varies from 6.5 to 7.3% in the different locations.

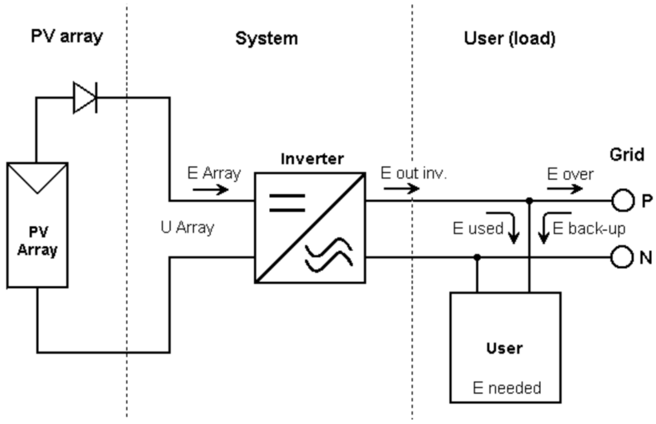

Figure 12. Schematic of the PV system, including the PV array, inverter and load (PVSyst)

Given the nominal power ratio of 1.05 for all cases in Standard Testing Conditions (STC), one inverter is proposed. The 1.2 Wac Santerno inverter (12.2 kW 315-630 V LF Tr 50/60 Hz SUNWAY TG 16-600V) is selected. The modules are arranged in 3 strings with 17 modules in series per string. In total, the system requires 51 modules and 83 m^2 for all locations, given that the power capacity is equal for all. However, energy generation will differ for each location. Table 20 shows a summary of the PV array characteristics for all locations. Given that that there are no sub-arrays, shadings or varying tilts or azimuths, one Maximum Power Point (MPP) is enough.

Table 20. PV array characteristics summary

Characteristic	Value
PV module	Silicon Monocrystalline 250 Wp 60 cells
PV module manufacturer	Generic
Number of PV modules	51
Number of strings	3 in parallel
Modules per string	17 in series
Unit Nominal Power	250 Wp
Array global power (Nominal power at STC)	12.75 kWp
Array global power (Operating cond. 50°C)	11.30 kWp
MPP Voltage	461 V
MPP Current	25 A
Unit module area	1.42 m^2
Total cell area	72.5 m^2
Total PV area	83.0 m^2
Inverter	SUNWAY TG 16 600 V
Inverter manufacturer	Santerno
Operating voltage	315-630 V
Unit nominal power	12.2 kWac
Number of inverters	1
Nominal power ratio	1.05

3.3.4 System Losses

Furthermore, the system losses are defined. The system unavailability due to maintenance is set to 2%, i.e. around 7 intervention days throughout the year allocated randomly. The modules are assumed to be freely mounted with air circulation (no air duct behind or insulation). As a consequence, the thermal loss factor is set to 29.0 W/m^{2}K and the wind loss factor to 0 W/m^{2}K / m/s. The thermal loss effect is portrayed in the loss diagram (Graph 43). The Ohmic or wiring losses occur due to the ohmic resistance ($E_{loss} = R_w \cdot I^2$) between the power output from modules and the array terminals, whereby the ohmic loss reacts to the square of the current. The global wiring resistance was set as default 320 mOhm and the loss fraction at STC 1.5%. Losses with regards to the module quality are also considered with respect to the manufacturer's performance description. The mismatch loss refers to variance between voltage and current characteristics between modules in the array. A string's current is defined by the lower-quality module. The soiling loss was increased for Barstow as it is surrounded by a desertic landscape. Maintenance and other causes for system halts require an unavailability factor of 2% defined as 7.3 days per year in three different periods for all scenarios.

A summary is provided in Table 21 showing the loss fractions which, for purposes of simplicity, remain constant throughout the year and seasons.

Table 21. PV system losses

Characteristic	Value
Thermal Constant Loss Factor	29.0 W/m^{2}K
Wind Loss Factor	0 W/m^{2}K / m/s
Ohmic Losses at STC	1.5 %
Module Efficiency Loss (default)	-0.8 % (over-performance)
Module Mismatch Losses at MPP	1.0 %
Loss when running at fixed voltage	2.5 %
Light Induced Degradation	2.0 %
Strings Voltage Mismatch	0.1 %
System Unavailability	2.0 %
Yearly Soiling Loss Factor	1 % for Panjib and Huelva 3% for Barstow
PV Degradation Factor	0.4 %/yr
I_{mpp} RMS Dispersion	0.4 %/yr
V_{mpp} RMS Dispersion	0.4 %/yr

The incidence effect (IAM) takes the factor n=1.526 for Fresnel smooth glass and has the following fractions for all locations:

Table 22. Incidence effect losses for Fresnel smooth glass (n=1.526) (PVSyst, 2019)

0°	30°	50°	60°	70°	75°	80°	85°	90°
1.000	0.998	0.981	0.948	0.862	0.776	0.636	0.403	0.000

At the same conditions, the array efficiency reduction and increase in losses throughout a time span of 30 years varies slightly for each country given the different ambience temperatures. However, the graphs follow the same curves for all cases. For illustration purposes the efficiency degradation and loss increase for Barstow in California are shown in Graph 41 and Graph 42.

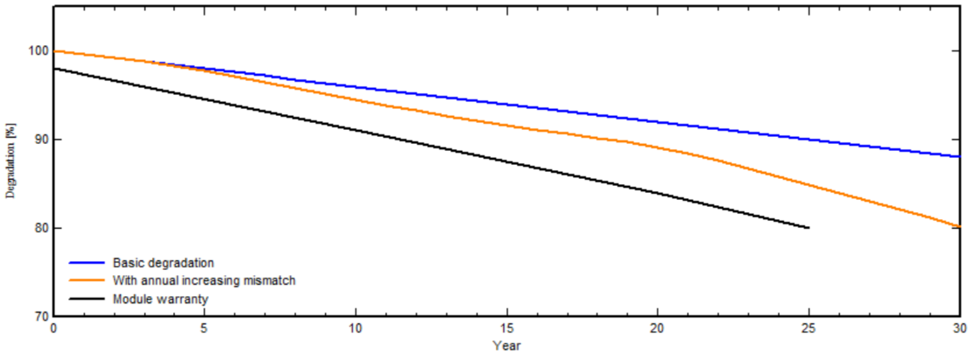

Graph 41. PV system efficiency degradation over time, Barstow (PVSyst, 2019)

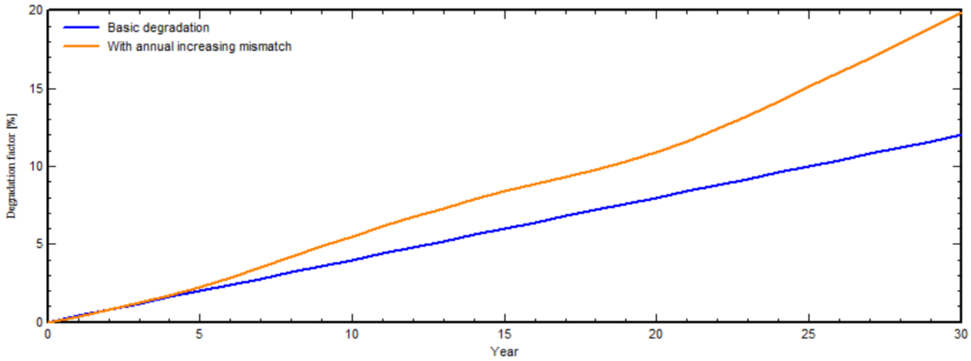

Graph 42. PV system loss increase over time, Barstow (PVSyst, 2019)

Graph 43 portrays the impact of defined losses on current reduction over voltage for the modelled modules with running conditions as follows: irradiance 800 W/m^2, incidence angle of 40°, a beam-global ratio of 80%, an ambient temperature of 20°C and a wind velocity of 1 m/s. The red line shows the nominal conditions.

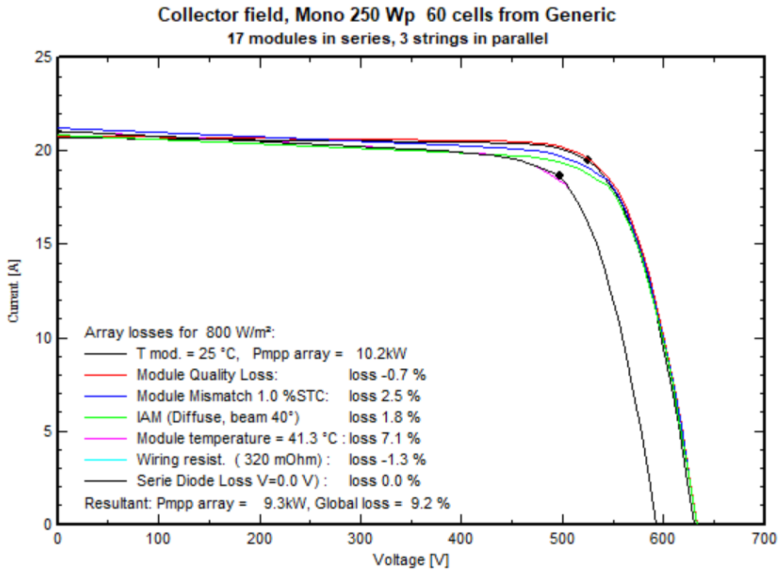

Graph 43. Current-Effect of losses on current-voltage graph (PVSyst, 2019)

3.3.5 Financial Inputs

First, the simulation is run without any financial specifications in order to understand its performance behaviour based on technical parameters. Once the results are satisfying and energy load requirements are met, the financial cost breakdown is inserted in the model. The PV module cost was taken as $212,49 per unit and the inverter as $2,550, equal for all locations.

Appendix A.3 (p.123) shows the sources for the values. Some of them have been slightly adjusted from guidelines to meet requirements. For the purposes of the model, the following financial assumptions in Table 23 have been used as inputs. No tax inputs have been inserted.

Table 23. Financial breakdown for the PV system in the different locations

	Panjib, India	Huelva, Spain	Barstow, US
Capital Costs			
PV modules	$ 10,837.50	$ 10,837.50	$ 10,837.50
Inverter	$ 2,550.00	$ 2,550.00	$ 2,550.00
Studies & Analysis	$ 100.00	$ 100.00	$ 100.00
Transport	$ 6,375.00	$ 7,650.00	$ 7,012.50
Wiring & Installation	$ 7,800.00	$ 9,562.50	$ 8,287.50
Insurance	$101.66	$ 150.00	$ 91.24
Land purchase	$ 6,225.00	$ 19,017.00	$ 2,000.00
Gross Investment	$ 33,989.16	$ 49,866.50	$ 30,878.74
Subsidies	- $ 8,497.29	- $ 17,505.80	- $
Net Investment	$ 25,491.87	$ 32,360.70	$ 30,878.74
Operating Costs			

Maintenance	$ 765.00 / yr	$ 975.32 / yr	$ 595.00 / yr
Inc. inflation (1.00%)	$ 855.99 / yr	$ 1,091.32 / yr	$ 665.77 / yr
Loan			
Rate	0.05 % / yr	0.05 % / yr	0.05 % / yr
Annuities	$ 1,026.32 / yr	$ 1,626.54 / yr	$ 1,560.20 / yr
Total yearly cost (inc. inflation)	$ 1,882.30 / yr	$ 2,392.56 / yr	$ 1,913.93
Cost of produced energy	$ 0.096 / kWh	$ 0.111 / kWh	$ 0.081 / kWh

The electricity sale follows the following inputs based on assumptions and current tariff values. The specific sources are provided in the Appendix A.3. Since solar energy in Huelva does not have the feed-in tariffs and instead competes with the electricity market price, the value has been set to the electricity market value obtained in August 7th, 2019 (Table 24).

Table 24. Tariff settings

	Panjib, India	Huelva, Spain	Barstow, US
Feed-in Tariff ($/kWh)	$ 0.10	$ 0.07	$ 0.14
Duration of tariff warranty (yrs)	30	30	30
Annual tariff variation (%/yr)	0.1 %	0.1 %	0.1 %
Feed-in tariff variation after warranty	-50 %	-50 %	-50 %

3.4 Surplus Energy Model Methodology

The solar capacity installed is able to generate surplus energy aside from the mining and this can be used to make additional profit from different ways. This part of the modelling focuses primarily on the energy storage revenue stream, but two more are analysed, as described in Table 25.

Table 25. Summary table for the surplus energy model methodology

Energy Storage Tab Name	Tab Description
Energy Storage	Calculations with respect to the available electricity generated are calculated here and contrasted with the energy usage for the mining system in each historical period. Battery characterization is performed here, where the model-user can choose different battery settings and see the impact on the cost. From there, profit for different scenarios are calculated: a) All electricity produced by PV is sold to the grid through local FiT and PPA b) Surplus electricity produced by PV is sold to the grid, without energy storage c) Surplus electricity produced by PV is stored and used to mine

	The historical varying feed-in tariffs have been taken for Panjib in India and Huelva in Spain. For Barstow a PPA constant value has been taken since 2013.
Replacement Cost	Sensitivity analysis looking at the impact on profitability based to different replacement costs, and how it differs for the different locations.
ES Analysis	Comparative analysis for the energy storage model.
Electricity Tariffs	Electricity peak and off-peak times for the different locations. For selling to the grid, the feed-in tariffs have been selected. A variation of 0.1% every year with a feed-in tariff warranty of 30 years and a variation of -50% thereafter have been modelled in PVSyst. Therefore, the tariff paid for electricity produced is assumed to remain constant.

For **scenario A** presented in Table 25, the whole of the electricity produced is sold to the grid at the country's tariff price, assumed previously, and the profitability of other system settings are compared against that one.

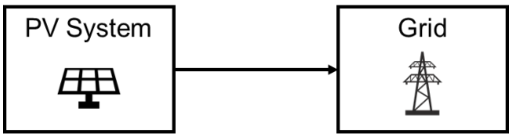

Figure 13. Scenario A system setting

For **scenario B**, the solar PV installation powers the mining system and additional energy generation is sold to the grid at standard pricing.

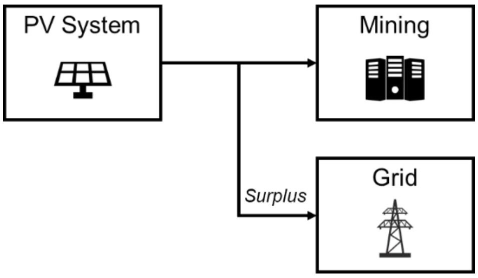

Figure 14. Scenario B system setting

Mining energy requirements versus the actual energy generation for each country is computed in a yearly basis in order to calculate the left-over energy generation yearly. Based on tariff values for each country, the yearly profit from the selling to the grid is calculated for the historical period.

For **scenario C**, the solar PV installation powers the miners and the surplus electricity produced is stored to mine during off-sun-hour period of the day.

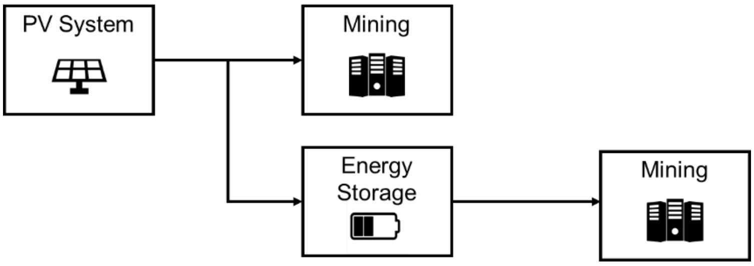

Figure 15. Scenario C system setting

When a battery is included, a Lithium-ion battery modelling scenario is presented with the technical and financial data provided in Appendix A.4 (p.126). Based on the power and capacity requirements, a 0.33 C-rating battery was selected with 15 kW of batter power and 45 kWh of battery capacity. This results in 3-hour charging and discharging rate. The cost of the battery is $800 per installed power (kW) which in turn gives a cost of the battery system of $12,000.

The average replacement cost of $329 per kWh was taken according to Graph 20, assuming a replacement time of 5 years (Zakeri & Syri, 2015). Over the historical duration, the replacement costs add to $20,727. Furthermore, a new mining model was developed calculating the extra hours of mining per day according to the left-over electricity generation as calculated previously and similarly to the initial cryptomining model, the profitability of directing the surplus electricity to mining was calculated. Results are presented in the following chapter.

4 Results, Analysis and Discussion

4.1 PV Model

4.1.1 System Output Results

Having set the previous system parameters, the simulation can be performed based on the dates available in the meteo-data file, and these cannot be modified. Therefore, throughout the years, the same monthly meteorological data is extrapolated to the years forward.

The main results are gathered in Table 26. The produced energy in MWh is the yearly energy output from the PV array design according to loss designation and local irradiation values. The specific production is the energy generated divided by the nominal power of the array at STC. This is an indicator of the system potential taking into account all environmental data and technology orientation. The performance ratio is the energy produced with respect to the energy which would be produced if the system was continuously working at its nominal STC efficiency. The performance ratio indicates the quality of the system, independent of the local irradiance on the collector plane or module efficiency. Appendix A.1 (p.115) provides a summary of the monthly values for the produced energy (E_Out) and the performance ratio (PR) for each location.

Table 26. Main PVSyst simulation results

Main Simulation Results	Panjib, India	Huelva, Spain	Barstow, US
Produced Energy (MWh/year)	19.56	21.58	23.55
Specific Production (kWh/kWp/year)	1,534	1,693	1,847
Performance Ratio	77.27 %	80.63 %	76.97 %

The following graphs (Graph 44, Graph 45 and Graph 46) show the normalized productions per installed capacity shown in *normalized performance index units*, namely kWh/m^2/day, as well as the performance ratio over the months (see values in Appendix A.1.1-2-3). As observed, energy output and capture losses are a function of temperature, which varies for each country with the same installed capacity.

They are higher in months of higher temperatures (contrast against ambient temperature values in Appendix A.1.1-2-3). The performance ratio includes optical losses, array losses and system losses and is not directly related to the monthly irradiation of the location. It is used to assess system quality from input energy and output energy in terms of in-between losses.

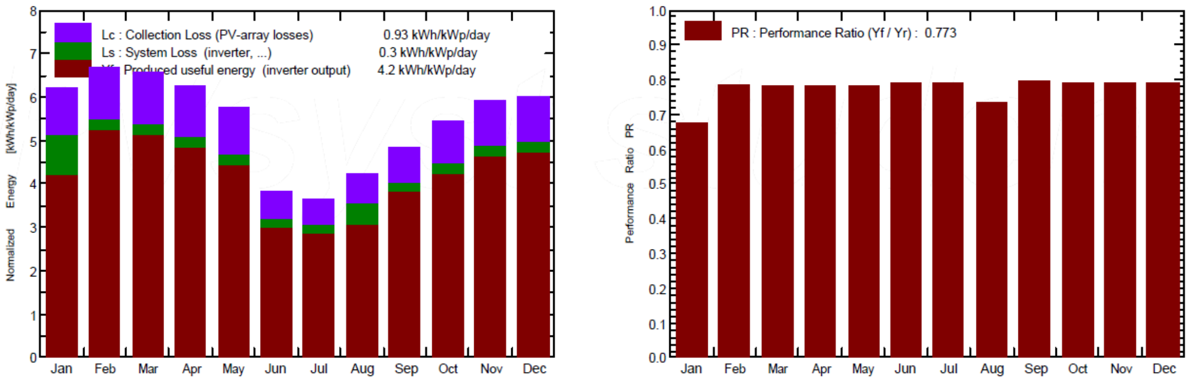

Graph 44. Normalized productions per installed kWp (nominal power 12.75 kWp) and the performance ratio for Panjib

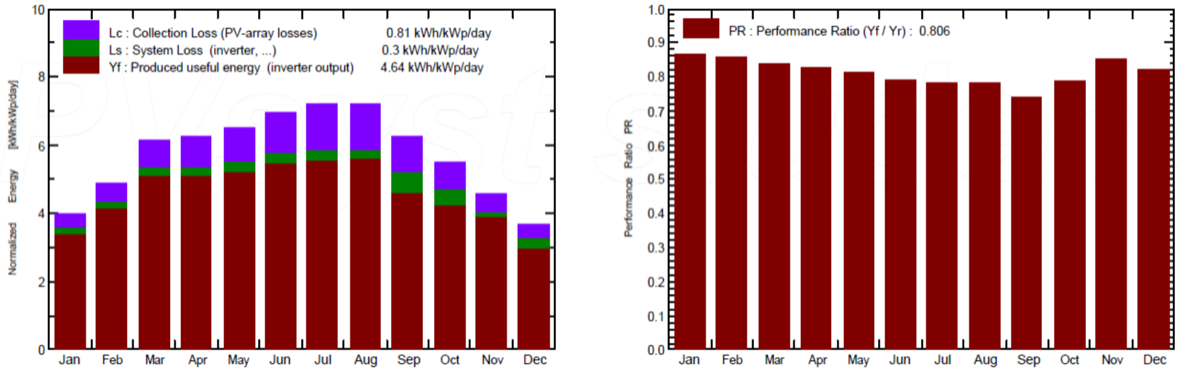

Graph 45. Normalized productions per installed kWp (nominal power 12.75 kWp) and the performance ratio for Huelva

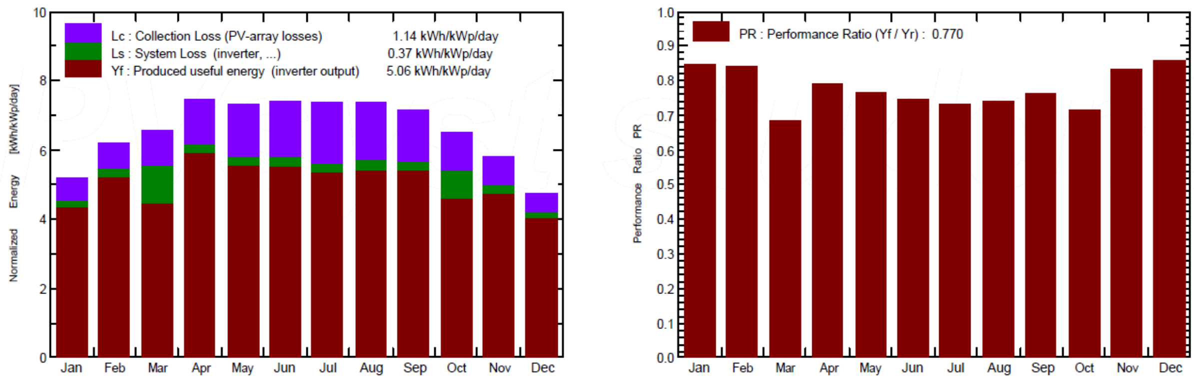

Graph 46. Normalized productions per installed kWp (nominal power 12.75 kWp) and the performance ratio for Barstow

Y_r refers to the reference yield, i.e. the energy production if the system was running at STC efficiency. Y_a is the energy production out of the array or the input for the inverter/ converter. Y_f is the final system yield, i.e. the energy injected into the grid, mining equipment or storage. L_C are the array capture losses, according to Equation 3. L_S are the system losses, as shown in Equation 4 and PR is the performance ratio, as in Equation 5.

$$L_C = Y_r - Y_a$$

Equation 3

$$L_S = Y_a - Y_f$$

Equation 4

$$PR = \frac{Y_f}{Y_r}$$

Equation 5

The Input/Ouput diagrams provided in Graph 47 portray the output energy for each location as a function of the injected energy, i.e. the global incident irradiation in the modules; thus, indicating the general behaviour of each designed system. The saturation of points for large values of the incident irradiation on the collector plane. A straight line indicates a well-designed system (such as for Panjib), whereas the slight curved shape shown for instance for Barstow is due to the temperature effect of the region in particular months. Points that deviate from the curve mean that the system has experienced overload conditions on the grid or that the battery connected reaches its complete capacity. Appendix A.5 (p.127) contains the system output power distribution for each location, whereby the energy injected into the grid is plotted against the power injected to the grid.

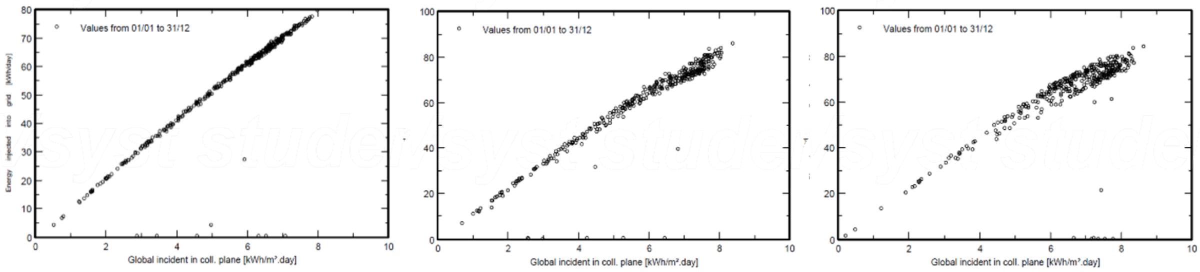

Graph 47. Daily input/output diagrams for Panjib, Huelva and Barstow, respectively

The detailed losses are presented in Appendix A.6 (p.129). Their purpose is to identify any sizing error. As observed, the temperature loss is the largest loss factor from the array nominal energy for all cases: -10.04% for Panjib, -7.14% for Huelva and -9.03% for Barstow. The second largest loss contributor is the inverter energy loss during operation.

4.1.2 Financial Results

Table 27 presents a summary of the main results. For the calculation of the LCOE, a warranty period of 30 years was taken, and Equation 6 was applied:

$$LCOE\ (\$/kWh) = \frac{I}{E_p \cdot 1{,}000 \cdot P_W}$$

Equation 6

Where I is the net investment, E_p is the energy produced in MWh which needs to be converted to kWh by multiplying times 1,000, and P_W is the warranty period selected.

Table 27. Main financial results

Main Financial Results	Panjib, India	Huelva, Spain	Barstow, US
Total Yearly Cost (incl. inflation 1%) ($/yr)	$ 1,882.30	$ 2,392.56	$ 1,913.93
Cost of Produced Energy ($/kWh)	$ 0.096	$ 0.11	$ 0.081
CAPEX per Capacity Installed ($/kW)	$ 2,665.82	$ 3,682.58	$ 2,416.79
OPEX per Energy Generated ($/kWh)	$ 0.04	$ 0.04	$ 0.03
Warranty Period (years)	30	30	30
Net Cost ($)	$ 25,491.87	$ 32,360.70	$ 30.878.74
Specific Cost ($/Wp)	$ 2.00	$ 2.54	$ 2.42
LCOE ($/kWh)	$ 0.043	$ 0.051	$ 0.044
Payback Period (years)	22.9	undefined	11.7
Net Profit at end of lifetime	$ 2,215.38	- $ 22.947.90	$ 34,825.45
ROI	8.7 %	-70.9 %	112.8 %

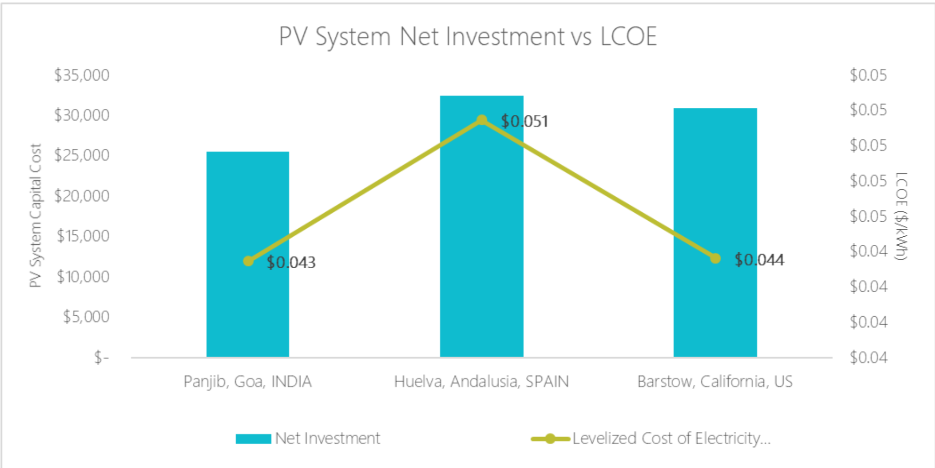

Graph 48. PV system net investment versus. calculated LCOE

According to the tariff values proposed and the financial inputs (Chapter 3.3.5), the financial results for each location, portrayed in Graph 63, Graph 62 and Graph 61 of Section 4.5.1, including the yearly net profit and the cumulative cashflow from selling to the grid. A detailed breakdown in numbers can be checked in the Appendix A.7 (p.131).

The simulation indicates that the project is not worth to develop in Huelva Spain, as the net profit from selling to the grid at electricity market price is too competitive for the high capital costs of a 12.75 kW capacity solar power plant. Only 29.1% of the costs are amortized at the end of the time frame and consequently, the ROI is negative. The most favourable option is the 12.75 kW solar plant in Barstow due to the low prices and high energy generation throughout the year with a ROI of 112.8%. The system in Panjib only achieves a modest ROI of 8.7% in a late amortization period due to the high capital costs and relatively low tariff.

4.1.3 CO_2 Balance

A CO_2 balance simulation was also performed. The energy generated from the solar PV farm in the different locations replace an equal amount of grid electricity and reduce the overall carbon footprint of the overall network. The CO_2 emissions savings across the entire length of the project is calculated, in this case set as 30 years.

The lifecycle emissions for the modules and supports based on the nominal power capacity help towards the calculation of produced emissions in tonnes of CO_2, whereby Equation 7 is used.

$$E_P = E_M + E_S = (LCE_M \cdot P_N) + (LCE_S \cdot Q_S)$$

Equation 7

Where E_P refers to the produced emissions, E_M to the modules' total emissions and E_S to the supports' total emissions. E_M is calculated by multiplying the lifecycle emissions of modules ($kgCO_2/kWp$) times the nominal power or installed capacity of solar panels P_N (kWp). E_S is calculated by multiplying the lifecycle emissions of supports ($kgCO_2/kg$) times the total quantity of supports required Q_S measured in mass units (kg).

Table 28 offers a summary of produced and replaced emissions for each system, based on grid lifecycle emissions data from the IEA for the corresponding country in 2010. The rest are calculated form the PVSyst database (PVSyst, n.d.). This only applies if the electricity produced is injected back into the grid and not used for mining.

Table 28. Produced and replaced emissions for each PV system

	Panjib, India	Huelva, Spain	Barstow, US
Modules			
LCE Modules ($kgCO_2$ / kWp)	1,713	1,713	1,713
Quantity (kWp)	12.75	12.75	12.75
Subtotal ($kgCO_2$)	21,837	21,837	21,837

Supports			
LCE Supports ($kgCO_2$ / kg)	6.24	1.91	3.52
Quantity (kg)	510	510	510
Subtotal ($kgCO_2$)	3,184	976	1,796
Produced emissions (tCO_2)	25.02	22.81	23.63
System Production (MWh/yr)	19.56	21.58	23.55
Lifetime (years)	30	30	30
Annual degradation	1.0 %	1.0 %	1.0 %
Grid Lifecycle Emissions (gCO_2/kWh)	936	287	528
Replaced emissions (tCO_2)	549.2	185.8	373.1
Emissions balance (tCO_2)	451.5	138.4	300.1

Over the entire duration of the PV installation, Panjib is the one that replaces more carbon savings over its lifetime (451.5 tCO_2), whereas Huelva saves the least (138.4 tCO_2). This is interesting because precisely Panjib has the highest LCE for the supports which contribute to higher produced emissions (25 tCO_2), and Huelva the least (22.81 tCO_2). In addition, Huelva and Barstow generate more green energy per year than Panjib and therefore one could expect that there would be a greater CO2 replacement potential from these two countries, rather than Panjib. However, replaced emissions take into account the grid lifecycle emissions for each country which is considerably larger for each country, using Equation 8.

$$E_R = G\left(\frac{\mathrm{gCO_2}}{\mathrm{kWh}}\right) \cdot 1000\left(\frac{\mathrm{kWh}}{\mathrm{MWh}}\right) \cdot E_G\left(\frac{\mathrm{MWh}}{\mathrm{year}}\right) \cdot t\ (\mathrm{years}) \cdot d(\%)$$

Equation 8

where E_R is the emissions replaced, G are the grid lifecycle emissions, E_G is the system generated energy, t is the lifetime of the PV installation and d is the annual degradation. Appendix A.8 (p.134) shows the gradual increase in the balance over time and Huelva takes a couple more years to reach positive CO_2 balance.

According to PVSyst, finding appropriate values for the lifecycle emissions of modules and supports is the major obstacle in this calculation, as there is little knowledge on how panels and supports have been manufactured (PVSyst, n.d.).

4.2 Mining Model

For each country, the following results shown in Table 29 are obtained at baseline conditions for mining from solar PV (Table 14), with no electricity injection from the grid in the historical timeframe. The capital costs are $22,132 for all countries when using the highest ROI configuration.

Table 29. Aggregate results for the historical period between 24th April 2013 to 23th July 2019

Country	Aggregate Revenue $	Net Electricity Savings	Return on Investment	Payback Time days
Panjib, Goa, India	$ 50,424.88	$ 3,320.47	127.84 %	50
Huelva, Andalusia, Spain	$ 52,808.60	$ 10,560.89	128.61 %	46
Barstow, California, US	$ 51,207.23	$ 8,378.13	131.37 %	48

Huelva is the most profitable location for mining. Even though it represents the country with the least number sun-hours (which is only one decimal smaller than India's), it has a very low sun unavailability rate across the year which elevates its potential to be able to have more mining capability throughout the year. Furthermore, Spain is the location where one can see gains from a savings approach. The savings gap is greater for Spain when mining from solar PV rather than using grid electricity, than for any other country, especially India. Nonetheless, the aggregate revenue for Spain is still the highest without considering the net electricity savings, and the one with the lowest payback time.

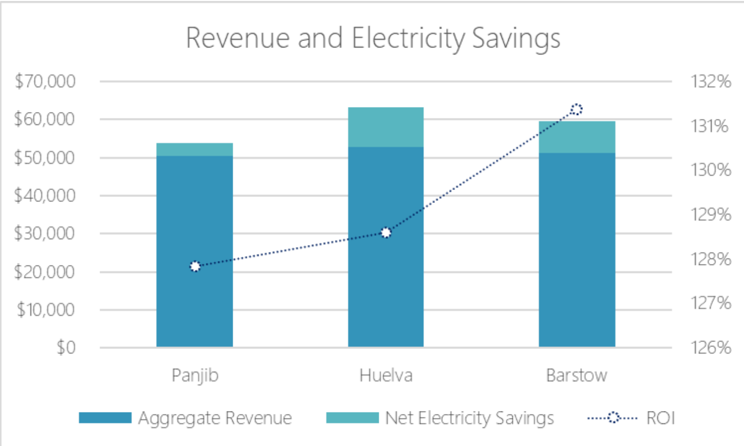

Graph 49. Mining revenue, electricity savings and ROI for each location during historical period

It is still worth mentioning that the peak sun-hours are roughly the same for all three countries, and that unavailability varies from 12.3% to 22.2% for all three countries (less than 10% difference). As observed in table the system profitability is not as varying for all three countries with a 4.7% minimum and maximum change, and yet the net electricity savings is what varies to a larger extent, namely 218% throughout the historical period of 2013 to 2019. However, the electricity savings should come in substituted by the solar PV capital costs and payback times. Given that a further analysis will be created, this will be discussed in Chapter 4.5, how all parts of the global system come together (PV, mining, storage, predictive modelling).

The concern with the approach modelled is that the reward is not always proportional to the amount of energy invested into mining, and that profitability is not made as daily contributions. The reality is that not always the model would be able to mine a block with the consequent bitcoin reward and it would only receive the bitcoins once this block is released into the network. Furthermore, the model assumes that the bitcoin value is sold instantaneously, acquiring the closing price value in US dollars of that day.

As observed in Graph 50 presented for Panjib in India (Huelva and Barstow follow the similar patterns), the daily revenue is very high during high Bitcoin price value and reaches a point where the daily profitability is not considerably large. The high-growing cumulative revenue stalls between 2013 and 2014, following a very gradual increase until 2019.

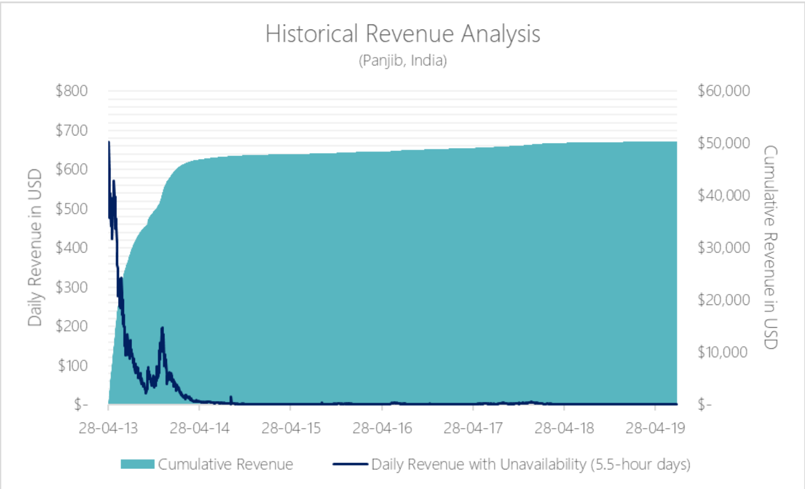

Graph 50. Historical revenue analysis for Panjib, India

4.2.1 ROI Sensitivity Analysis

A sensitivity analysis has been performed to understand the impact on the model's ROI if the peak-sun hours, power unavailability or electricity costs change.

The model includes two ROI formulas: one that only takes into account revenue and CAPEX (Equation 9), and the second takes into account the energy savings from otherwise consuming electricity from the grid (Equation 10). The first is used to calculate the model's ROI and to understand the impact of a change in sun-hours and power unavailability on that ROI. The second is used to understand the impact of a change in electricity cost on the ROI from Equation 10.

$$ROI_1 = \frac{R - CAPEX}{CAPEX}$$

Equation 9

$$ROI_2 = \frac{(R + S) - CAPEX}{CAPEX}$$

Equation 10

Where R refers to the revenue after the unavailability factor has been included, S refers to the electricity savings incurred depending on the electricity cost for each location, and the $CAPEX$ are the capital costs for the mining equipment.

Power Unavailability Impact on ROI

As previously explained, power unavailability refers to the number of days where the sky is not clear, and it is assumed that there is no solar irradiation reaching the collector planes. For Panjib, Huelva and Barstow, 65, 45 and 81 days a year are assumed which leads to a 17.8%, 12.3% and 22.2% power unavailability factor. This data is only used for the mining model as the PVSyst model has more intricate data knowledge in its simulation performance.

The sensitivity analysis seeks to understand the impact that a power unavailability of 5%, 10%, 15%, 20% and 25% would have on the overall ROI, keeping the sun-hours and electricity cost inputs as constant, as presented in Table 14.

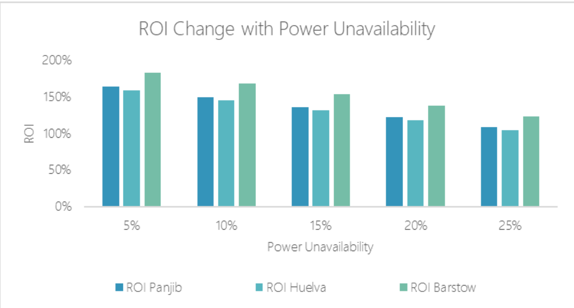

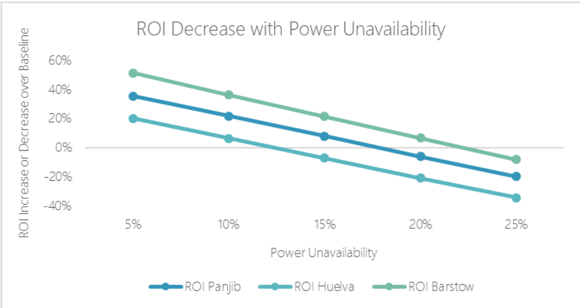

Graph 51. Mining ROI change with power unavailability at each location (absolute value and % change)

As expected, the ROI would be negatively impacted in all countries if power unavailability increases (Graph 51). A 5% power unavailability factor would have a greater impact on the ROI for Barstow than Huelva and Panjib for instance because in addition to more availability it has a greater number of sun-hours, and because it is the one that has most to gain since it has a very high baseline power unavailability factor.

Sun-Hours Impact on ROI

The average sun-hours vary from region to region. Barstow is the location with the highest number of hours, but for all countries the sun-hours vary from 5 to 7.5. The more sun-hours, the more energy generation potential and therefore, the more mining potential as well as consequent profitability. A sensitivity analysis has been performed to understand the impact on the ROI based on the number of sun hours from 4.5 to 7.5 in steps of 0.5 hours, keeping power unavailability and electricity price inputs as constant, as presented in Table 14.

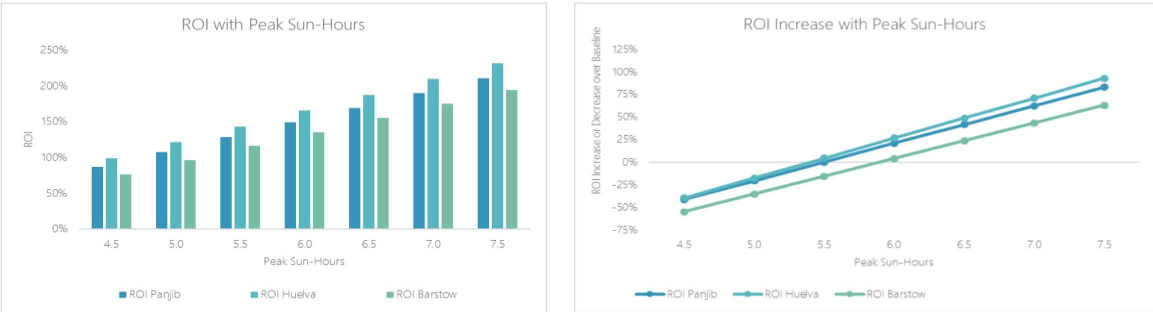

Graph 52. Mining ROI change with sun-hours at each location (absolute value and % change)

As observed in Graph 52, ROI follows an upward trend with greater number of sun-hours. The trend line for Huelva follows a much larger rise as the number of sun hours is what limited it from being as irradiated as the other countries, since its power unavailability factor is the smaller of all options (Table 14).

Electricity Costs Impact on ROI

Electricity costs tend to be readjusted year on year and a small percentage increase or decrease tends to be put forward. An analysis to understand the impact on electricity costs in the electricity savings has been performed as a function of the ROI shown in Equation 10. The variability of the electricity costs ranges from -5% to 5% in steps of 0.01, keeping power unavailability and sun-hours inputs as constant, as presented in Table 14.

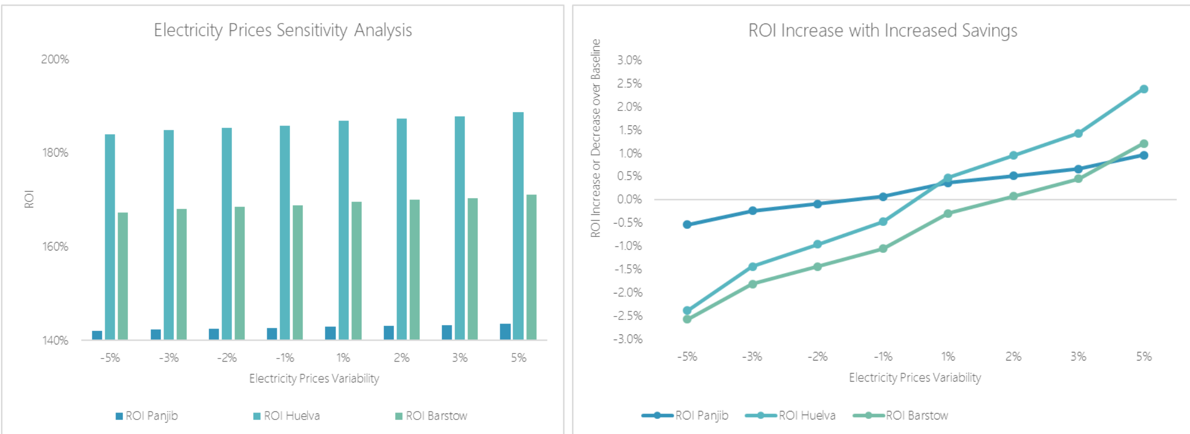

Graph 53. Mining ROI change with sun-hours at each location (absolute value and % change)

As observed in Graph 53, the change in electricity prices does not change the ROI exceedingly compared to the previous change in variables, the maximum change being of -2.6% from baseline in the case of Barstow. The impact of electricity price changes is much greater in Huelva for which the baseline value is the highest, and therefore the percentage decrease or rise is the greatest as well.

4.2.2 NPV and IRR Analysis

The Net Present Value (NPV) and Internal Rate of Return (IRR) where calculated for the years of the historical model. The IRR indicates that at that hurdle rate the NPV would be zero. Because it is positive, it indicates a positive value for the project. All three locations have a positive IRR, mainly due to the revenues made during the first year. For purposes of simplicity, the whole mining CAPEX was assumed on Year 0 and not according to technology evolution. Furthermore, because it has been looked at the time period of the historical account, some years have experienced some profitability all days of the year (2014 to 2018) and others only partially (2013, 2019).

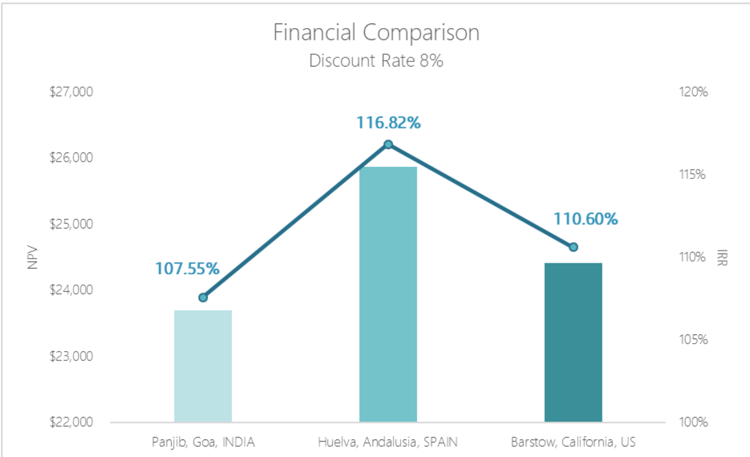

Graph 54. NVP comparison of the mining system located in different locations

From Graph 54 it is observed that Huelva in Spain has the highest NPV and IRR, whereas Panjib in India has the least, albeit still profitable for the time-period presented. This is mainly because even though Spain has the least sun-hours (i.e. mining time in the day) it has the lower power unavailability (i.e. mining days in a year) which gives it an advantage for mining potential from solar PV. Barstow on the other hand, has the highest sun-hours but it also has the highest power unavailability and therefore it's mining potential and consequent profitability are lower.

The discount value taken for the analysis was 8%. Performing a sensitivity analysis of the discount value (Graph 55), the impact is perceived greater in the system of Panjib in India and the least in Huelva. This is related to the absolute value of cashflows, lower in India than in other locations.

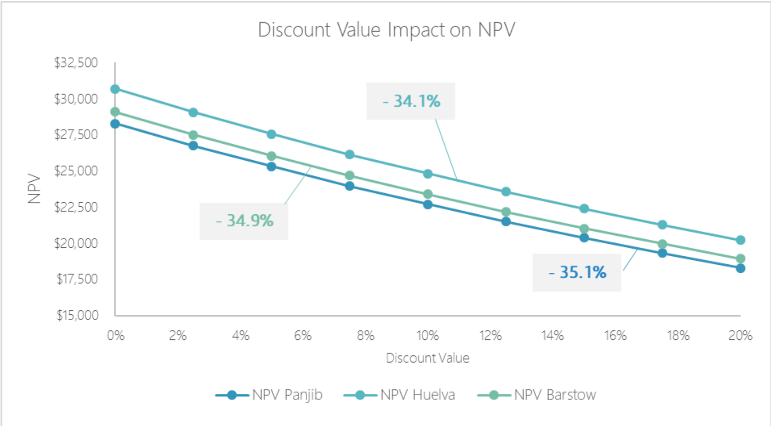

Graph 55. Discount value impact on mining NPV for all locations

4.3 Additional Profitability from Surplus Electricity

The energy storage results page gathers results for more than just energy storage calculations. If we retake on the scenarios presented in Chapter 3.4, the following results shown in Table 30 are presented for each country and case.

Table 30. Summary of additional profitability from surplus electricity

	Panjib	Huelva	Barstow
Scenario A All PV electricity generation is sold to the grid	$11,792.33	$9,437.16	$22,962.80
Scenario B PV electricity generation is used to mine, and surplus is sold to the grid	$7,490.04	$6,193.99	$15,306.88
Scenario C PV electricity generation is used to mine, surplus is stored and then used to mine in off-sun-hour periods	$487.99	$8,479.18	$22,907.72

Graph 56 represents the same data in a way that it is more intuitive to see the long-term profitability of each scenario for each country.

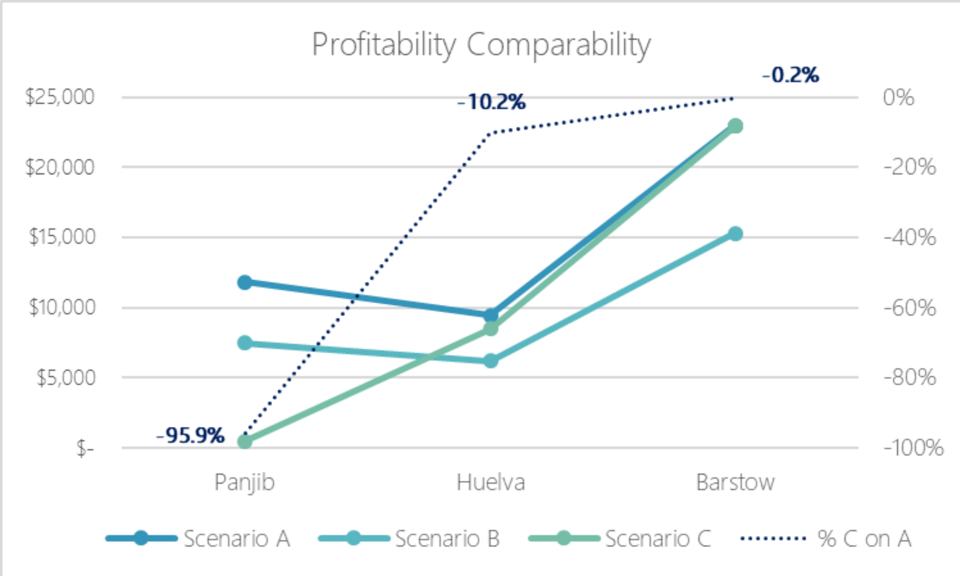

Graph 56. Profitability comparison between the different countries with respect to additional revenue streams

As one can observe, the profitability of Panjib in India would much better off selling all PV electricity to the grid, as the tariff considered is high and steady. Investing in mining equipment (Scenario B) would still be profitable, but 36.5% less so. Additionally, investing in batteries to store surplus electricity (Scenario C) would in the long-run leave the system with a profitability of merely $488, a profit loss of 95.9% from selling all electricity to the grid, represented by the line of Scenario C on Scenario A.

Huelva in Spain presents a different case. In this case, investing in energy storage to continue mining (Scenario C) is more profitable than just investing in mining equipment and selling surplus to the grid (Scenario A). Scenario C on A appears much more favourable than for the case in India as it only represents a 10.2% profit loss over the maximum. However, the market value changes and whilst the electricity price for generated was chosen as $0.7 per kWh, it can reach $0.4 values making Scenario A and B less favourable towards profit-making. Nonetheless, at the established electricity price, Scenario A still appears to be the most profitable.

The case for Barstow favours even more energy storage (Scenario C). Whilst Scenario A remains the most profitable due to the high tariffs for solar energy in California, Scenario C only diverges 0.2% below the top value. Investing in energy storage in Barstow is 94.3% more profitable than selling the electricity to the grid in India. In this case one would recommend to invest in energy storage as mining profitability historically renders worth it when facing grid electricity changes in price and allows for the mining profitability to be completely independent from the grid.

4.3.1 Replacement Cost Sensitivity Analysis

As aforementioned, the average value for battery replacement costs was taken. However, a sensitivity analysis of the replacement cost which can range from $185/kWh to $550/kWh for Lithium-ion batteries was performed against the profitability of an energy storage system, giving different results for the different countries. It is concluded that the energy replacement costs have a considerable impact on the profitability of the energy storage model and therefore should not be overlooked.

For Panjib, the profitability reaches a negative point with a battery replacement cost of $472 per kWh (Graph 57). The profitability ranges from $12,890 in the lower limit of replacement cost to a negative value of -$3,535 from the upper limit of the replacement cost. The profit variability compares how much profit changes with respect to the previous profit value calculated from $1 less of replacement cost.

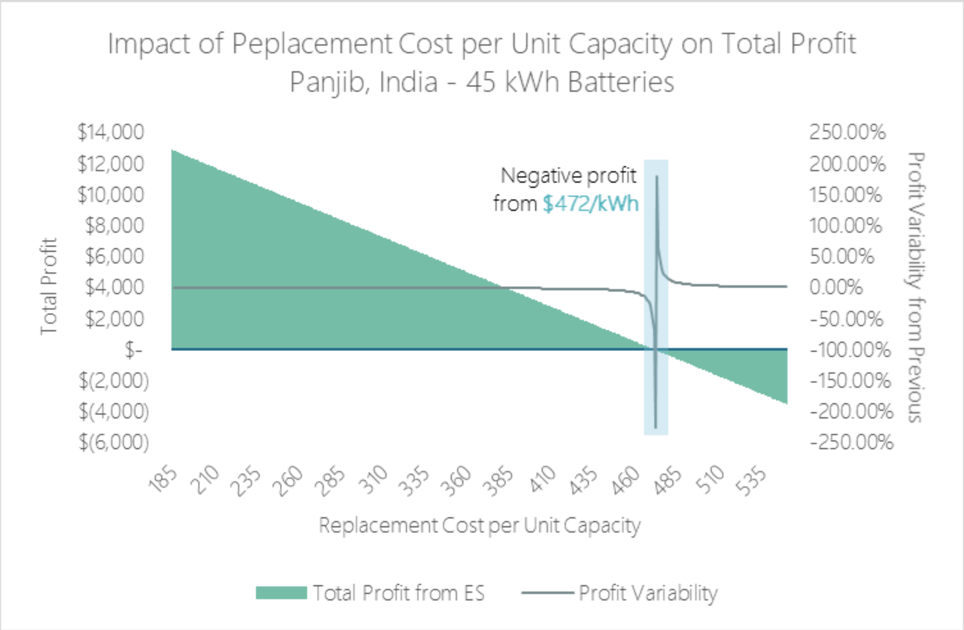

Graph 57. Impact of replacement cost per unit capacity on total profit for Panjib

For Huelva and Barstow, the profitability does not reach a negative value but reduces substantially the overall profit. For Huelva, at the lower limit of cost replacement profitability reaches $20,881 and at the upper limit it can still make a profit of $4,456 (Graph 58). For Barstow, the profitability is at $35,310 in the upper limit and $18,885 in the lower limit (Graph 59), where the variability is presented as lower (-0.24%) than for Huelva (-1.00%).

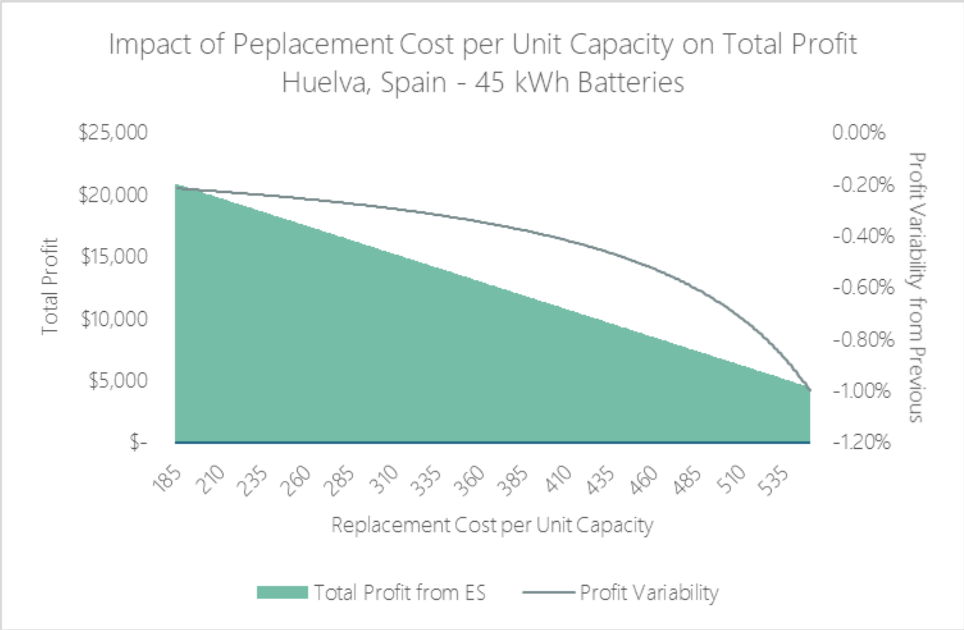

Graph 58. Impact of replacement cost per unit capacity on total profit for Huelva

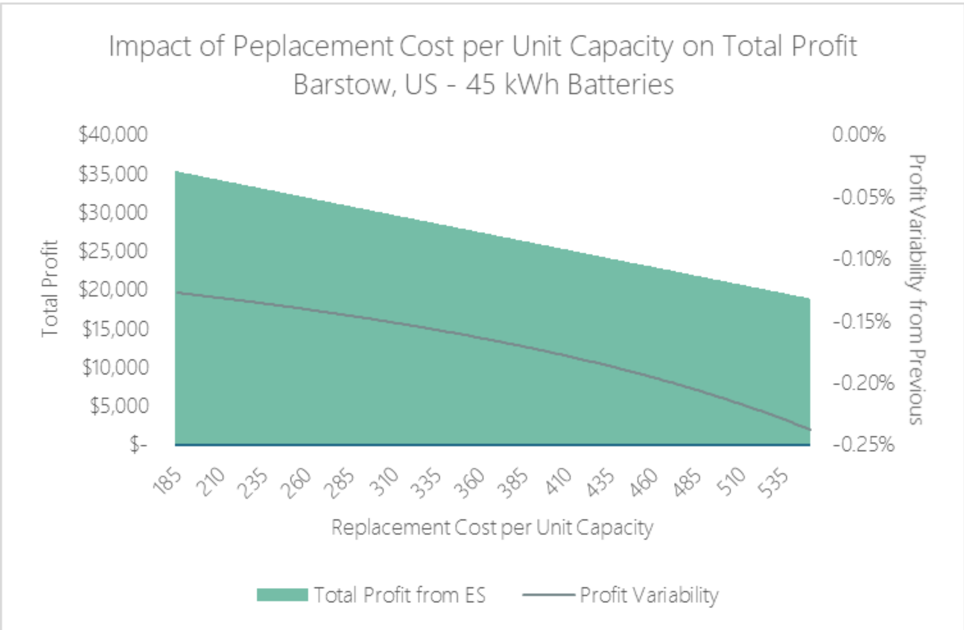

Graph 59. Impact of replacement cost per unit capacity on total profit for Barstow

4.4 Predictive Profitability for Mining

Based on the methodology discussed in Chapter 3.2.2, the following data is obtained for the combination of models presented in Table 31, based on Table 16:

Table 31. Model combinations analysed for the predictive results

Analysed Model Combination	Definition
B0-H0	Random scenario
B1-H1	Optimistic scenario

B2-H2	Medium-high profitability scenario
B3-H3	Medium-low profitability scenario
B4-H4	Pessimistic scenario

The profit simulation was analysed assuming that in 2018 a mining technology was using a hashrate of 1.35E+13 H/s with a power consumption of 3.08 kW (like the ASIC Antminer S9, 16nm). It was assumed that every 2 years there would be a new adoption of more efficient mining technology with an increased hashrate of 900% (i.e. an additional order of magnitude) with a starting cost of $7,000 but with an increasing rate of 10% per technology adoption.

Appendix A.9 (p.135) presents the detailed prediction results for each location (Panjib, Huelva and Barstow), including the daily revenue as well as the cumulative revenue for each scenario combination (B0-H0, B1-H1, B2-H2, B3-H3, B4-H4). The results have been summarized in Graph 60. Huelva experiences the higher predicted profit and ROI based on the 2008 pattern and the baseline conditions. Considering the same technological assumptions, Panjib and Barstow follow a similar pattern given a similar number of sun-hours and varying power unavailability factors. As expected, the optimistic scenario (B1-H1) is the most profitable setting. It is 65.5-65.9% greater than B2-H2 for all scenarios, whilst B2-H2 is 52.4-52.6% than B3-H3 for all scenarios, and B3-H3 is 52.7-52.9%. The ROI presented in Graph 60 was calculated using Equation 9, after having calculated a net capital cost from technology substitution (based on the data provided in the preceding paragraph) which amounted to $111,562 at the end of the project lifetime, with a 10% increase on the starting cost upon the 2 years of technology duration.

The ROI is very high for all cases (between 1,000% and 1,500%) considering only capital costs and no operating costs, as the energy would come from the “free” solar energy.

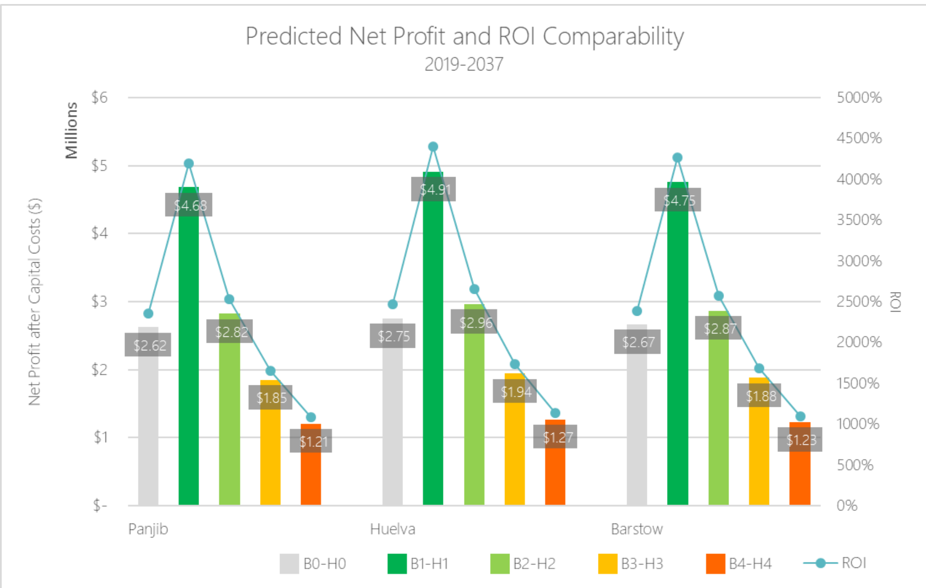

Graph 60. Predicted net profit and ROI comparability from the period 2019-2037

4.5 Integrated Analysis

The integrated approach seeks to analyse the profitability of the three scenarios with all system components, namely the PV system, the mining system and the energy storage, when applicable, and at different predicted scenarios. Capital costs, operating costs and so on are considered in this case, as the analysis is approached from a financial point of view.

4.5.1 Scenario A

Scenario A analysed the profitability of selling the electricity generated to the grid for each location. This analysis was performed through PVSyst 6.3.8 assuming a constant feed-in tariff as outlined in the solar methodology (Chapter 3.3) and in the case specification for each location. According to the input data, the solar profitability achieves a net profitability of $34,825 at the end of project lifetime for Barstow after paying-off capital costs and annuities, with an overall project ROI of 112.8% and a payback of 11.9 years. The yearly net profit and cashflow are presented in Graph 61.

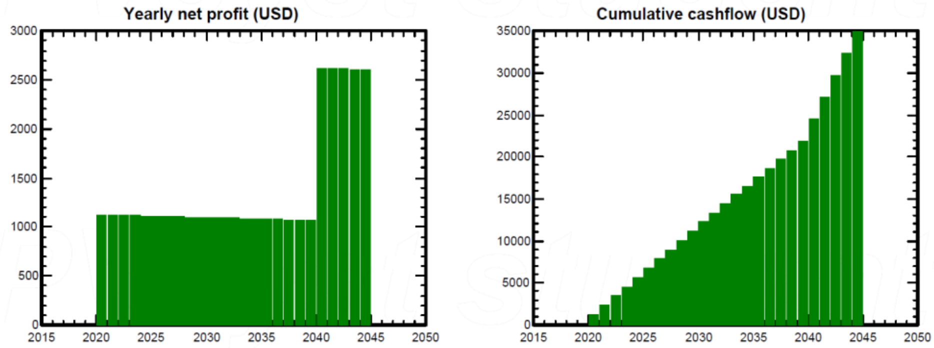

Graph 61. Yearly net profit and cumulative cashflow for Barstow, US

Huelva follows the opposite reaction. Given the competitive reward for providing electricity in the energy market, it does not gather enough yearly profit to have a positive cumulative outcome at the end of the project lifetime. At the end of the project lifetime is would be in a negative value of -$22,948 with a ROI of -70.9%. In addition, these values would be further aggravated as the solar tax wasn't included in the model. The yearly net profit and cashflow are presented in Graph 62.

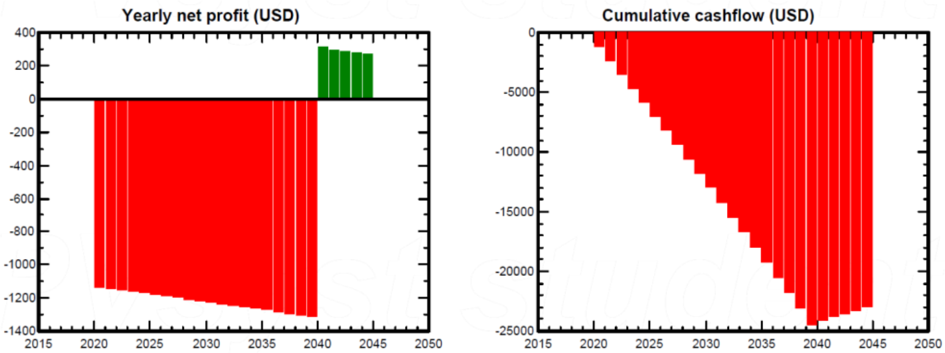

Graph 62. Yearly net profit and cumulative cashflow for Huelva, Spain

Panjib experiences an intermediate outcome. Selling the generated energy to the grid at the set tariff, it would only make \$2,215 after paying off capital costs and annuities, with an overall project ROI of 8.7% and a payback time of 22.9 years, without considering local taxes. The yearly net profit and cashflow are presented in Graph 63.

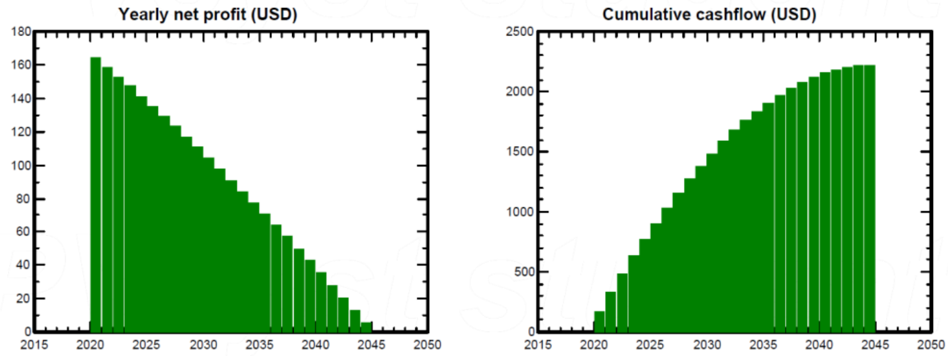

Graph 63. Yearly net profit and cumulative cashflow for Panjib, India

4.5.2 Scenario B

Scenario B considered the case whereby electricity produced by solar PV is used to mine for 25 years and the surplus is sold to the grid. The surplus electricity was calculated in order to find out how much this would pay at baseline tariff rate, assuming a PPA or a tariff agreement was performed at the beginning of the project for 25 to 30 years, even though 25 years is the time of interest.

In this scenario the PV and mining infrastructure were subtracted from the total profitability coming from the mining activities and electricity generation costs as shown in Equation 11.

$$P_{n,2} = P_{M,h} + P_{M,p}\left(B_0 - H_0 \,||B_1 - H_1||B_2 - H_2||B_3 - H_3||B_4 - H_4\right) + P_{G,h} + P_{G,p} - I_{PV} - I_{M,h} - I_{M,p}$$

$$\forall \; Locations \; (Panjib, Huelva, Barstow)$$

Equation 11

Where $P_{n,2}$, the net profitability for scenario 2 is calculated by subtracting investment requirements from the revenue each investment brings forth. $P_{M,h}$ is the historical mining profitability, $P_{M,p}$ is the predicted mining profitability which can be either for models $B_0 - H_0$, $B_1 - H_1$, $B_2 - H_2$, $B_3 - H_3$ or $B_4 - H_4$. Furthermore, $P_{G,h}$ is the profitability made from selling to the grid up to 2019 and $P_{G,p}$ is the predicted grid gains. On the investment side, I_{PV} is the net investment required to build the solar PV farm, $I_{M,h}$ is the historical net investment for the mining equipment modelled and $I_{M,p}$ is the predicted net capital costs for the mining equipment in the future.

The overall outcome is shown in Graph 64 whereby the net profitability for each predicted scenario is modelled for each country. Huelva is the most profitable location even though in Scenario 1 the model predicted the opposite. Under the pessimistic scenario of Bitcoin value and network difficulty (B4-H4) at the end of the lifetime it would have produced $1.27 million dollars and on the most optimistic scenario it would have reached $4.9 million dollars within the 25-year spam, 2% more than the B1-H1 of Barstow and 4% greater than the same for Panjib.

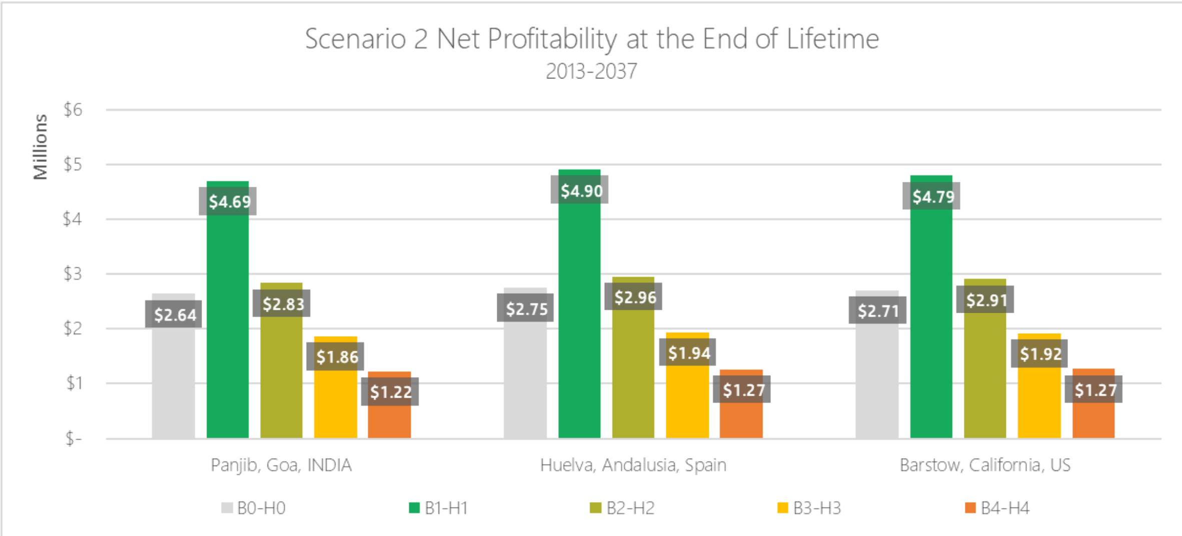

Graph 64. Net profitability at the end of lifetime for Scenario 2 (2013-2037)

This means that compared to Scenario 1 whereby no mining activities were carried out, the following percentage of profitability growth presented in Graph 65 are observed throughout the project lifetime for each location. It was calculated by averaging the percentage difference of the model combinations (B0-H0 /B1-H1/ B2-H2/ B3-H3/ B4-H4) from the results in Scenario 1. In Huelva, given the large profitability contrast, the percentage increase is considerably higher. In essence, Graph 65 epitomizes the value added of Bitcoin mining powered by the sun for each country based on the geographical as well as electricity market conditions. For instance, mining from the sun is more valuable in a location such as Huelva rather than in Panjib, given that there is a greater loss from potentially injecting the generated electricity to the grid at under-valued prices compared to India or the US.

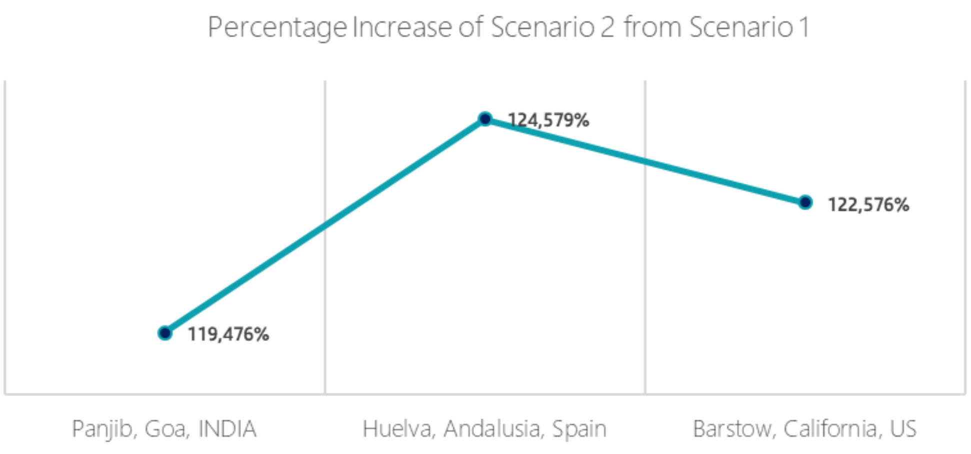

Graph 65. Percentage increase from Scenario 2 on Scenario 1

4.5.3 Scenario C

Scenario C considered the case whereby electricity produced by solar PV is used to mine for 25 years and the surplus is then stored and used to mine for more hours during the day, making further mining profitability. The surplus electricity was calculated in order to find out how much this would pay at baseline tariff rate, assuming a PPA or a tariff agreement was performed at the beginning of the project for 25 to 30 years, even though 25 years is the time of interest.

The additional predicted profitability shown in Graph 66 was reached by computing the number of extra mining hours per day, through the mining equipment power consumption and the available energy generated after mining during the sun-hours. According to the different mining difficulty and bitcoin price, the following results were obtained.

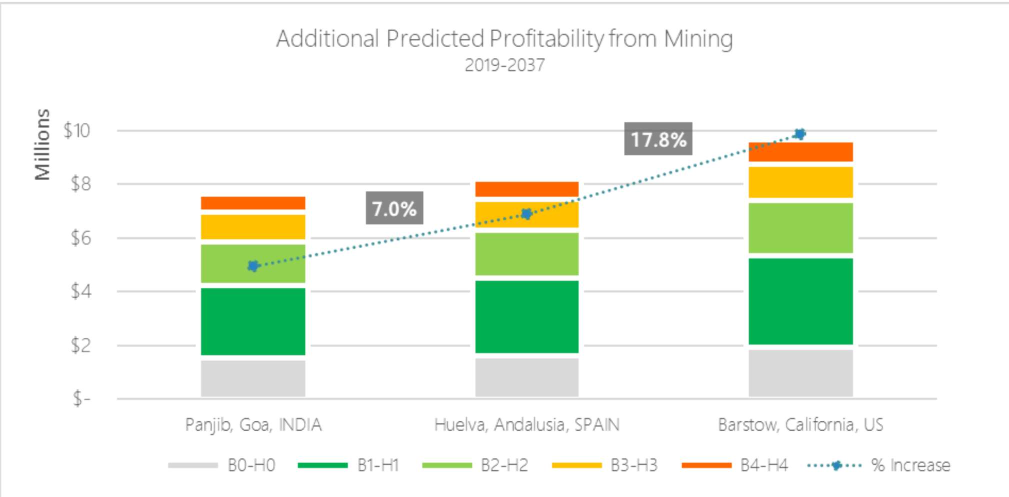

Graph 66. Additional predicted profitability

In this scenario, the solar PV, mining and energy storage infrastructure were subtracted from the total profitability coming from the mining activities and electricity generation costs as shown in Equation 12.

$$P_{n,3} = P_{M,h} + P_{M,p}\big(B_0 - H_0 \,\big|\big|B_1 - H_1\big|\big|B_2 - H_2\big|\big|B_3 - H_3\big|\big|B_4 - H_4\big) + P_{a,h}$$
$$+ P_{a,p}\big(B_0 - H_0 \,\big|\big|B_1 - H_1\big|\big|B_2 - H_2\big|\big|B_3 - H_3\big|\big|B_4 - H_4\big) - I_{PV} - I_{M,h} - I_{M,p} - I_S - I_{R,p}$$

$$\forall\ Locations\ (Panjib, Huelva, Barstow)$$

Equation 12

Where $P_{n,3}$, the net profitability for scenario 3 is calculated by subtracting investment requirements from the revenue each investment brings forth. In addition to the parameters mentioned in Scenario 2, $P_{a,h}$ is the historical profitability that comes from storing electricity and using for additional mining, $P_{a,p}$ is the predicted profitability that comes from storing electricity and using for additional mining which can be either for models $B_0 - H_0$, $B_1 - H_1$, $B_2 - H_2$, $B_3 - H_3$ or $B_4 - H_4$. On the investment side, I_S is the energy storage computed cost (including the battery's capital cost as well as the replacement costs recurring every 5 years within the historical period) and $I_{R,p}$ is the additional replacement cost estimation based on the average Li-ion replacement cost for the predicted period.

The overall outcome of Scenario 3 is shown in Graph 67 whereby the net profitability for each predicted scenario is modelled for each country. Even though Huelva was the most profitable location for Scenario 2, with energy storage Barstow became the most profitable location for mining from the sun. Huelva is still 59% more profitable than its own profitability performance (Graph 68) but less than Barstow which increased by 70% from its Scenario 2 performance and surpassed in absolute values Huelva's profitability by $0.38 million dollars (Graph 67). Under the pessimistic scenario of Bitcoin value and network difficulty (B4-H4) at the end of the lifetime it would have produced $2.13 million dollars and on the most optimistic scenario it would reach $8.16 million dollars in the 25-year time span.

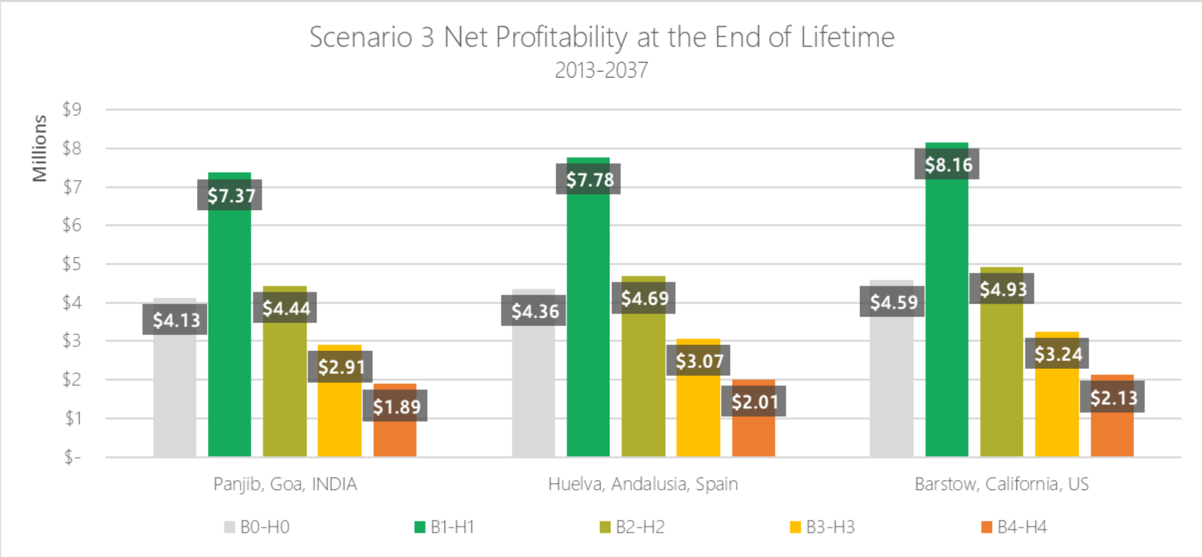

Graph 67. Net profitability at the end of lifetime for Scenario 3 (2013-2037)

Compared to Scenario 2, whereby no energy storage and further mining was used, the following percentage of profitability growth presented in Graph 68 are observed throughout the project lifetime for each location. It was calculated by averaging the percentage difference of the model combinations (B0-H0 /B1-H1/ B2-H2/ B3-H3/ B4-H4) from the results in Scenario 2. In essence, Graph 68 epitomizes the value added of Bitcoin mining powered by the sun with energy storage for higher mining capability for each country based on the geographical conditions.

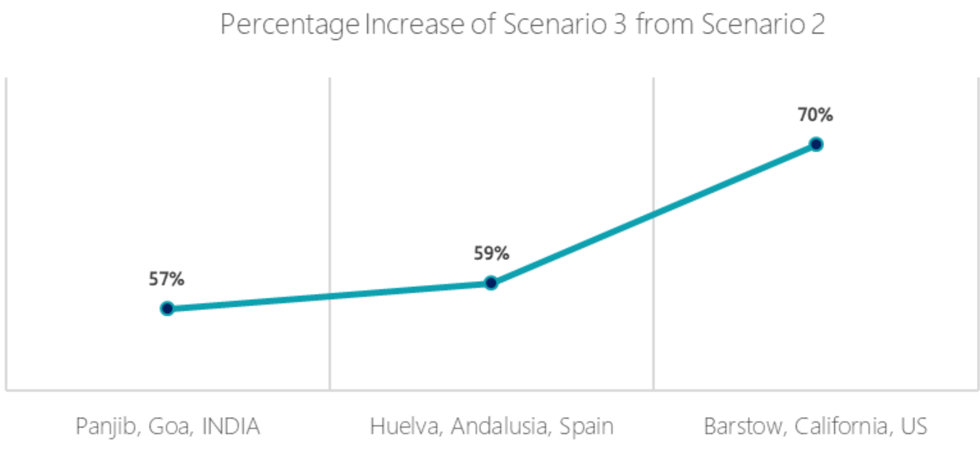

Graph 68. Percentage increase from Scenario 3 on Scenario 2

4.6 Model Weaknesses

Meteorological variability was assumed as steady throughout the 25 years, based on a one-year database with climate averages for each location provided in PVSyst. A technology degradation profile was selected but the impact of change in climate conditions was not considered for 25 years forward. Furthermore, the financial PV model did not include taxes in its assessment, and the data obtained was gathered from different web sources, reports and experts, and yet they could differ from country to country greatly. In some parameters this has been viewed, but it could be further defined with access to more accurate and updated data.

All obtained data for each country were in different currencies, namely US dollars, euros (EUR) and Indian rupees (INR). The EUR/US currency exchange used was of 1.112 and the INR/US was of 0.0145. Variation of currency exchange rates will have an impact on the results obtained in this model.

Furthermore, this model does not consider future changes in tariff systems and solar electricity compensation might change in the future. It does not consider a reduced price in PV system, as it is a one-time installation of 2013 and it envisions a mining software increase of 10% every 2 years. Even though this can be changed in the Excel model, a sensitivity analysis wasn't performed with regards to the impact the future prices of assets would have on the overall system profitability, as it was done for battery replacement costs for the historical period.

Results obtained may vary greatly with different assumptions and therefore it is worth dedicating a section to discussing these and the approach taken to measure profitability, both historical and predicted. First of all, the way the mining reward profitability was calculated takes as an assumption that the profitability is proportional to the energy input by the mining technology, as it would be in a mining pool. However, no percentage of participation payment was introduced and also no probability factor of block-mining non-achievement was considered. Therefore, the results may present an upper limit benefit. Furthermore, the profitability was also modelled as if the bitcoins gained were sold at the same daily closing value of bitcoin which has a variation range of a historical maximum 29.42% to a historical minimum -29.75% from close to open on one same day, and from 42.38% difference between high and low Bitcoin prices on one day.

The predicted bitcoin value and network hashrate is a random estimation based on historical data and some growth patterns that have been forced to be more profitable or less profitable according to the percentages included. The truth is it is very difficult, if not impossible in the long-term, to accurately predict the future worth of bitcoin is US dollars and to assess the mining difficulty of the network. Therefore, a large impact on the calculated profit could come from error in the predictive approach.

5 Conclusions

Based on the obtained on the results summarized in the integrated analysis (Chapter 4.5), which includes both the historical and predictive account of the modelling, the following can be assessed for each geographical location selected.

In Panjib, selling the solar PV in India does not render much profit at the end of the project lifetime as the solar tariffs are quite low and still depend on subsidies provided by the state and the Ministry as previously outlined. Efforts had to be made with regards to the financial PV in order to make the tariff of $0.10/kWh a profitable one. However, the process is able to replace 549.2 tons of CO_2 throughout the lifetime of the project. Redirecting the electricity generated to Bitcoin mining, according to the predictions in Appendix A.9.1 (p.135) the profitability is much greater, and depending on the outlook on the Bitcoin value and network, the profitability can range between $1.2M and $4.7M and with an investment that represents 6.8% of the net profitability for Scenario 2. However, profitability increases when adding energy storage as in Scenario 3. The net investment increases by 36.1% from the model without energy storage (Scenario 2), but the average net profit increases by more than half (56.5%) as shown in Graph 69.

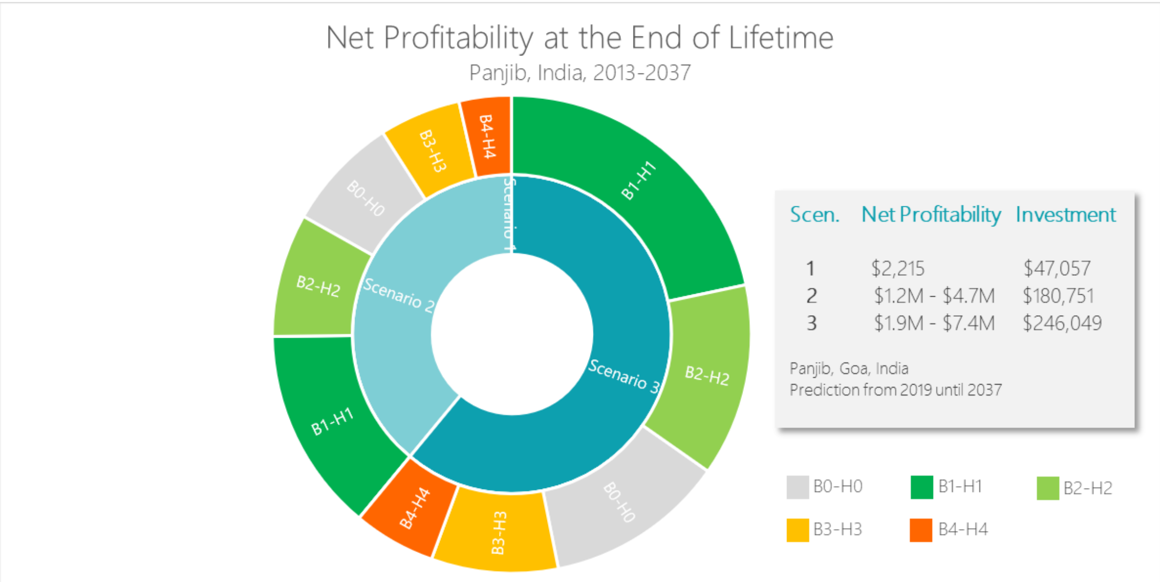

Graph 69. Net profitability at the end of lifetime for Scenario 1, 2 and 3 in Panjib, India (2013-2037)

Selling the solar electricity in Spain is not at all profitable considering the assumptions that went into the Spanish PV model. As shown in Chapter 4.5.1, it is able to make some annual profit only from 2040, which expands past the tariff duration of 30 years, but does not render profit during the 25-year period that is the scope of this analysis. The issue with Spain for solar energy is the high energy tax, which has not been considered in the model, and the highly competitive environment in which solar electricity is expected to compete in terms of electricity selling. Certain regions of Spain, such as Andalusia and Castilla La Mancha, have high degree of PV installation and subsidies. However, competing against market-value prices – which can go to as low as $0.04/kWh – for electricity that can come from conventional sources, does not make it easy for the renewable transition at stand-alone scale.

However, redirecting the electricity generated to Bitcoin mining, according to the predictions in Appendix A.9.2 (p.136) the profitability is the greatest from all analysed locations, and depending on the outlook on the Bitcoin value and network, the profitability can range between $1.3M and $4.9M and with an investment that represents 7.0% of the net profitability for Scenario 2. However, profitability increases when adding energy storage as in Scenario 3. The net investment increases by 33.7% from the model without energy storage (Scenario 2), but the average net profit increases by more than half (58.6%) as shown in Graph 70.

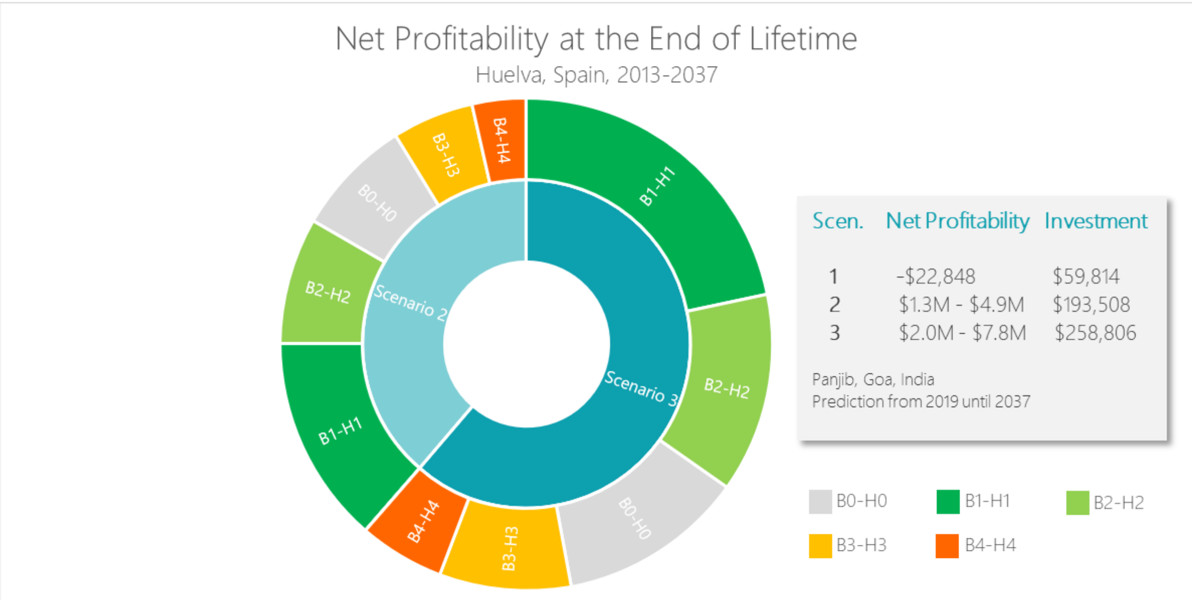

Graph 70. Net profitability at the end of lifetime for Scenario 1, 2 and 3 in Huelva, Spain (2013-2037)

With regards to the PV model, Barstow presents the best location and weather conditions to implement the 12.75 kW solar plant with 51 monocrystalline modules. It generates 9.1% more electricity than Huelva and 20.4% more than Panjib. Its ROI is of 112.8% and the profitability after the project's lifetime is of $34,825 – fifteen times fold the positive profitability from Panjib's solar farm – paying back all the capital costs in 11.7 years.

However, redirecting the electricity generated to Bitcoin mining, according to the predictions in Appendix A.9.3 (p.137) the profitability is much greater, and depending on the outlook on the Bitcoin value and network, the profitability can range between $1.3M and $4.8M and with an investment that represents 6.7% of the net profitability for Scenario 2. However, profitability increases even further (the highest of all compared countries) when adding energy storage as done in Scenario 3. The net investment increases by 36.0% from the model without energy storage (Scenario 2), but the average net profit increases by more than half (69.6%) as shown in Graph 70.

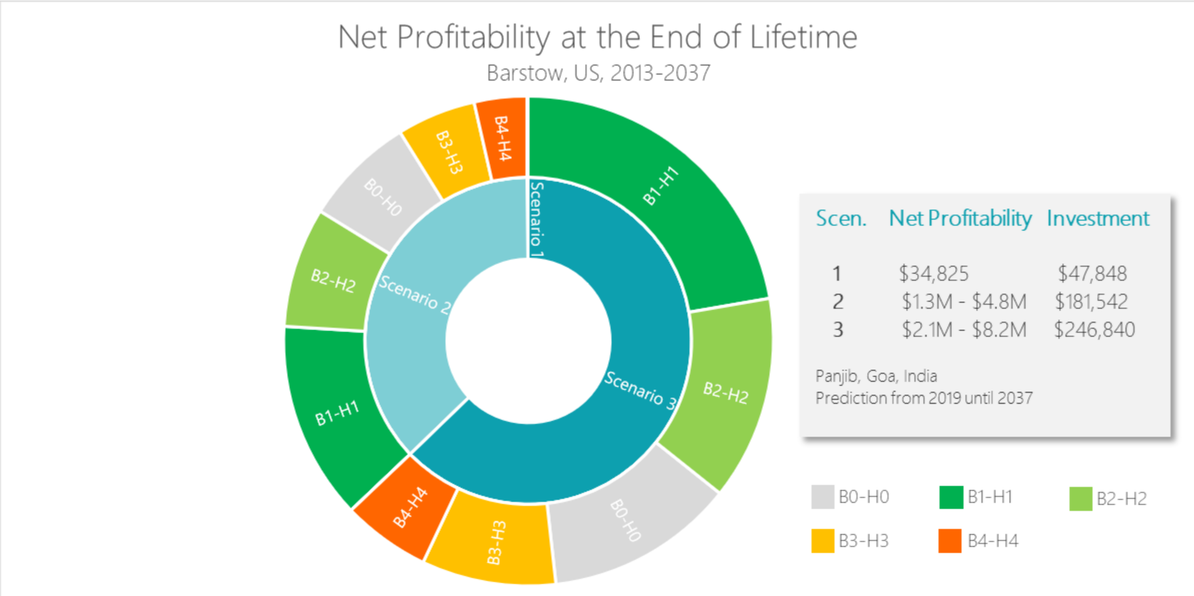

Graph 71. Net profitability at the end of lifetime for Scenario 1, 2 and 3 in Barstow, US (2013-2037)

The results indicate that PV solar installations are not always profitable depending on the market conditions and on the generation capacity of the installation (see results for Scenario 1 in Huelva, Spain). However, finding new ways of securing profit and covering initial and yearly expenses can be key in the deployment of renewable energy, in this case of solar PV systems. This thesis concluded that, despite the high risk and they highly irregular profile of Bitcoin, under all represented scenarios the costs of solar PV installations are covered even in places where it would not be compensated by just the varying market value of electricity. It seems that the future for renewables competing in the energy market system is going to be ever more competitive in an environment that urges price parity between renewables, fossil fuels and other conventional sources. Therefore, finding these new revenue streams are a major asset and play a key role in the innovative and resourceful financing in the long-run.

Furthermore, the model presented is not inflexible to the profitability needs of every timestep. The solar plant owner could adapt the revenue stream from selling to the local electricity grid, mining or any other profit-making application that they could identify, in order to maximize benefits in both the short and the long-run.

5.1 Personal Reflection

All in all, the results of this thesis indicate the same conclusion for all locations studied, even though they become more intricate as we look at different variables such as geographical and electricity market conditions. The conclusion is that energy storage is worth having because Bitcoin can provide value under the set conditions. The profit changes slightly to a greater or lesser given the solar irradiation profiles and geographical conditions of each location. However, based on the Bitcoin value, mining difficulty and technological adoption, this research seems to indicate that there is profitability potential within the crypto-mining space. Looking at the graphs presented in Appendix A.9 one might even decide to stop mining after 2025, as most of the profitability is covered by the first 12 years of mining. After those 12 years, perhaps it would be of interest to turn to selling electricity to the grid as perhaps future conditions of renewable energy could be more favorable; or perhaps they become even more competitive and therefore it might be worth to keep making a bit more of profit in hope that the Bitcoin value of mining difficulty increase further. Notwithstanding, the Bitcoin network presents some fundamental and technical concerns that the public is putting on inspection and technological changes might lead to re-adjustments.

Carrying out this work was by no means easy, especially with regards to the assumptions to be made in an unpredictable field that is the future of renewables and the crypto scope. Nonetheless, it was a very challenging project that does not come with its own set of discoveries and gratitude towards being given the chance to perform such an investigation. All related assumptions can be found in several Excel files: one for the PV model, another includes the crypto assessment, additional means of profitability such as energy storage and the prediction model, and the last one for the integrated analysis and country comparison. Additional attachments include the country selection and number of miners' optimization. These have been organized as a tool where the user can input numbers of their liking so to get results with different assumptions from the ones presented in this thesis.

6 References

Alves, L., 2016. *OviMagazine | Photovoltaic Solar in Portugal.* [Online] Available at: http://www.ovimagazine.com/art/3270 [Accessed 28 August 2019].

Andoni, M. et al., 2018. Blockchain Technology in the Energy Sector: A Systematic Review of Challenges and Opportunities. *ElSevier Renewable and Sustainable Energy Reviews,* Issue 100, pp. 143-174.

Andoni, M. et al., 2019. Blockchain Technology in the Energy Sector: A Systematic Review of Challenges and Opportunities. *ElSevier Renewable and Sustainable Energy Reviews,* Issue 100, pp. 143-174.

Arvind, K., Dong, W. & Mihir, N., 2018. *CAP Theorem,* Vancouver: University of British Colombia.

Bachrach, Y. et al., 2015. *Bitcoin Mining Pools: A Cooperative Game Theoretic Analysis,* Jerusalem, Cambridge: School of Computer Science and Engineering, The Hebrew University of Jerusalem & Microsoft Research .

Badejani, M. M., Masoum, M. A. S. & Kalanta, M., 2007. *Optimal Design and Modeling of a Stand-Alone Hybrid PV-WInd Systems,* Perth: IEEE.

Bahar, H., 2019. *IEA | Solar PV Tracking Clean Energy Progress.* [Online] Available at: https://www.iea.org/tcep/power/renewables/solarpv/ [Accessed 24 August 2019].

Bahga, A. & Madisetti, V. K., 2016. *Blockchain Platform for Industrial Internet of Things,* Georgia: Scientific Research Publishing.

Baliga, A., 2017. *Understanding Blockchain Consensus Models,* s.l.: Persistent Systems Ltd. .

Bellini, E., 2019. *PV Magazine | Spain hits 5 GW milestone.* [Online] Available at: https://www.pv-magazine.com/2019/02/05/spain-hits-5-gw-milestone/ [Accessed 24 August 2019].

Bestplaces, n.d.. *Climate in Los Angeles, California.* [Online] Available at: https://www.bestplaces.net/climate/city/california/los_angeles [Accessed 2019 August 28].

Bird, L., Cochran, J. & Wang, X., 2014. *Wind and Solar Energy Curtailment: Experience and Practices in the United States,* Colorado: National Renewable Energy Laboratory.

Bitcoin Block Half, 2019. *Bitcoin Block Reward Halving Countdown.* [Online] Available at: https://www.bitcoinblockhalf.com/ [Accessed 28 March 2019].

Bitcoin, n.d.. *Bitcoin Mining.* [Online] Available at: https://www.bitcoin.com/bitcoin-mining [Accessed 4 April 2019].

Bitcoin, n.d.. *Bitcoin.com Pool.* [Online] Available at: https://pool.bitcoin.com/ [Accessed 4 April 2019].

Bitnodes, 2019 . *Global Bitcoin Nodes Distribution.* [Online] Available at: https://bitnodes.earn.com/?The [Accessed 1 April 2019].

Blockchain, 2019. *Hash Rate.* [Online] Available at: https://www.blockchain.com/en/charts/hash-rate?timespan=all [Accessed 3 April 2019].

Blockgeeks, 2018. *Blockchain Scalability: When, Where, How?.* [Online] Available at: https://blockgeeks.com/guides/blockchain-scalability/#The_scalability_problem_of_cryptocurrencies
[Accessed 28 March 2019].

Bohme, R., Christin, N., Edelmand, B. & Moore, T., 2015. Bitcoin: Economics, Technology and Governance. *Journal of Economic Perspectives,* 29(2), pp. 213-238.

BRE, 2014. *Planning Guidance for the Development of Large Scale Ground Mounted Solar PV Systems,* s.l.: BRE National Solar Centre.

Brilliantova, V. & Thurner, T. W., 2018. Blockchain and the Future of Energy. *ElSevier Technology in Society.*

Burke, M., 2015. Solar Farms: Funding, Planning and Impacts. *House of Commons Library,* Issue 7434.

CAISO, 2016. *Impacts of Renewable Energy on Grid Operations,* Folsom: California Independent System Operator .

CAISO, 2016. *What the Duck Curve Tells us about Managing a Green Grid,* Folsom: California Independent System Operator.

CAISO, 2019. *Price Map.* [Online] Available at: http://www.caiso.com/TodaysOutlook/Pages/Prices.aspx [Accessed 2019 August 28].

Center for Climate and Energy Solutions, n.d.. *Electric Energy Storage.* [Online] Available at: https://www.c2es.org/content/electric-energy-storage/ [Accessed 10 April 2019].

Clayton, M. E., Kjellsson, J. B. & Webber, M. E., 2018. *Can Renewable Energy and Desalination Tackle Two Problems at Once?.* [Online] Available at: https://www.earthmagazine.org/article/can-renewable-energy-and-desalination-tackle-two-problems-once
[Accessed 10 April 2019].

Climate Council, 2019. *11 Countries Leading the Change on Renewable Energy.* [Online] Available at: https://www.climatecouncil.org.au/11-countries-leading-the-charge-on-renewable-energy/
[Accessed 10 April 2019].

Coin Telegraph, n.d.. *What is Bitcoin Cash?.* [Online] Available at: https://cointelegraph.com/bitcoin-cash-for-beginners/what-is-bitcoin-cash [Accessed 11 April 2019].

Coindesk, n.d.. *Bitcoin Price (BTC).* [Online] Available at: https://www.coindesk.com/price/bitcoin [Accessed 9 April 2019].

CoinMarketCap, n.d. *CoinMarketCap - Bitcoin.* [Online]
Available at: https://coinmarketcap.com/currencies/bitcoin/historical-data/?start=20130428&end=20190724
[Accessed 23 July 2019].

CPUC, 2018. *Renewable Feed-In Tariff (FIT) Program.* [Online]
Available at: https://www.cpuc.ca.gov/feedintariff/
[Accessed 2019 August 28].

Credits Blockchain, 2018. *Why is CREDITS faster than other blockchains?.* [Online]
Available at: https://medium.com/@credits/why-is-credits-faster-than-other-blockchains-1555a5f3e995
[Accessed 11 April 2019].

Croman, K. et al., 2016. *On Scaling Decentralized Blockchains,* s.l.: Initiative for CryptoCurrencies and Contracts (IC3).

Data.Gov, n.d.. *U.S. Government's open data.* [Online]
Available at: https://www.data.gov/
[Accessed 2019 August 28].

Deetman, S., 2016. *Bitcoin Could Consume as Much Electricity as Denmark by 2020.* [Online]
Available at: https://motherboard.vice.com/en_us/article/aek3za/bitcoin-could-consume-as-much-electricity-as-denmark-by-2020
[Accessed 4 April 2019].

Deng, D., 2015. Li-ion Batteries: Basics, Progress, and Challenges. *Energy Science and Engineering,* 3(5), p. 385–418.

Dimitri, N., 2017. *Bitcoin Mining as a Contest,* Siena: Ledger.

Doman, L., 2017. *EIA Projects 28% Increase in World Energy Use by 2040.* [Online]
Available at: https://www.eia.gov/todayinenergy/detail.php?id=32912
[Accessed 9 April 2019].

EIA, 2018. *U.S. Battery Storage Market Trends.* [Online]
Available at: https://www.eia.gov/analysis/studies/electricity/batterystorage/
[Accessed 10 April 2019].

Endesa, 2018. *Cities in the World with Most and Least Sunlight.* [Online]
Available at: https://www.endesaclientes.com/blog/cities-hours-sunlight
[Accessed 2019 August 28].

European Commission, n.d.. *Renewable Energy: Moving Towards a Low Carbon Economy.* [Online]
Available at: https://ec.europa.eu/energy/en/topics/renewable-energy
[Accessed 6 April 2019].

Evergreen Energy, 2017. *How Much do Solar Panels Cost on Average?.* [Online]
Available at: https://www.evergreenenergy.co.uk/solar-panels/how-much-do-solar-panels-cost/
[Accessed 9 April 2019].

Farrokhfal, Y. G., Kazhamiaka, F., Rosenberg, C. & Keshav, S., 2015. Optimal Design of Solar PV Farms with Storage. *IEE Transactions on Sustainable ENergy,* 6(4).

Gilbert, S. & Lynch, N. A., 2012. *Perspectives on the CAP Theorem,* s.l.: National University of Singapore & Massachusetts Institute of Technology.

Glance, D., 2017. *Bitcoin Splits and Bitcoin Cash is Created. Explaining Why and What Happens Now.* [Online]
Available at: https://theconversation.com/bitcoin-splits-and-bitcoin-cash-is-created-explaining-why-and-what-happens-now-81943
[Accessed 11 April 2019].

Goldie-Scot, L., 2019. *A Behind the Scenes Take on Lithium-ion Battery Prices.* [Online]
Available at: https://about.bnef.com/blog/behind-scenes-take-lithium-ion-battery-prices/
[Accessed 10 April 2019].

Goldthau, A., 2018. *The International Political Economy of the Low Carbon Transition,* Madrid: Andreas Goldthau conference on the 16th March 2018.

Greenberg, P. & Budgen, D., 2018. Energy Consumption Boomtowns in the United States: Community Responses to a Cryptocurrency Boom. *ElSevier Energy Research & Social Science,* Issue 50, pp. 162-167.

Hayes, A. S., 2018. *Bitcoin Price and its Marginal Cost of Production: Support for a Fundamental Value,* Madison, Cyprus: Department of Sociology, University of Wisconsis-Madison | University of Nicosia.

Huang, Z., Snyder, S. & Schillinger, G., 2018. *Aura Protocol: A Peer-to-Peer Blockchain Scaling Solution for Highly Interactive Decentralized Applications,* s.l.: s.n.

IBEF, 2018. *Renewable Energy,* s.l.: India Brand Equity Foundation.

IEA, 2016. *IEA | Solar PV electricity generation in India.* [Online]
Available at:
https://www.iea.org/statistics/?country=INDIA&year=2016&category=Renewables&indicator=SolarGen&mode=chart&dataTable=ELECTRICITYANDHEAT
[Accessed 24 August 2019].

IEA, 2019. *Electricity in the United States.* [Online]
Available at: https://www.eia.gov/energyexplained/electricity/electricity-in-the-us.php
[Accessed 2019 August 28].

IEA, 2019. *Uttar Pradesh renewable energy feed-in tariff 2014 - 2019 levels.* [Online]
Available at: https://www.iea.org/policiesandmeasures/pams/india/name-140455-en.php?s=dHlwZT1yZSZzdGF0dXM9T2s,&return=PG5hdiBpZD0iYnJlYWRjcnVtYiI-PGEgaHJlZj0iLyI-SG9tZTwvYT4gJnJhcXVvOyA8YSBocmVmPSIvcG9saWNpZXNhbmRtZWFzdXJlcy8iPlBvbGljaWVzIGFuZCBNZWFzdXJlczwvYT4gJnJhcXV
[Accessed 28 August 2019].

IEA, 2019. *World Energy Prices,* s.l.: International Energy Agency.

IEA, n.d.. *Solar PV Global Status.* [Online]
Available at: https://www.iea.org/tcep/power/renewables/solarpv/
[Accessed 2019 August 28].

India Times, 2016. *Times of India | New Consumers will Earn Less for Selling Solar Power.* [Online]
Available at: https://timesofindia.indiatimes.com/city/bengaluru/New-consumers-will-earn-less-for-selling-solar-power/articleshow/52099912.cms
[Accessed 28 August 2019].

IPCC, 2018. *Global warming of 1.5°C,* Switzerland: Intergovernmental Panel on Climate Change.

IRENA, 2012. *Renewable Energy Technologies: Cost Analysis Series,* s.l.: International Renewable Energy Agency.

Kar, S. K., Sharma, A. & Roy, B., 2016. Solar Energy Market Developments in India. *ElSevier Renewable and Sustainable Energy Reviews,* 121(62), pp. 121-133.

Khan, M. & Salah, K., 2018. IoT Security: Review, Blockchain Solutions and Open Challenges. *Future Generat Comput Syst,* Issue 82, pp. 395-411.

Kim, Y. & Chang, N., 2014. *Design and Management of Energy Efficient Hybrid Electrical Energy Storage Systems.* 1st ed. s.l.:Springer International Publishing.

Kost, C. et al., 2018. *Levelized Cost of Electricity for Renewable Energy Technologies,* Freiburg: Fraunhofer Institute for Solar Energy Systems.

Kroll, J. A., Davey, I. C. & Felten, E. W., 2013. *The Economics of Bitcoin Mining or Birtcoin in the Presence of Adversaries,* Princeton: Princeton University.

Lazard, 2018. *Lazard's Levelized Cost of Energy Analysis Version 12.0,* Hamilton: Lazard.

Lewis, K., 2016. *Portugal Runs Entirely on Renewable Energy for Four Consecutive Days.* [Online]
Available at: https://www.independent.co.uk/news/world/europe/portugal-runs-entirely-on-renewable-energy-for-four-consecutive-days-a7035561.html
[Accessed 10 April 2019].

Li, J. et al., 2018. Energy Consumption of Cryptocurrency Mining: A Study of Electricity Consumption in Mining Cryptocurrencies. *ElSevier Energy,* Issue 168, pp. 160-168.

Marcy, C. & Fields, F., 2018. *Costs of Different Battery Storage Technologies Depend on Technical Characteristics.* [Online]
Available at: https://www.eia.gov/todayinenergy/detail.php?id=36432
[Accessed 10 April 2019].

Monera, F., 2018. *¿Es interesante vender los kWh vertidos a red en una instalación de autoconsumo con baterías?.* [Online]
Available at: https://www.energias-renovables.com/fotovoltaica/es-interesante-vender-los-kw-vertidos-20181029
[Accessed 25 August 2019].

Motyka, M. & Sanborn, S., 2015. *US Solar Power Growth through 2040: Exponential or Inconsequential?,* s.l.: Deloitte Center for Energy Solutions.

Nakamoto, S., 2008. *Bitcoin: A Peer-to-Peer Electronic Cash System,* s.l.: Bitcoin .

Nelson, J., 2018. *Solar Energy Conversion ,* LOndon: Imperial College London.

NREL, n.d.. *U.S. State Solar Resource Maps.* [Online]
Available at: https://www.nrel.gov/gis/solar.html
[Accessed 2019 August 28].

Nyberg, M., 2018. *California's Installed Electric Power Capacity and Generation,* s.l.: California Energy Commission.

O'Dwyer, K. J. & Malone, D., 2014. Bitcoin Mining and its Energy Footprint. *Irish Signals & Systems Conference 2014 and 2014 Chine-Ireland International Conference on Information and Communications Technologies,* pp. 280-285.

OMIE, 2018. *Operador Del Mercado Ibérico De Energía Polo Español S A.* [Online]
Available at: http://www.omie.es/inicio
[Accessed 28 August 2019].

Palz, W., 2011. *Power for the World: The Emergence of Electricity from the Sun.* 1st ed. Singapore: Pan Stanford Publishing Pte. Ltd..

Park Insurance, 2019. *Setting Up a Solar Farm: Costs, Funding and How To Run It Effectively.* [Online]
Available at: https://parkinsurance.co.uk/solar-farm-cost-setting-up/
[Accessed 6 April 2019].

Parker, G. & Greene, L., 2014. *Biodiversity Guidance for Solar Developments,* s.l.: BRE National Solar Centre .

Partain, L. et al., 2016. *Swanson's Law Plan to Mitigate Global Climate Change,* s.l.: IEEE 43rd Photovoltaic Specialists Conference.

Paulos, B., 2017. *Too Much of a Good Thing? An Illustrated Guide to Solar Curtailment on California's Grid.* [Online]
Available at: https://www.greentechmedia.com/articles/read/an-illustrated-guide-to-solar-curtailment-in-california#gs.5e2c9s
[Accessed 13 April 2019].

Pearson, P., 2018. *Energy System Transitions: Past and Prospective,* London: Imperial College London.

Peleg, R., 2018. *Microquanta reaches 17.9% efficiency for perovskite solar mini-module. Perovskite-info..* [Online]
Available at: https://www.perovskite-info.com/microquanta-reaches-179-efficiency-perovskite-solar-mini-module
[Accessed 9 April 2019].

Pilkington, M., 2015. *Blockchain Technology: Principles and Applications,* Besançon: SSRN.

Pressman, M., 2017. *Understanding Tesla's Lithium Ion Batteries.* [Online]
Available at: https://evannex.com/blogs/news/understanding-teslas-lithium-ion-batteries
[Accessed 10 April 2019].

PV Europe, 2019. *Predicted European solar growth jump of over 42% in 2019.* [Online]
Available at: https://www.pveurope.eu/News/Markets-Money/Predicted-European-solar-growth-jump-of-over-42-in-2019
[Accessed 9 April 2019].

PVSyst, 2019. *PVSyst 6.8.3.* s.l.:s.n.

PVSyst, n.d.. *PVSyst Files | Carbon Balance Tool.* [Online]
Available at: http://files.pvsyst.com/help/carbon_balance_tool.htm
[Accessed 28 August 2019].

PVSyst, n.d.. *PVSyst Files | Detailed System LCE.* [Online]
Available at: http://files.pvsyst.com/help/detailed_system_lce.htm
[Accessed 28 August 2019].

REE, 2017. *Renewable Energy in the Spanish Electricity System,* s.l.: Red Eléctrica de España.

REE, 2019. *Series estadísticas nacionales.* [Online]
Available at: https://www.ree.es/es/datos/publicaciones/series-estadisticas-nacionales
[Accessed 28 August 2019].

Schermeyer, H., Vergara, C. & Fichtner, W., 2018. Renewable Energy Curtailment: A Case Study on Today's and Tomorrow's Congestion Management. *ElSevier Energy Policy,* Issue 112, pp. 427-436.

Schlogl, R., 2013. *Chemical Energy Storage.* 1st ed. Berlin/Boston: Walter de Gruyter GmbH.

Scurlock, J., 2014. *Agricultural Good Practice Guidance for Solar Farms,* s.l.: BRE National Solar Centre .

SEIA, 2019. *Solar Industry Research Data.* [Online] Available at: https://www.seia.org/solar-industry-research-data [Accessed 2019 August 28].

Seibert, J., 2019. *"Storage of Value in bitcoin is a fucking joke" - with Jason Seibert!* [Interview] (6 January 2019).

Serrano, R., 2007. Cooperative Games: Core and Shapley Value. *CEMFI Center for Monetary and Financial Studies,* Issue 709.

Shi, N., 2016. A New Proof-of-Work Mechanism for Bitcoin. *Financial Innovation.*

Shrestha, P., 2019. *UK to scrap Feed-in Tariff scheme in April 2019.* [Online] Available at: https://www.energylivenews.com/2018/07/20/uk-to-scrap-feed-in-tariff-scheme-in-april-2019/
[Accessed 6 April 2019].

Sigurdardottir, R. & Rigillo, N., 2018. *Bloomberg Technology | Extreme Bitcoin Mining Aids an Unexpected Revolution in Iceland.* [Online] Available at: https://www.bloomberg.com/news/articles/2018-07-03/extreme-bitcoin-mining-aids-an-unexpected-revolution-in-iceland
[Accessed 4 April 2019].

Skea, J., 2018. *Global Energy Markets: Drivers and Prospects,* London: Imperial College London.

Solar Energy Centre, 2008. *Solar Radiation Hand Book,* s.l.: Solar Energy Cenre, MNRE ,Indian Meteorologival Department.

SolarChoice, 2019. *AC vs DC Battery Storage Explained.* [Online] Available at: https://www.solarchoice.net.au/blog/ac-vs-dc-solar-battery-storage-explained [Accessed 10 April 2019].

Tapscott, D., 2016. *How Blockchain is Changing Money and Business.* [Online] Available at: https://www.ted.com/talks/don_tapscott_how_the_blockchain_is_changing_money_and_business?language=en
[Accessed 2 April 2019].

Taylor, M. B., 2017. *The Evolution of Bitcoin Hardware | Blockchain Technology in Finance,* Washington: The IEEE Computer Society .

The Electric Energy, n.d.. *Lithium and Lithium-Ion Battery Technology.* [Online] Available at: http://theelectricenergy.com/lithium-and-lithium-ion-battery/ [Accessed 10 April 2019].

Truby, J., 2018. Decarbonizing Bitcoin: Law and Policty Choices for Reducing the Energy COnsumption of Blockchain Technologies and Digital Currencies. *ElSevier Energy Research & Social Science,* Issue 44, pp. 399-410.

Tsagas, I., 2018. *PV Magazine | Spain covers 45.8% of H1 2018 electricity demand with renewables.* [Online] Available at: https://www.pv-magazine.com/2018/07/12/spain-covers-45-8-of-first-half-electricity-demand-with-renewables/
[Accessed 28 August 2019].

UCS, 2018. *Electric Vehicle Battery: Materials, Cost, Lifespan.* [Online] Available at: https://www.ucsusa.org/clean-vehicles/electric-vehicles/electric-cars-battery-life-materials-cost
[Accessed 10 April 2019].

UTE, 2018. *Composición Energética de Uruguay por Fuente.* [Online] Available at: https://apps.ute.com.uy/SgePublico/ConsComposicionEnergeticaXFuente.aspx
[Accessed 10 April 2019].

Vranken, H., 2017. Sustainability of Bitcoins and Blockchains. *Elsevier Current Opinion in Environmental Sustainability,* Issue 28, pp. 1-9.

Vujičić, D., Jagodić, D. & Ranđić, S., 2018. *Blockchain Technology, Bitcoin, and Ethereum: A Brief Overview,* Čačak: University of Kragujevac.

Waters, N., Pendered, O. & Hartnell, G., 2015. *Community Engagement Good Practice Guidance for Solar Farms,* s.l.: BRE National Solar Centre .

Wattenhofer, R., 2016. *The Science of the Blockchain.* First ed. s.l.:Inverted Forest Publishing.

Whattomine.com, n.d.. *What To Mine Main Page.* [Online] Available at: https://whattomine.com/
[Accessed 11 April 2019].

Zakeri, B. & Syri, S., 2015. Electrical Energy Storage Systems: A Comparative Life Cycle Cost Analysis. *ElSevier Renewable and Sustainable Energy Reviews,* Issue 42, pp. 569-596.

A.1 Appendix : Meteorological & Solar

Parameter	Panjib, India	Huelva, Spain	Barstow, US
Latitude	15.48°	37.28°	34.85°
Longitude	73.82°	-6.92°	-116.78°
Altitude (m)	55	32	585
Data Source	Meteonorm 7.2 (1998-2013)	Meteonorm 7.2 (1996-2010)	Meteonorm 7.2

A.1.1 Meteorological Data for Panjib, India

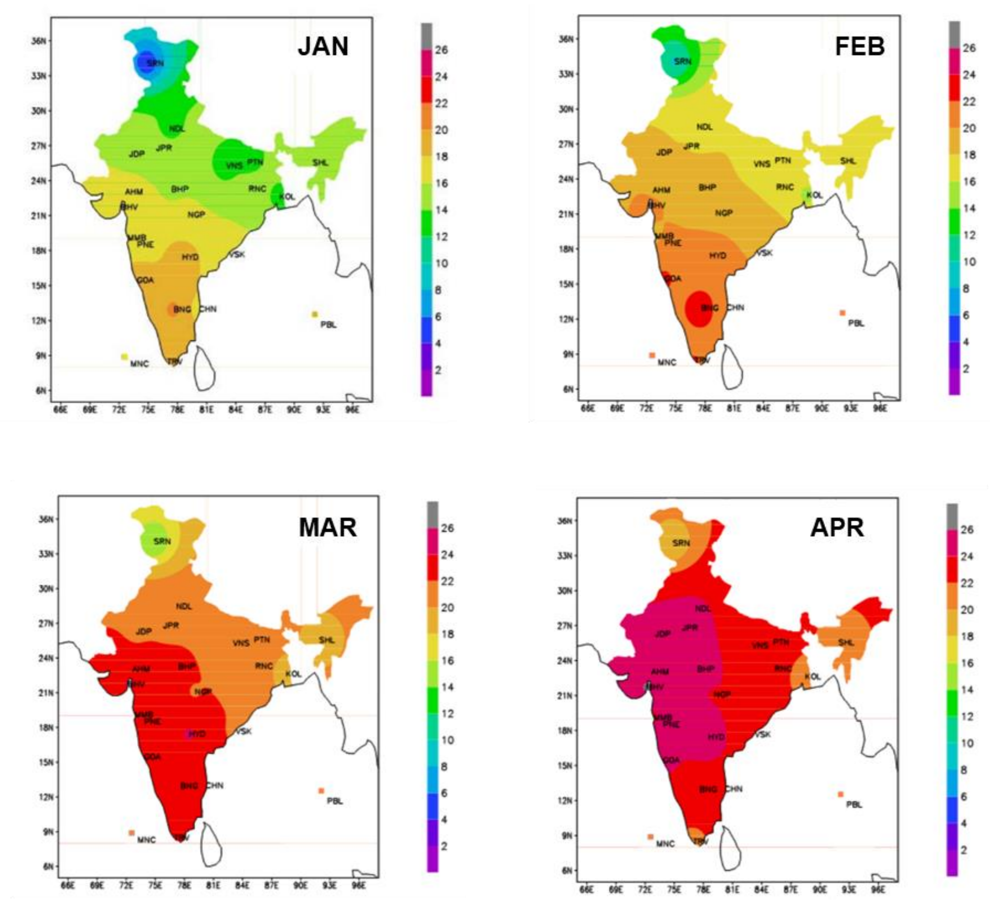

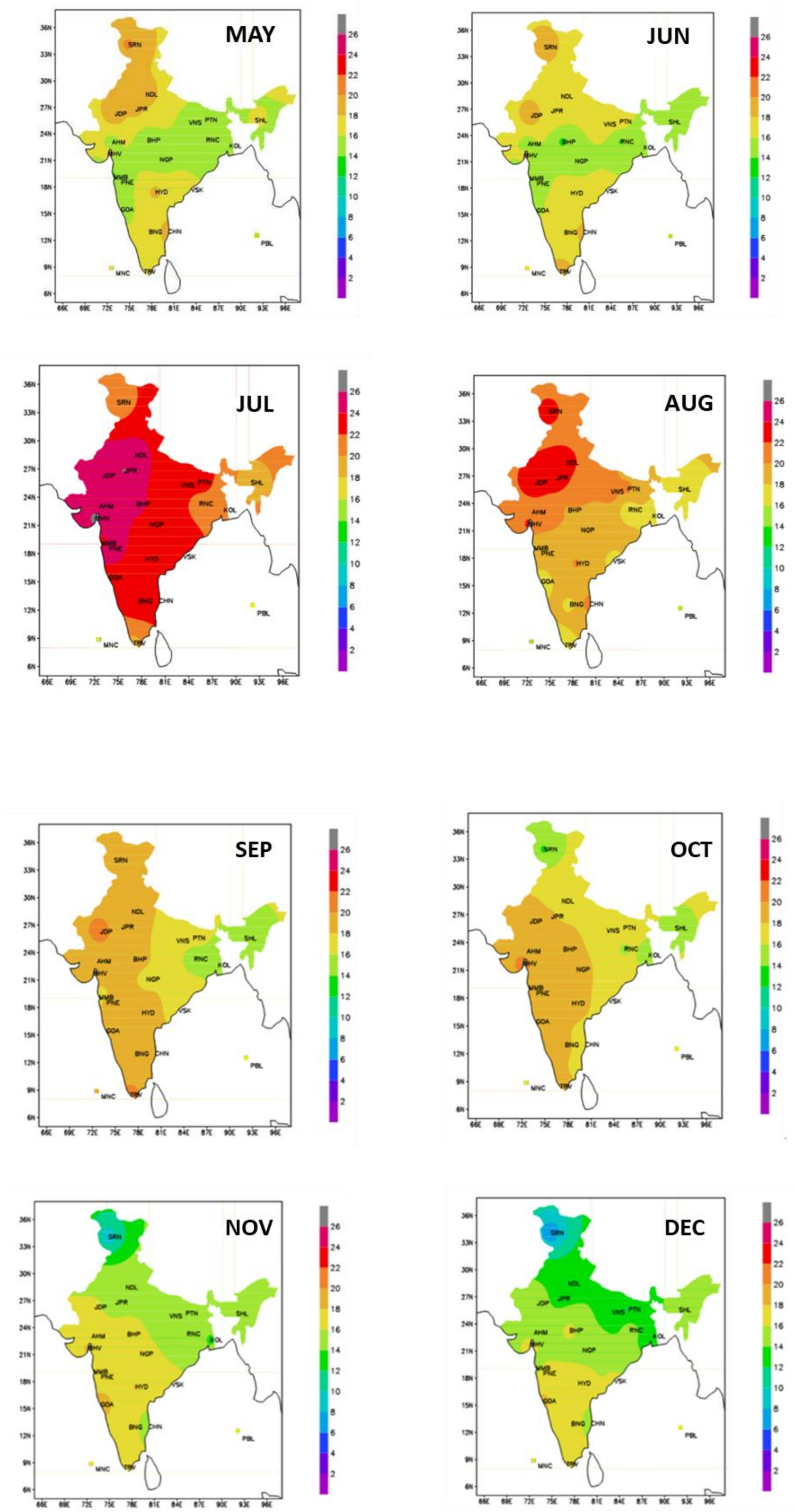

Source: (Solar Energy Centre, 2008)

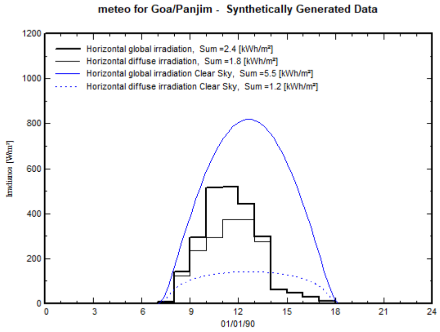

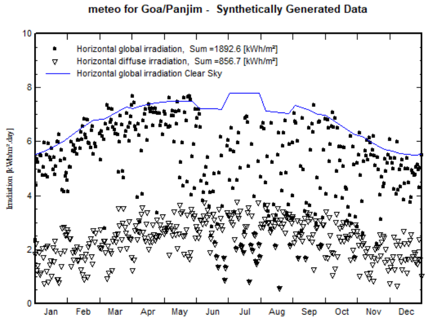

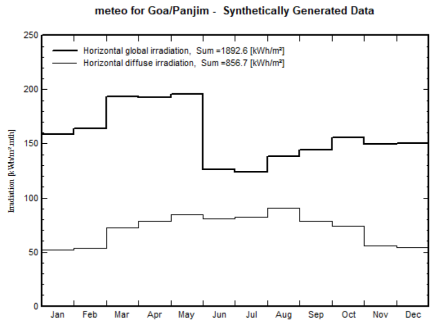

Month	GlobHor kWh/m^2	DiffHor kWh/m^2	T_Amb °C	GlobInc kWh/m^2	GlobEff kWh/m^2	EArray MWh	E_Out MWh	PR %
Jan	158.8	52.02	25.72	192.7	186.1	2.040	1.662	67.7
Feb	163.9	53.43	26.20	187.0	180.5	1.969	1.878	78.7
Mar	193.3	72.26	27.72	204.1	196.0	2.136	2.036	78.3
Apr	192.4	78.13	29.02	186.8	178.7	1.949	1.857	78.0
May	195.5	84.18	29.76	178.4	170.2	1862	1.772	77.9
Jun	126.4	80.90	27.24	114.4	108.5	1.223	1.155	79.2
Jul	124.0	82.39	26.94	113.3	107.6	1.214	1.144	79.2
Aug	138.6	90.92	26.57	131.5	125.2	1.414	1.229	73.3
Sep	144.1	78.75	26.42	145.0	138.4	1.546	1.470	79.5
Oct	155.5	75.09	27.61	168.3	161.3	1.776	1.691	78.8
Nov	149.9	55.40	27.14	177.9	171.5	1.875	1.788	78.8
Dec	150.2	54.24	26.21	186.0	179.1	1.966	1.876	79.1
Year	1892.6	856.71	27.22	1985.2	1903.1	20.970	19.557	77.3

A.1.2 Meteorological Data for Huelva, Spain

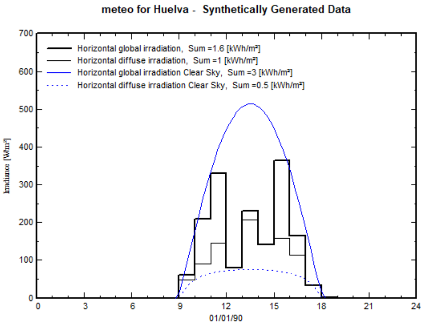

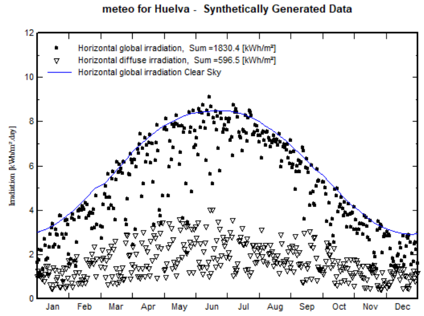

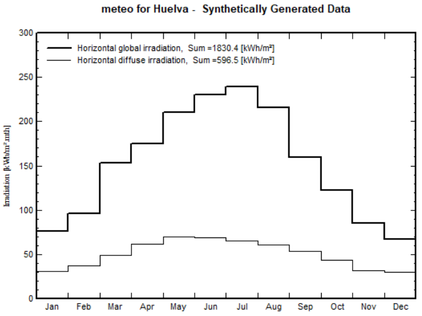

Month	GlobHor kWh/m^2	DiffHor kWh/m^2	T_Amb °C	GlobInc kWh/m^2	GlobEff kWh/m^2	EArray MWh	E_Out MWh	PR %
Jan	75.8	30.40	10.75	122.4	118.4	1.422	1.354	86.8
Feb	95.7	36.51	12.35	136.5	132.1	1.564	1.490	85.6
Mar	153.2	48.41	15.03	191.0	184.1	2.134	2.033	83.5
Apr	174.7	61.22	16.58	187.1	179.7	1.067	1.966	82.4
May	210.7	69.36	20.39	200.8	192.2	2.177	2.070	80.9
Jun	230.3	68.33	24.20	208.9	199.7	2.212	2.103	79.0
Jul	239.8	65.04	26.27	222.9	213.1	2.326	2.214	77.9
Aug	216.0	60.48	26.19	222.8	213.9	2.334	2.222	78.2
Sep	159.9	53.00	23.01	187.5	180.6	2.008	1.763	72.8
Oct	122.5	42.86	19.82	169.3	163.7	1.863	1.691	78.3
Nov	85.1	31.05	14.30	137.0	132.5	1.562	1.489	85.3
Dec	66.7	29.88	11.72	113.2	109.4	1.316	1.187	82.3
Year	1830.4	596.54	18.42	2099.4	2019.3	22.984	21.582	80.6

A.1.3 Meteorological Data for Barstow, US

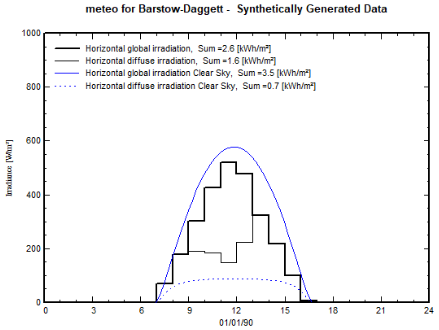

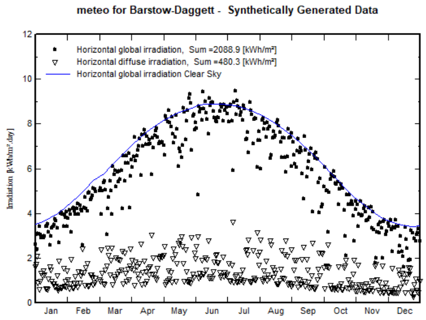

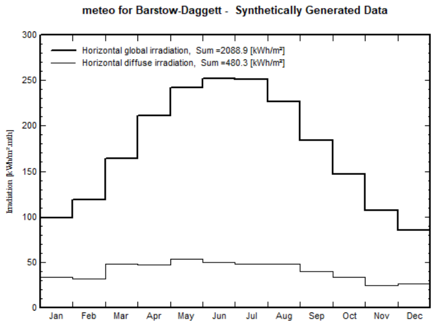

Month	GlobHor kWh/m^2	DiffHor kWh/m^2	T_Amb °C	GlobInc kWh/m^2	GlobEff kWh/m^2	EArray MWh	E_Out MWh	PR %
Jan	98.8	33.10	9.50	160.0	152.0	1.813	1.728	84.7
Feb	118.8	31.90	10.60	173.8	165.0	1.949	1.861	84.0
Mar	164.4	48.20	15.10	202.8	191.9	2.202	1.771	68.5
Apr	210.9	47.10	18.20	224.1	211.0	2.376	2.263	79.2
May	242.5	53.00	25.10	225.8	212.0	2.312	2.201	76.4
Jun	252.2	49.20	29.00	222.5	208.5	2.226	2.117	74.6
Jul	251.7	47.40	33.00	227.3	213.1	2.227	2.118	73.1
Aug	227.1	47.50	31.40	228.4	214.8	2.257	2.150	73.8
Sep	184.0	39.60	26.50	214.3	202.2	2.178	2.077	76.0
Oct	146.4	33.10	19.80	201.8	191.4	2.137	1.836	71.4
Nov	107.0	24.60	12.90	172.9	164.7	1.921	1.834	83.2
Dec	85.1	25.60	7.80	146.5	139.3	1.676	1.598	85.6
Year	2088.9	480.30	19.97	2400.2	2265.9	25.275	23.555	77.0

A.2 Angle Optimization

	Global Incidence kWh/m²	**Global Effective** kWh/m²	**Energy out of the array** MWh	**Energy output** MWh
Panjib Tilt 21.2° Azimuth -4.7°	1,985.2	1,903.1	21.0	19.6
Huelva Tilt 34.2° Azimuth 4.7°	2,099.3	2,019.3	23.0	21.4
Barstow Tilt 34.2° Azimuth -4.7°	2,402.1	2,266.1	25.3	23.6

A.2.1 Angle Optimization for Panjib, India

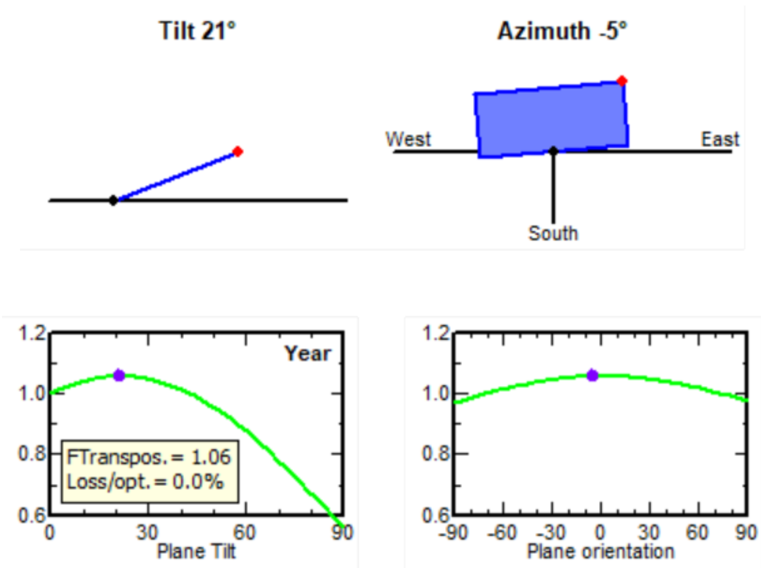

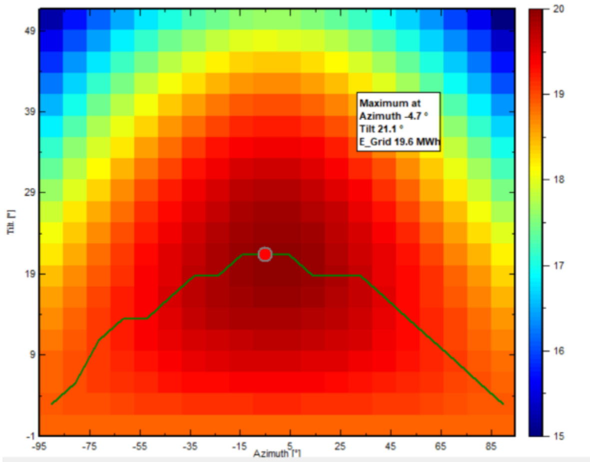

A.2.2 Angle Optimization for Huelva, Spain

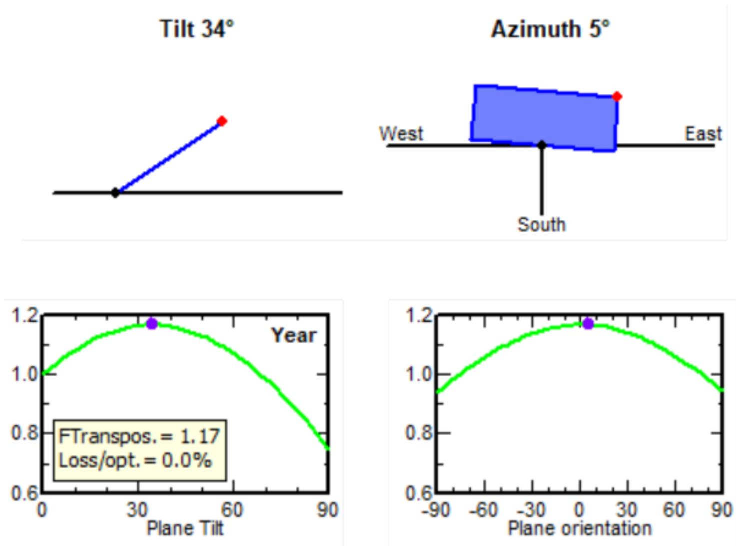

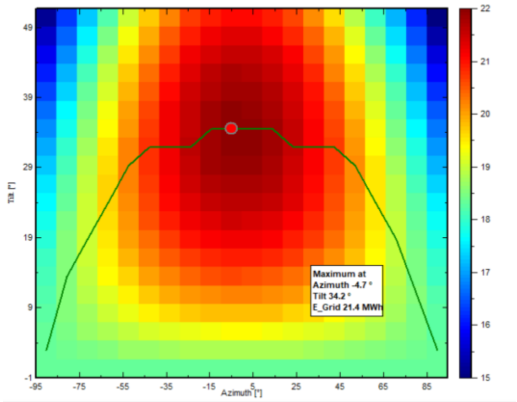

A.2.3 Angle Optimization for Barstow, US

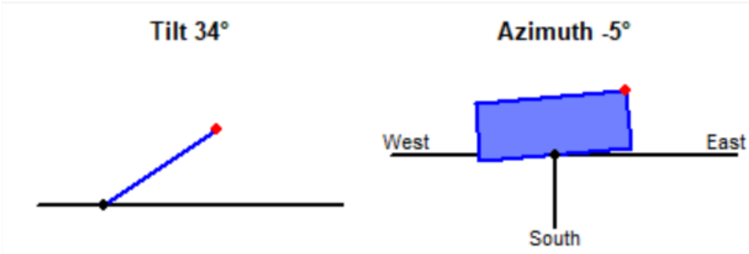

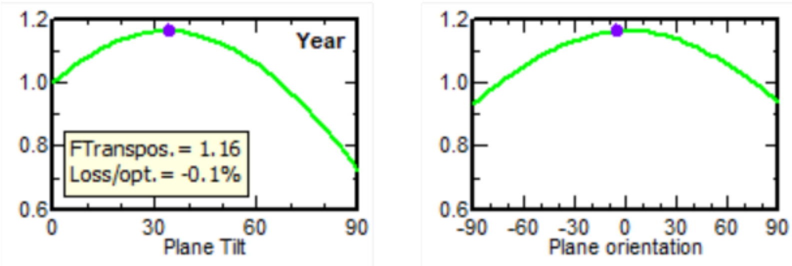

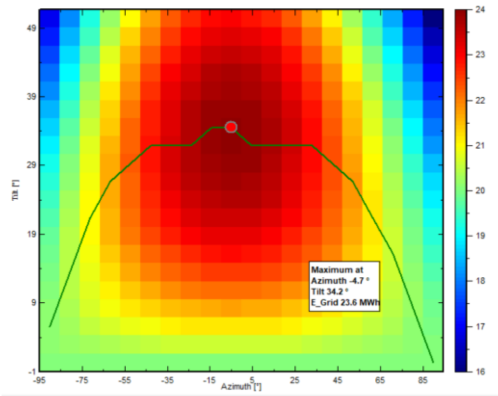

A.3 Financial Inputs

PV Installation and Technology

PVSyst 6.8.3 Financial Guidelines

Financial Data	Specific	
PV modules specific cost, < 1 kWp	1.5	€/W
PV modules specific cost, < 10 kWp	1.0	€/W
PV modules specific cost, < 100 kWp	0.85	€/W
PV modules specific cost, >100 kWp	0.7	€/W
Custom modules over-cost (ratio)	1.3	
Inverters specific cost, < 5 kWp	300	€/kW
Inverters specific cost, > 5 kWp	250	€/kW
Inverters specific cost, > 20 kWp	200	€/kW
Flat roof supports specific cost	0.65	€/W
Façade integration specific cost	1.0	€/W
Free-mounting supports specific cost	0.6	€/W
Specific transport and mounting costs (5 kWp grid system)	1500	€/kW
Specific Maintenance cost (5 kWp grid system)	80	€/kW
Scale exponential factor (mounting and maintenance) (ratio)	80	%
Specific cost of batteries (per kWh capacity)	150	€/kWh
Specific cost of regulator (basis 500 Wp)	0.8	€/W
Specific cost of surface pumps	1.5	€/W
Specific cost of submersible (well) pumps	2.0	€/W
Specific cost of controllers for pumping (basis 500 W)	0.4	€/W
Specific cost of control/converters for pumping	0.5	€/W
Specific transport and mounting (stand-alone 500 Wp)	6,000	€/W
Scale exponential factor (stand-alone mounting and regulator) (ratio)	70	%

Meeting with expert: OPEX and insurance can be assumed to be 3% and 0.3%, respectively, of the capital costs. A PV system cost can be 1.6 €/Wp, whereas a simpler system can be assumed to cost 1.4 €/Wp. For their project, inflation was taken as 2% yearly.

IEA, 2017, *Technical Assumptions Used in PV Financial Models – Review of Current Practices and Recommendations,* Photovoltaic Power Sysems Programme, Report IEA-PVPS T13-08:2017, p. 63-64

IRENA, 2012, *Renewable Energy Technologies: Cost Analysis Series, International Renewable Energy Agency, Volume 1: Power Sector, Issue 4/5. Link last accessed (22nd August 2019):* https://www.irena.org/documentdownloads/publications/re_technologies_cost_analysis-solar_pv.pdf

Sunmetrix, n.d., Cost of Solar Panels, Link last accessed (22nd August 2019) https://sunmetrix.com/cost-of-solar-panels/

Economic Times, 2019, *Solar panel cost: Price range of different types of solar panels and how much govt. subsidy can you avail for installing one.* Link last accessed (22nd August 2019) https://economictimes.indiatimes.com/small-biz/productline/power-generation/solar-panel-cost-price-range-of-different-types-of-solar-panels-and-how-much-govt-subsidy-can-you-avail-for-installing-one/articleshow/69327365.cms?from=mdr

Richardson, L., 2019, Solar panel cost and typical prices in California, Energy Sage. Link last accessed (22nd August 2019) https://news.energysage.com/compare-solar-panel-prices-california/

Land Costs

Panjib: Residential prices for the Goa region. Link last accessed (22nd August 2019) https://www.makaan.com/goa-residential-property/buy-plot-land-in-goa-city

Huelva: Terrenos Andalucía. Link last accessed (22nd August 2019) https://www.idealista.com/geo/venta-terrenos/andalucia/con-metros-cuadrados-mas-de_100/

Barstow: Average California Farm Real Estate Value. Link last accessed (22nd August 2019) https://www.farmprogress.com/markets/average-california-farm-real-estate-value-7200-acre

Land for Sale in San Bernadino County. Link last accessed (22nd August 2019) https://www.point2homes.com/US/Land-For-Sale/CA/San-Bernardino-County/San-Bernardino.html

Subsidies

Panjib: 25% was taken even if the subsidy currently is at 50% of capital costs. Link last accessed (22nd August 2019) https://mercomindia.com/small-solar-prosumers-goa-subsidy/

Huelva: Subsidies range from 20-50%. 35% subsidy was taken. SotySolar, n.d., *Subvenciones placas solares 2019 - Subvenciones placas solares Andalucia*. Link last accessed (22nd August 2019) https://sotysolar.es/placas-solares/subvenciones

California: No need for subsidies. Link last accessed (22nd August 2019) https://solartechonline.com/blog/california-solar-tax-credit/

Feed-in Tariffs

Panjib: Uttar Pradesh renewable energy feed-in tariff 2014 - 2019 levels. Link last accessed (22nd August 2019)

https://www.iea.org/policiesandmeasures/pams/india/name-140455-en.php?s=dHlwZT1yZSZzdGF0dXM9T2s,&return=PG5hdiBpZD0iYnJlYWRjcnVtYiI-PGEgaHJlZj0iLyI-SG9tZTwvYT4gJnJhcXVvOyA8YSBocmVmPSIvcG9saWNpZXNhbmRtZWFzdXJlcy8iPlBvbGljaWVzIGFuZCBNZWFzdXJlczwvYT4gJnJhcXVvOyA8YSBocmVmPSIvcG9saWNpZXNhbmRtZWFzdXJlcy9yZW5ld2FibGVlbmVyZ3kvIj5SZW5ld2FibGUgRW5lcmd5PC9hPjwvbmF2Pg,,

Huelva: In Spain there is no special tariffs for solar. Solar electricity is sold to the market at normal value. The value data for Operador Del Mercado Ibérico De Energía Polo Español (OMIE) was used as a stable value for tariffs in Spain as 0.07 $/kWh.

https://www.energias-renovables.com/fotovoltaica/es-interesante-vender-los-kw-vertidos-20181029

http://www.omie.es/inicio

A.4 Battery Specifications

C-rating	Charge/Discharge duration hours	Battery Power kW	Battery Capacity kWh	Nominal Voltage V	Max. Charge Current A	Nominal Capacity Ah	Price per kW $/kW	Battery Cost $
1		5	5	120	41666.7	41.7	$ 440.00	$ 2,200.00
1	1	10	10	120	83333.3	83.3	$ 440.00	$ 4,400.00
1		15	15	120	125000.0	125.0	$ 440.00	$ 6,600.00
0.5		5	10	120	41666.7	83.3	$ 600.00	$ 3,000.00
0.5	2	10	20	120	83333.3	166.7	$ 600.00	$ 6,000.00
0.5		15	30	120	125000.0	250.0	$ 600.00	$ 6,600.00
0.33		5	15	120	41666.7	125.0	$ 800.00	$ 4,000.00
0.33	3	10	30	120	83333.3	250.0	$ 800.00	$ 8,000.00
0.33		15	45	120	125000.0	375.0	$ 800.00	$ 9,000.00
0.25		5	20	120	41666.7	166.7	$ 1,000.00	$ 5,000.00
0.25	4	10	40	120	83333.3	333.3	$ 1,000.00	$ 10,000.00
0.25		15	60	120	125000.0	500.0	$ 1,000.00	$ 12,000.00
0.2		5	20	120	41666.7	166.7	$ 1,200.00	$ 6,000.00
0.2	5	10	40	120	83333.3	333.3	$ 1,200.00	$ 12,000.00
0.2		15	60	120	125000.0	500.0	$ 1,200.00	$ 15,000.00

A.5 System Output Power Distribution

A.5.1 Power Distribution in Panjib, India

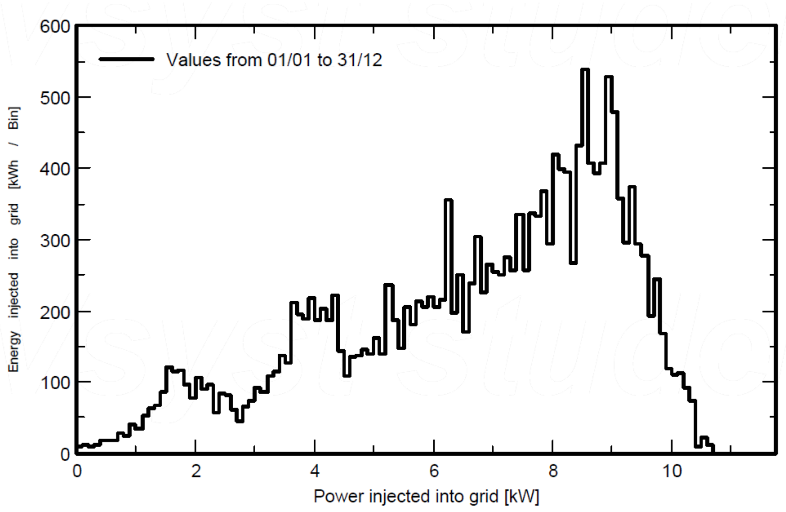

A.5.2 Power Distribution in Huelva, India

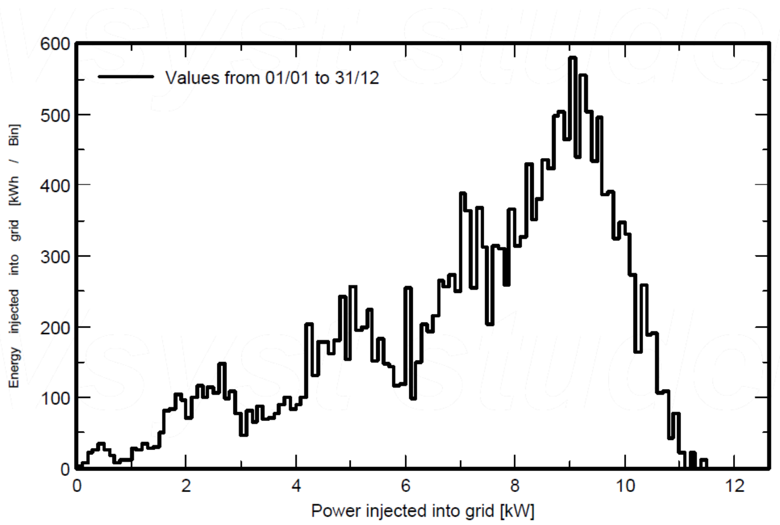

A.5.3 Power Distribution in Barstow, U.S.

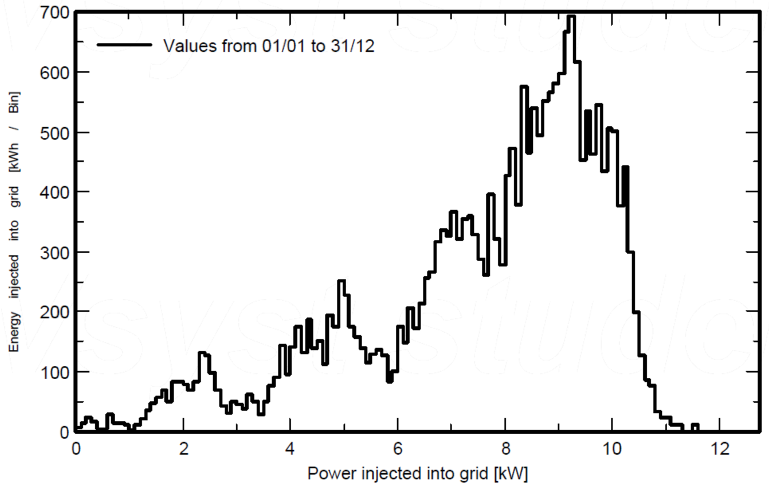

A.6 Loss Diagrams

A.6.1 Loss Diagram for the PV System in Panjib, India

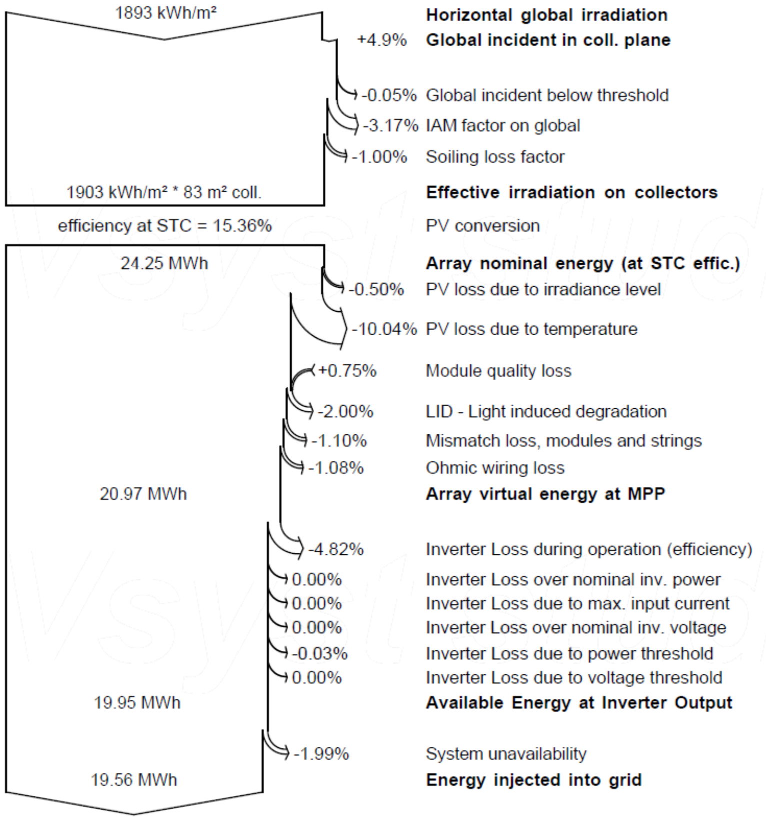

A.6.2 Loss Diagram for the PV System in Huelva, Spain

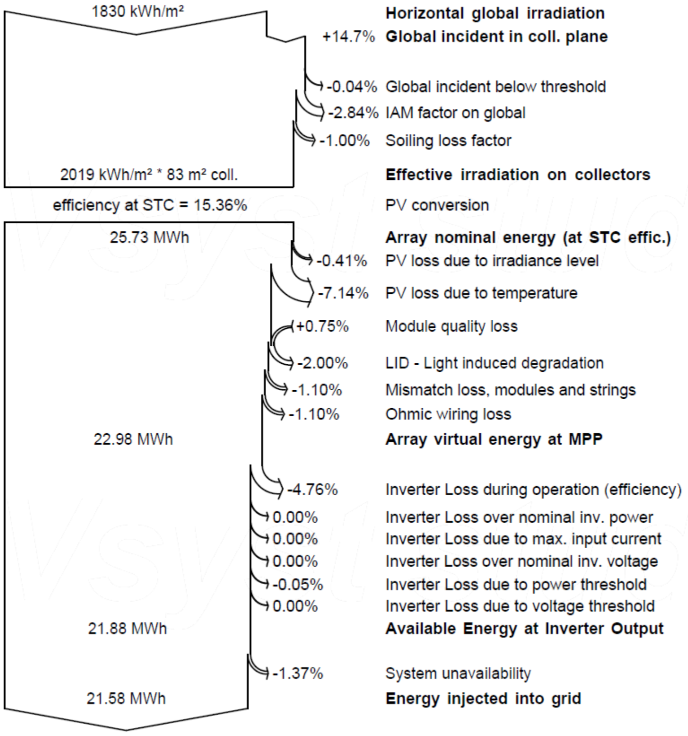

A.6.3 Loss Diagram for the PV System in Barstow, U.S.

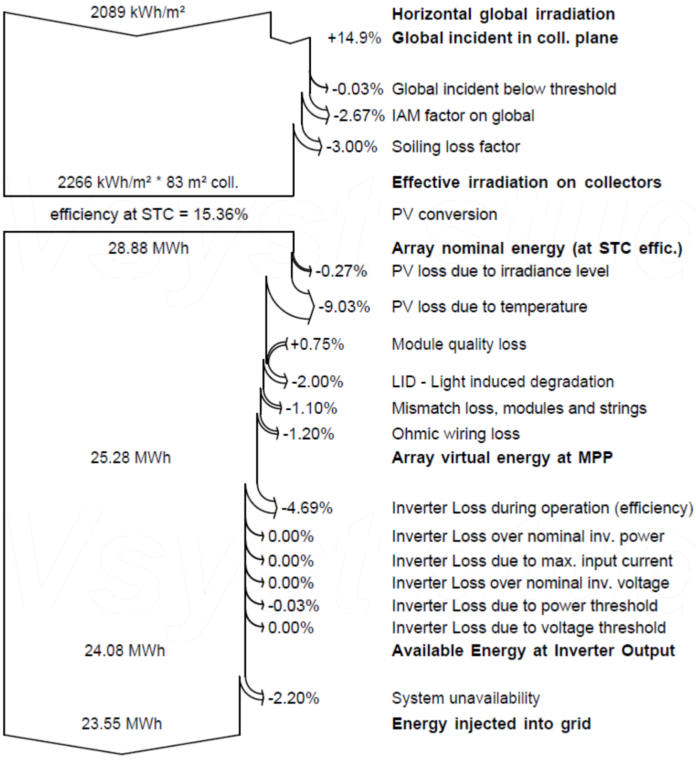

A.7 Economic Results

A.7.1 Detailed Economic Results for Panjib, India

Year	Sold Energy	Loan principal	Interest 0.05%	Running Costs	Deprec. Allow.	Profit	Cumulative Profit	% Amortization
2013	$1,956	$1,014	$13	$765	$1,360	$164	$164	4.6%
2014	$1,958	$1,014	$12	$773	$1,360	$159	$323	9.2%
2015	$1,960	$1,015	$12	$788	$1,360	$153	$476	13.8%
2016	$1,962	$1,015	$11	$796	$1,360	$147	$623	18.4%
2017	$1,964	$1,016	$11	$804	$1,360	$142	$764	22.9%
2018	$1,965	$1,016	$10	$812	$1,360	$135	$899	27.4%
2019	$1,967	$1,017	$10	$820	$1,360	$129	$1,028	31.9%
2020	$1,969	$1,017	$9	$828	$1,360	$123	$1,151	36.4%
2021	$1,971	$1,018	$9	$837	$1,360	$117	$1,268	40.8%
2022	$1,973	$1,018	$8	$845	$1,360	$110	$1,378	45.3%
2023	$1,975	$1,019	$8	$853	$1,360	$104	$1,482	49.7%
2024	$1,977	$1,019	$7	$862	$1,360	$97	$1,580	54.0%
2025	$1,979	$1,020	$7	$871	$1,360	$91	$1,670	58.4%
2026	$1,981	$1,020	$6	$879	$1,360	$84	$1,755	62.7%
2027	$1,983	$1,021	$6	$888	$1,360	$77	$1,832	67.0%
2028	$1,985	$1,021	$5	$897	$1,360	$71	$1,903	71.3%
2029	$1,987	$1,022	$5	$906	$1,360	$64	$1,966	75.6%
2030	$1,989	$1,022	$4	$915	$1,360	$57	$2,023	79.8%
2031	$1,991	$1,023	$4	$924	$1,360	$50	$2,072	84.0%
2032	$1,993	$1,023	$3	$933	$1,360	$42	$2,115	88.2%
2033	$1,995	$1,024	$3	$943	$1,360	$35	$2,150	92.3%
2034	$1,997	$1,024	$2	$952	$1,360	$28	$2,178	96.5%
2035	$1,999	$1,025	$2	$962	$1,360	$20	$2,198	100.6%
2036	$2,001	$1,025	$1	$971	$1,360	$13	$2,211	104.6%
2037	$2,003	$1,026	$1	$979	$1,360	$5	$2,215	108.7%
Total	$49,479	$25,492	$166	$21,606	$1,360	$2,215	$2,215	108.7%

A.7.2 Detailed Economic Results for Huelva, Spain

Year	Sold Energy	Loan principal	Interest 0.05%	Running Costs	Deprec. Allow.	Profit	Cumulative Profit	% Amortization
2013	$1,468	$1,610	$16	$975	$1,995	-$1,134	-$1,134	1.5%
2014	$1,469	$1,611	$15	$985	$1,995	-$1,143	-$2,277	2.9%
2015	$1,470	$1,612	$15	$995	$1,995	-$1,151	-$3,428	4.3%
2016	$1,472	$1,613	$14	$1,005	$1,995	-$1,159	-$4,587	5.7%
2017	$1,473	$1,614	$13	$1,015	$1,995	-$1,168	-$5,755	7.1%
2018	$1,475	$1,614	$12	$1,025	$1,995	-$1,177	-$6,932	8.5%
2019	$1,476	$1,615	$11	$1,035	$1,995	-$1,186	-$8,118	9.8%
2020	$1,478	$1,616	$11	$1,046	$1,995	-$1,194	-$9,312	11.1%
2021	$1,479	$1,617	$10	$1,056	$1,995	-$1,203	-$10,515	12.4%
2022	$1,481	$1,618	$9	$1,067	$1,995	-$1,212	-$11,728	13.6%
2023	$1,482	$1,618	$8	$1,077	$1,995	-$1,222	-$12,950	14.9%
2024	$1,484	$1,619	$7	$1,088	$1,995	-$1,231	-$14,181	16.1%
2025	$1,485	$1,620	$6	$1,099	$1,995	-$1,240	-$15,421	17.2%
2026	$1,487	$1,621	$6	$1,110	$1,995	-$1,250	-$16,671	18.4%
2027	$1,488	$1,622	$5	$1,121	$1,995	-$1,260	-$17,930	19.5%
2028	$1,490	$1,622	$4	$1,132	$1,995	-$1,269	-$19,200	20.6%
2029	$1,491	$1,623	$3	$1,144	$1,995	-$1,279	-$20,479	21.7%
2030	$1,493	$1,624	$2	$1,155	$1,995	-$1,289	-$21,768	22.7%
2031	$1,494	$1,625	$2	$1,167	$1,995	-$1,299	-$23,067	23.7%
2032	$1,495	$1,626	$1	$1,178	$1,995	-$1,309	-$24,377	24.7%
2033	$1,497	$0	$0	$1,190	$1,995	$307	-$24,070	25.6%
2034	$1,498	$0	$0	$1,202	$1,995	$296	-$23,773	26.5%
2035	$1,500	$0	$0	$1,214	$1,995	$286	-$23,487	27.4%
2036	$1,501	$0	$0	$1,226	$1,995	$275	-$23,212	28.3%
2037	$1,503	$0	$0	$1,238	$1,995	$264	-$22,948	29.1%
Total	$37,129	$32,361	$170	$27,546	$49,867	-$22,948	-$22,948	29.1%

A.7.3 Detailed Economic Results for Barstow, U.S.

Year	Sold Energy	Loan principal	Interest 0.05%	Running Costs	Deprec. Allow.	Profit	Cumulative Profit	% Amortization
2013	$3,274	$1,529	$31	$595	$1,235	$1,119	$1,119	8.6%
2014	$3,277	$1,531	$29	$601	$1,235	$1,116	$2,235	17.1%
2015	$3,281	$1,532	$28	$607	$1,235	$1,113	$3,349	25.7%
2016	$3,284	$1,534	$26	$613	$1,235	$1,111	$4,459	34.3%
2017	$3,287	$1,535	$25	$619	$1,235	$1,108	$5,567	42.8%
2018	$3,290	$1,537	$23	$625	$1,235	$1,105	$6,672	51.4%
2019	$3,294	$1,539	$22	$632	$1,235	$1,102	$7,774	59.9%
2020	$3,297	$1,540	$20	$638	$1,235	$1,099	$8,873	68.5%
2021	$3,300	$1,542	$19	$644	$1,235	$1,096	$9,968	77.0%
2022	$3,304	$1,543	$17	$651	$1,235	$1,093	$11,061	85.6%
2023	$3,307	$1,545	$16	$657	$1,235	$1,089	$12,150	94.1%
2024	$3,310	$1,546	$14	$664	$1,235	$1,086	$13,237	102.6%
2025	$3,313	$1,548	$12	$670	$1,235	$1,083	$14,319	111.1%
2026	$3,317	$1,549	$11	$677	$1,235	$1,079	$15,399	119.7%
2027	$3,320	$1,551	$9	$684	$1,235	$1,076	$16,474	128.2%
2028	$3,323	$1,552	$8	$691	$1,235	$1,072	$17,546	136.7%
2029	$3,326	$1,554	$6	$698	$1,235	$1,069	$18,615	145.2%
2030	$3,330	$1,556	$5	$705	$1,235	$1,065	$19,680	153.6%
2031	$3,333	$1,557	$3	$712	$1,235	$1,061	$20,741	162.1%
2032	$3,336	$1,559	$2	$719	$1,235	$1,057	$21,798	170.6%
2033	$3,340	$0	$0	$726	$1,235	$2,614	$24,412	179.1%
2034	$3,343	$0	$0	$733	$1,235	$2,610	$27,021	187.5%
2035	$3,346	$0	$0	$741	$1,235	$2,606	$29,627	195.9%
2036	$3,349	$0	$0	$748	$1,235	$2,601	$32,228	204.4%
2037	$3,353	$0	$0	$755	$1,235	$2,597	$34,825	212.8%
Total	$82,834	$30,879	$325	$16,805	$30,879	$34,825	$34,825	212.8%

A.8 CO2 Balance

A.8.1 System Lifecycle Emissions for Panjib, India

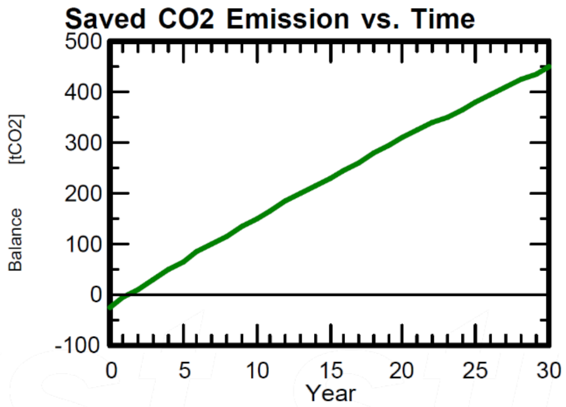

A.8.2 System Lifecycle Emissions for Huelva, Spain

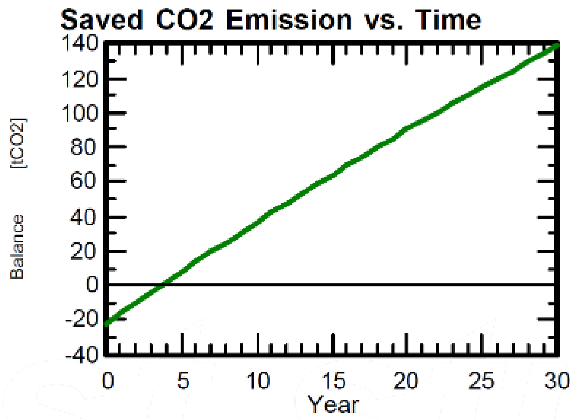

A.8.3 System Lifecycle Emissions for Barstow, U.S.

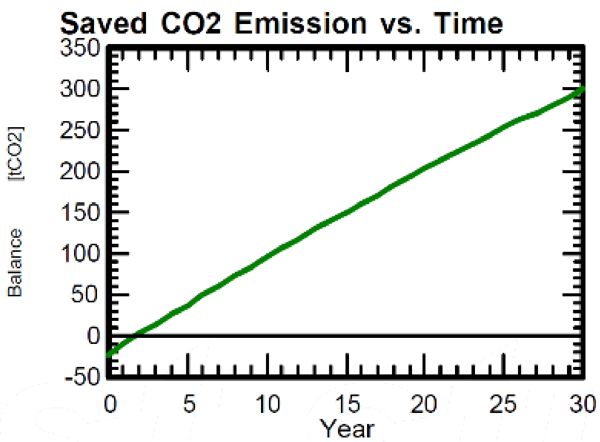

A.9 Predicted Revenue per Model and Country

A.9.1 Daily and Cumulative Predicted Revenue for Panjib, India

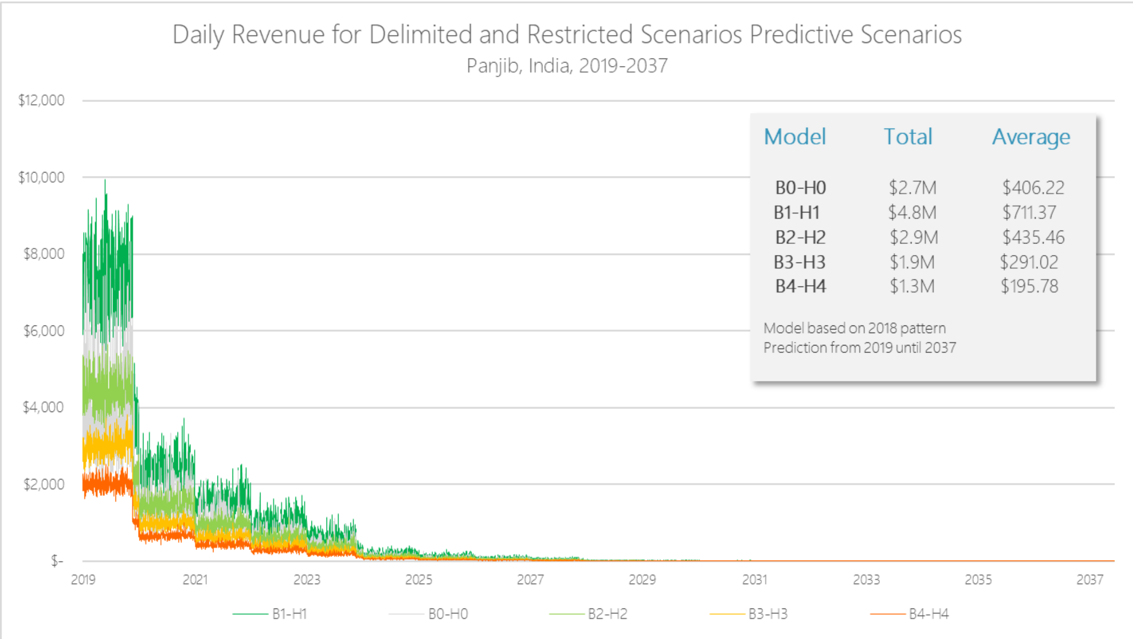

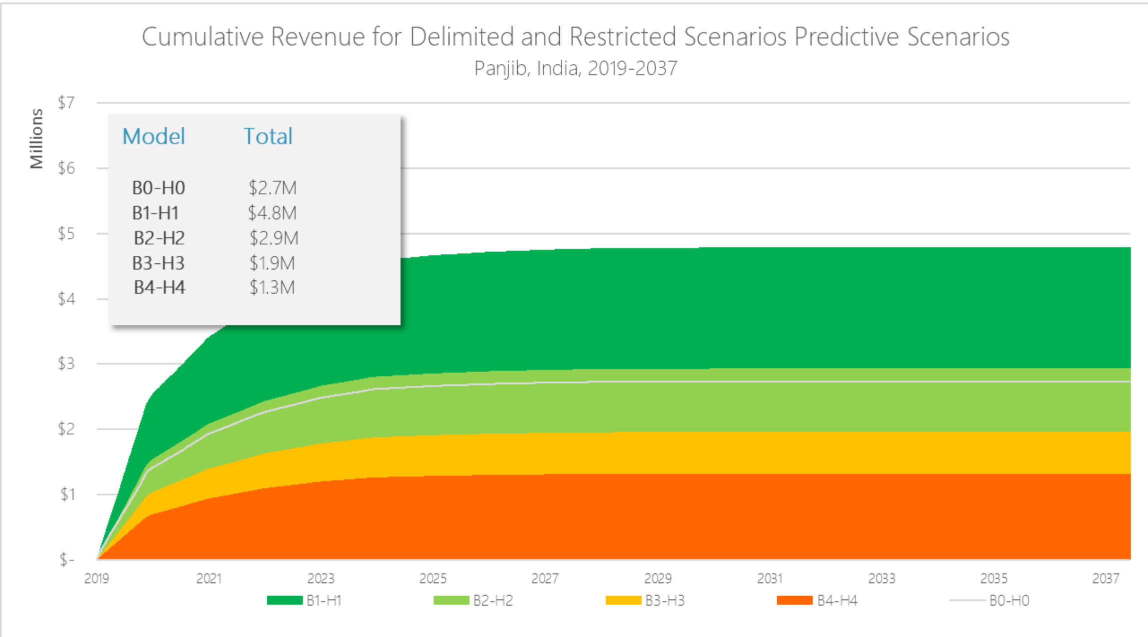

A.9.2 Daily and Cumulative Predicted Revenue for Huelva, Spain

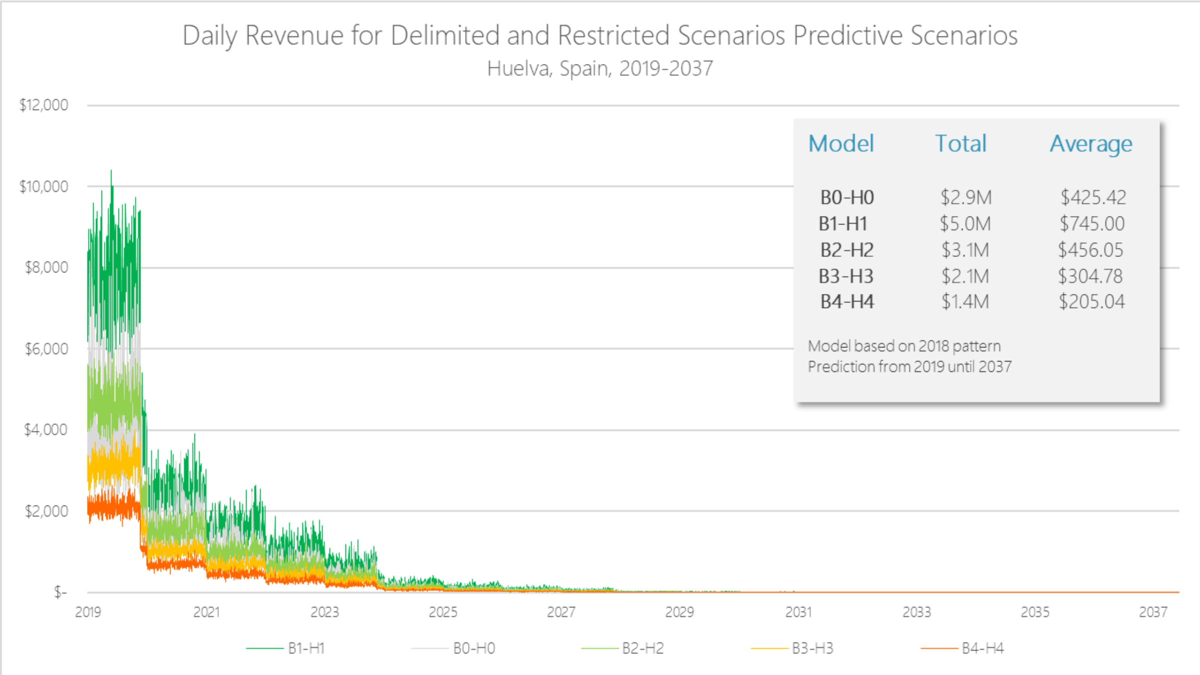

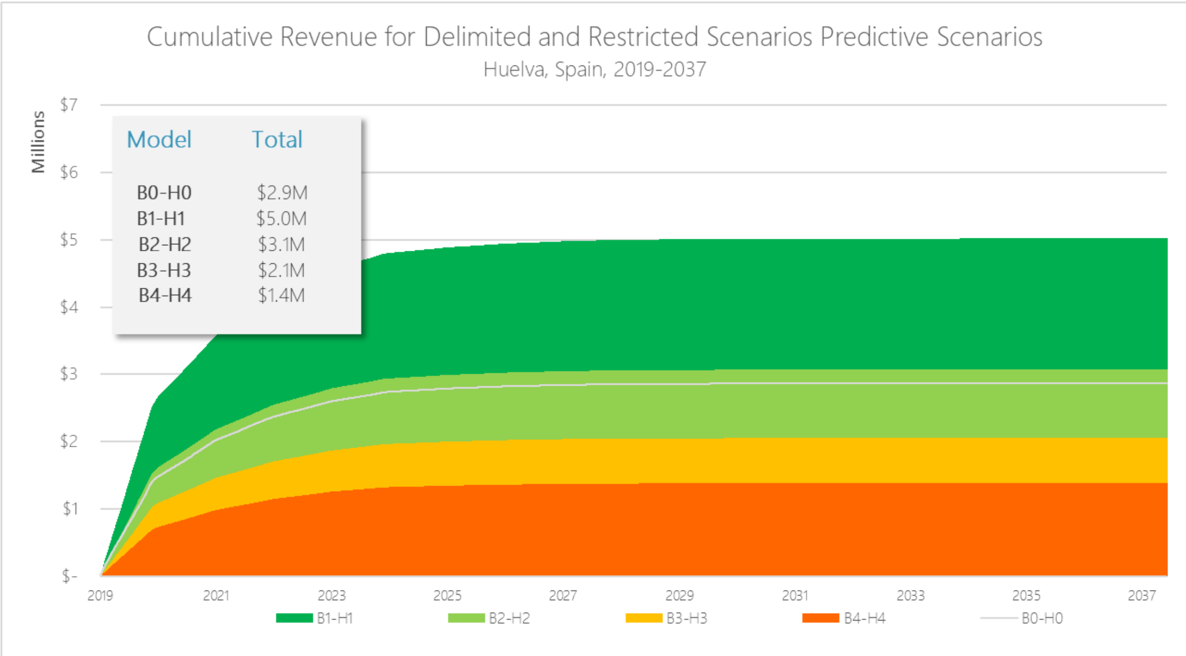

A.9.3 Daily and Cumulative Predicted Revenue for Barstow, U.S.